PROCESS SIMULATION AND TECHNO-ECONOMIC ANALYSIS OF CESAR-1 SOLVENT IN POST COMBUSTION CARBON CAPTURE, AND BENCHMARKING WITH MEA SOLVENT

Master Thesis in Chemical Engineering @

Author:

Yasemin Mertdağ

AALBORG UNIVERSITY
DENMARK

Title: Process simulation and techno-economic analysis of CESAR-1 solvent in post combustion carbon capture, and benchmarking with MEA solvent

Project supervisor: Rudi P. Nielsen
Anders Andreasen

Project period: Autumn Semester 2022 & Spring Semester 2023

Authors: Yasemin Mertdağ

Page Number: 122

Project submitted: 1st of June 2023

Chemistry and Bioscience Department
Aalborg University
https://www.aau.dk

Abstract

Mono-Ethanol-Amine (MEA) solvent has been widely used in the Carbon Capture industry. However, it has some drawbacks (e.g. it requires an extensive amount of energy for regeneration, the CAPEX of the plant operating with MEA is high etc.). Thus, a more promising solvent CESAR 1, an aqueous solution of 2-amino-2-methyl-propanol (AMP) and piperazine (PZ), from CESAR project has been studied to overcome these drawbacks. In this study, the performance of CESAR 1 solvent in Post-combustion Carbon Capture Plant has been evaluated in technical and economical point of view with respect to simple yet well-studied aqueous solvent MEA. The Process has been modelled in a process simulation software called ProMax, V6 (Bryan Research & Engineering). Pilot plant studies have been performed, and bigger scale production with real flue gas data was studied. Six parameter sensitivity analysis was performed, and the most significant reboiler duty reduction was observed in the sensitivity analysis performed by L/G ratio, minimum temperature approach, and stripper pressure. Respectively, the lowest reboiler duty at the best conditions of these were found to be 2.8 GJ/t CO_2, 2.77 GJ/t CO_2 and 2.73 GJ/t CO_2 for CESAR, 3.5 GJ/t CO_2, 3.45 GJ/t CO_2, and 3.43 GJ/t CO_2 for MEA. The L/G ratio and the minimum temperature difference were the most significant parameters affecting the cost. At the best L/G ratio, total cost of 460 million € for CESAR, and 544 million € for MEA was obtained. At the best minimum temperature difference, total cost of 502 million € for MEA, and 419 million € for CESAR were found. In every case of sensitivity analysis, CESAR performed better than MEA, and almost at every condition, CESAR design was less costly.

Keywords: Carbon capture, CO_2 capture, post-combustion carbon capture (PCC), MEA, CESAR 1, techno-economic analysis, CAPEX, amines, flue gas, ProMax, modelling, pilot plant, simulation

Preface

This study, Process simulation and techno-economic analysis of CESAR-1 solvent in Carbon capture, and MEA benchmarking, has been completed in the period from 09/2022 - 06/2023 as a long Master Thesis in Chemical Engineering at Aalborg University Esbjerg. The author would wish to express her gratitude to the project supervisors Rudi P. Nielsen and Anders Andreasen, who have provided help and guidance throughout the entire time.

Aalborg University, June 01, 2023

Table of Contents

Table of Figures

List of Tables

1 Introduction

The world has been fighting with climate change for over 70 years now. Human activities such as transportation vehicles, industrial activities, incineration causes change in chemical composition of atmosphere. This composition change leads to global temperature increase called global warming which in long term causes weather change like change in global humidity, rainfall pattern, seasonal temperature in other words, climate change. Gases like Methane (CH_4), Halocarbons, Nitrous Oxide (N_2O), Water vapor (H_2O), and Carbon Dioxide (CO_2), namely Green-house gases (GHG), are the major contributors to this change in the composition. When released, these gases act as a blanket over the surface of the Earth, causing all the radiated heat trapped inside the atmosphere which in return heats up the world causing a global temperature change which is defined as global warming.

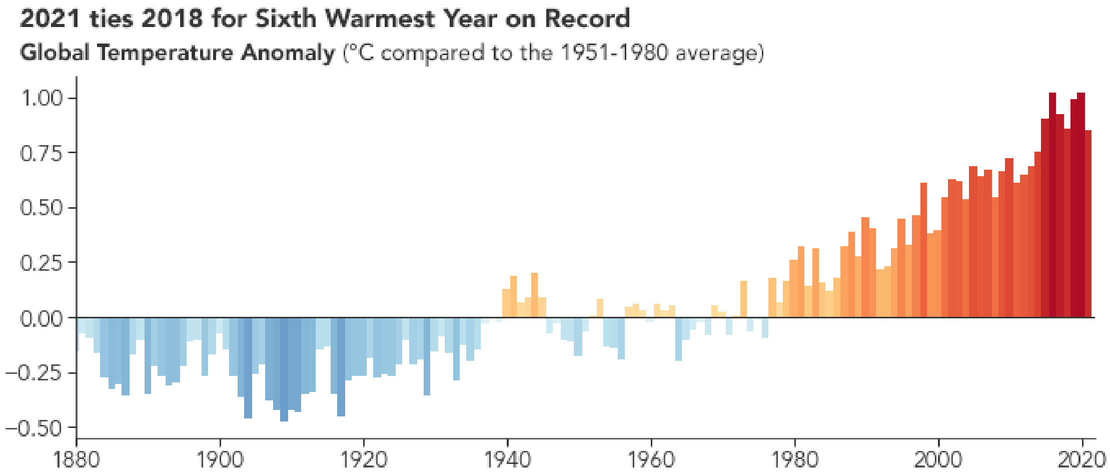

Figure 1: Global temperature increase over years [1]

The World is almost 1.1^{o}C warmer than it used to be 200 years ago. However, if it keeps getting warmer and reaches over 1.5^{o}C, it will have damaging consequences to earth and to humanity. Water shortage, super hurricanes, drying out of underground reservoirs, strong heat waves and many other consequences will be triggered if the temperature keeps rising. Therefore, scientists have come to a conclusion that to maintain a livable environment, the temperature rise should be limited to 1.5^{o}C. In Paris Agreement, it was decided to achieve net zero emissions, and to decrease the CO_2 emissions by 45% by 2050 [2]. Various solutions have been found to limit CO_2 emissions such a using green energy, reducing air travel, capturing carbon and many more.

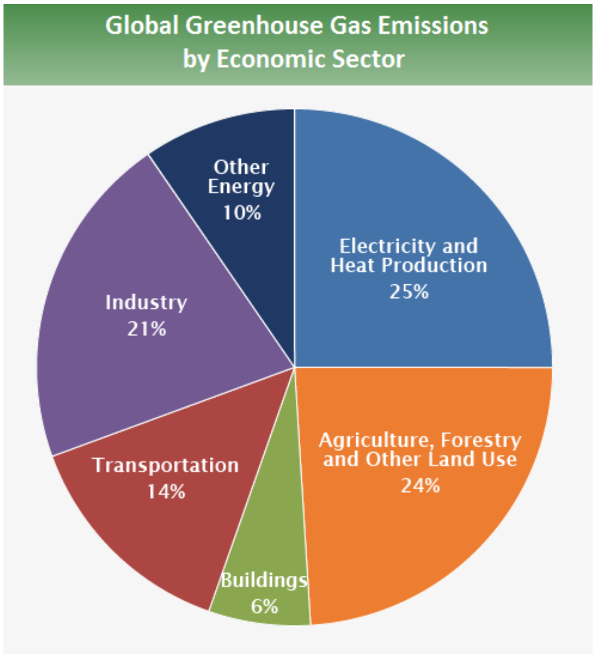

Figure 2: Greenhouse gas emissions by different sectors [3]

Industrial activities, and heat and electricity production are responsible of almost 50% of greenhouse emissions. However, fossil fuels are still very important source of energy and electricity production, as well as fuel in used in various industries. At this point, carbon capture and storage (CCS) or utilization (CCU) show great importance as they focus on capturing carbon from flue gases of industries where the carbon is source is relatively large. By 2050, it is expected to reduce global carbon emissions by around 14% with CCS or CCU [4] at 90% removal rate. However, it should also be noted that to achieve net zero goal by 2050, no single emission reduction solution will be enough.

Carbon capture and storage focuses on capturing carbon and storing it in the depleted oil and gas reservoirs or deep-water aquifers whereas carbon capture and utilization involves utilization of captured carbon in various production/manufacturing activities. Three main steps are included: the capture, the transportation, and the storage/utilization [5].

Three main types of carbon capture technologies are currently available namely post-combustion capture, pre-combustion capture, and oxy-fuel combustion capture while post-combustion carbon capture being the most promising one. More detailed explanation of each technology will be given in the following sections.

2 Carbon Capture Technologies

Finding a way to reduce CO_2 emissions is becoming more important every passing day. Numerous studies have been made to decrease these emissions associated with using fossil fuels which include replacing high carbon content fuels with low ones, using advanced fossil fuels to improve the plant efficiencies, and Carbon capture and storage/utilization. Carbon capture and storage/utilization show good potential among these solution strategies. Carbon could be captured by three main techniques shown in Figure 3. Post combustion capture techniques will be explained in the following section. Depending on when the carbon is captured, technologies differ from each other. If the capturing process takes place before the combustion is done, it is called pre-combustion capture. Similarly, capturing the carbon after combustion is done is called post-combustion carbon capture. Finally, if pure Oxygen instead of air is used for the combustion, it is called oxy-fuel carbon capture.

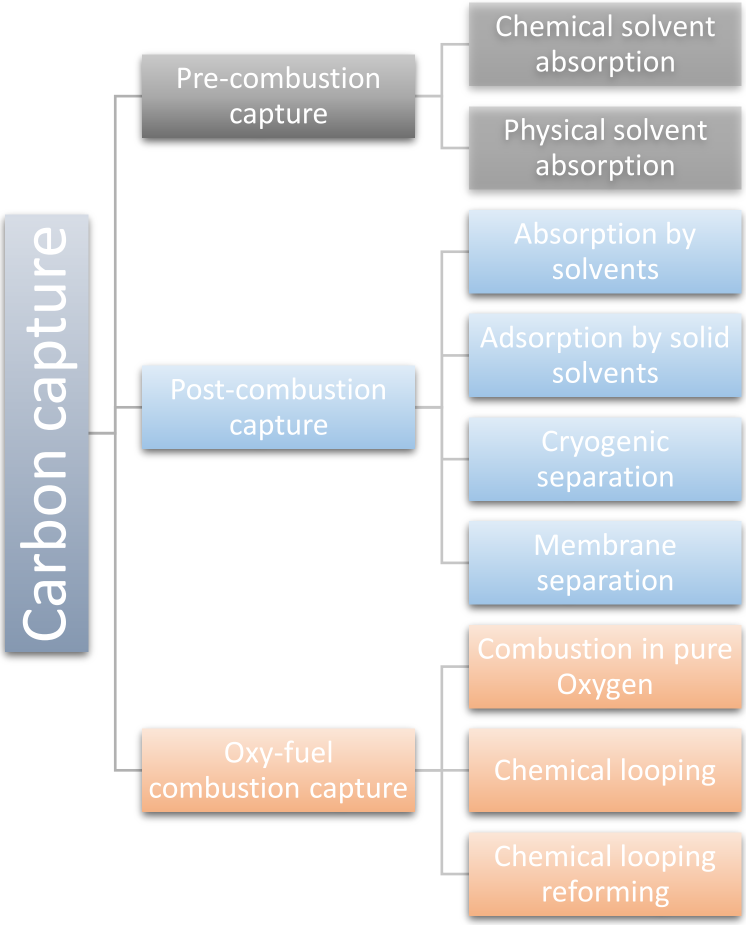

Figure 3: Types of carbon capture technologies [6]

2.1 Pre-combustion carbon capture

In pre-combustion capture, the carbon is separated from the flue gas before the combustion cycle ends but after conversion of CO to CO_2. This technology can be used with Integrated Gasification Combined Cycle (IGCC) [6]. Processes such as coal gasification and natural gas reforming which produces synthesis gas (syngas) use this capture technology [7].

In IGCC, syngas is produced by gasification of solid fuels by adding pure Hydrogen or steam. Later, water gas shift reaction in the shift reactor increases the Hydrogen content of the syngas making it mainly H_2 and CO_2 (around 40%) making the capture process more effective. Then, this converted CO_2 can be separated from syngas by physical absorption [7] [6]. The remaining gas rich in H_2 can be further used for power generation or transported to customer sites [6] [8]. Low energy penalty of the process is the major advantage of this technology [6]. Less cooling water requirement compared to post-combustion, and lower energy requirement due to the higher CO_2 concentration are other advantages of this technology [9]. The disadvantages of this technology include high CAPEX and OPEX, extensive auxiliary requirement, limited retrofitting option to existing plants, and barriers in large scale application [9] [10].

2.2 Post combustion carbon capture

Post combustion carbon capture from the flue gases of the industries run by fossil fuels is the most studied method among carbon capture technologies. In this technology, carbon is captured after the combustion cycle ends. This technique is applied to the downstream to power plant processes thus, it is the most suitable one for retrofitting purposes for power plants with lowest impact to their processes [6]. This technology is the most widely used and mature technology which can be applied to the existing plants. Furthermore, it is commercially available, and suitable for retrofitting to the existing plants which makes the adapting cost effective [10] [11]. Also, resulting product has high purity [9]. Low CO_2 partial pressure combined with low operating pressure makes the capture process a cost intensive technology as the specific energy demand and the CAPEX would be high [6]. Smaller process efficiency due to lower CO_2 concentration, requirement for larger equipment and cooling associated with high reboiler temperature are other disadvantages [9]. Several ways are used in PCC to capture carbon from flue gasses including absorption, adsorption, membrane separation and cryogenic separation [6] . Post combustion carbon capture can be done in various ways but the most used one is absorption/desorption technique where amine-based solvents are used to capture carbon from the flue gas [6]. The techniques are explained in the following sections.

2.2.1 Absorption by chemical solvents

This technology is the most widely used technology in capturing carbon from low-pressure flue gasses. It is based on selective absorption where the primary, secondary and tertiary amines are used as solvents for the separation. As the name implies, absorption by chemical solvents relies on the chemical reaction between absorbent and CO_2. After the flue gas is mostly separated from the impurities, it is contacted counter-currently in the absorber with chemical solvent. Mono-ethanolamine (MEA) is the most used amine solvent in absorption-based post combustion carbon capture. CO_2 reacts with the solvent in the absorber and forms loosely bound intermediate products. The solvent enriched in CO_2 is then fed to the stripper where it is regenerated by the reverse reaction. Heat supplied by the reboiler causes the loosely formed bonds between the solvent and CO_2 to break, and the solvent previously fed to absorber is regenerated. The solvent mainly free of CO_2 is recycled back to the absorption column to keep the continuous process going. Purity of the product generated by this technology is above 99%. [6]

The advantage of this technology includes high purity product, high absorption capacity at low CO_2 partial pressures, mature technology, and high recovery up to 95% [11] [12]. High regeneration energy requirement, solvent losses, requiring large equipment for circulating large volumes of regenerated solvent, thus high CAPEX are the main disadvantages [6]. Other disadvantages include limited CO_2 loadings, and corrosion are the main disadvantages [6].

2.2.2 Adsorption by solid solvents

Adsorption by solid solvents is due to the strong intermolecular interactions between the solvent surface and the gas molecules. Difference in the strength of intermolecular interactions forms the selectivity of the towards different gases. Solid materials such as activated carbon, zeolites or calcium oxides are used to capture carbon due to their high surface areas. Normally, fixed beds are filled these materials for adsorption. In this technology, the process is based on simple adsorption then desorption cycle where the flue gas is passed through the fixed bed filled with spherical adsorbent particles. CO_2 is selectively adsorbed, and the other materials pass through the adsorber. The regeneration takes place when the adsorbent is fully saturated with the CO_2, meanwhile the gas to be treated is sent to another clean adsorber bed. Adsorbent pore size, temperature, pressure, and the surface forces play important role in the adsorption of single or multiple layers of gases. [6]

Different adsorption methods are available including Pressure Swing Adsorption (PSA), Temperature Swing Absorption (TSA), and Electric Swing Adsorption (ESA). PSA is based on a principle where the flue gas is passed through the beds operating at elevated temperatures and pressures until the equilibrium conditions are met at the bed exit. Then, the bed is regenerated by lowering the pressure. In TSA, the regeneration takes place by raising the temperature by either externally heating up the bed or supplying hot inert gas. In ESA, low-voltage electric current is supplied for regeneration. TSA and PSA are the commercially used technologies, but PSA is superior due to lower energy requirement and higher regeneration speed. [13]

This technology gives; high capacity at low CO_2 partial pressures, high selectivity, has; fast kinetics, and low energy consumption. However, degradation due to the impurities and thermal and oxidative degradation of the solvent are the main disadvantages [11].

2.2.3 Membrane absorption

Solvent and gas use membranes as the contact surface where the selectivity is determined by the solvent. Zeolites, polymeric membranes, porous inorganic membranes, and palladium membranes exists for membrane absorption [13]. Although the process is like the conventional absorption-desorption technique, it shows some advantages over the conventional method like low flooding, channeling, foaming, and solvent discharge [6]. It requires multiple stages and/or recycle stream for achieving desired removal which gives increased cost, energy consumption and complexity [13].Even several membranes with different characteristics are required depending on the required level of purity of CO_2 [13].In gas absorption membranes, the gas mixture is introduced into the microporous membrane where the CO_2 diffuse through the pores and is absorbed by liquid solvent where the removal depends on the selectivity of the solvent [6].

Easy operation, high recovery, and requiring no chemical process are the main advantages of this technology [12] [11]. Some disadvantages of membrane absorption are high membrane and production costs, poor membrane resistance, membrane contamination, and pressure drop of flue gas through the membrane [6] [11].

2.2.4 Cryogenic separation

Cryogenic separation includes compressing and cooling the gas mixture containing CO_2 to form liquid or solid CO_2 after it is pre-treated to remove most of the components like H_2O, SO_2, and NO_x [6]. Formed liquid and solid CO_2 is removed from the gas mixture. This technology enables easy liquid CO_2 production with high purity which then simplifies the transportation and storage of CO_2 [6]. This technique has high capture efficiency up to 99.9%, low corrosion, pure CO_2 recovery in the liquid form which allows for easier transportation an reduces extra liquefaction costs [12]. The disadvantage of this technology is the high energy requirement for compression and refrigeration required for the process and the possible blockage caused by solid CO_2 or H_2O [13] [6]. Especially, application of this technology to the gas mixtures having low CO_2 content is not economic because of the mentioned disadvantages [6] [13]. Therefore, this technology is not suitable for large scale carbon capture from flue gases from power stations. It is a good option for high pressure gases from pre-combustion and oxy-fuel combustion which have high CO_2 content [6]. Other disadvantage of this technology is the possible blockage caused by solid CO_2 or H_2O [13].

2.3 Oxy-fuel combustion carbon capture

Provides that the concentrated Oxygen is used in oxy-fuel combustion, the main problem associated with this technology is the separation of N_2. Cryogenic air separation is used for producing Oxygen [13].Burning the fuels with concentrated/pure Oxygen meaning that in the absence of N_2 results in increased combustion temperatures [6]. To decrease the combustion temperature near that of normal air blown combustor, some CO_2 containing gas is recycled back to the combustor [13]. The main advantage of using oxy-fuel method is relatively easier separation of CO_2 due to high CO_2 concentration in the flue gas, around 80%. Thus, CO_2 can be separated from the flue gas by a simple flue gas cleaning system combustor [13].This technology has been already used in steel, cement, and glass industries [6]. The advantage of Oxy-fuel technology is that the very high CO_2 concentration increases the absorption capacity, and the amount of gas to be treated is relatively low [14]. However, significant energy drops, costly cryogenic O_2 production, low process efficiency and corrosion problems are the main disadvantages [14] [10] [9].

2.4 Summary

Table 1 shows the summary of different capture technologies. After discussing about them and comparing the advantages and disadvantaged it was decided to go with Post Combustion Capture.

Table 1: Advantages and disadvantages of main capture technologies [9] [10] [14]

Technology	Advantages	Disadvantages
Pre-combustion	• High absorption efficiency due to high CO_2 concentration • Lower cooling requirement • Lower energy penalty	• High CAPEX and OPEX • Extensive auxiliary requirement • Limited retrofitting option • Barriers in larger scale production
Post-combustion	• Mature technology • Easily retrofitted to existing plants • Low impurities in the product • Suitable for commercial usage	• High solvent regeneration requirement • High CAPEX • Smaller process efficiency due to low CO_2 concentration • High cooling requirement
Oxy-fuel combustion	• Increased absorption capacity due to very high CO_2 concentration • Lower amount of gas to be treated	• Significant energy drop • Costly cryogenic O_2 production • Low process efficiency • Corrosion problems • Only tested at small scale

As it is seen from Table 1, all three technologies have advantages and disadvantages. Pre-combustion has high absorption capacity, low cooling requirement, and low energy penalty. However, the CAPEX and OPEX are high for this technology. Also, the retrofitting and bigger scale production options are limited. Oxy-fuel combustion has higher absorption capacity due to very high CO_2 concentration, too. Smaller amount of gas to be treated is another advantage of this technology. However, high energy drop, costly cryogenic O_2 production, low process efficiency, small scale production, and corrosion problems are the drawbacks. Post combustion carbon capture overweighs with its advantages and the possibility of larger scale application. Easier retrofitting, high purity product, and being mature technology are the other advantages of this technology. Therefore, it has been selected to be studied in more details. This technology has different capturing techniques which are already discussed in the previous sections. One technique should be selected based on the advantages and the disadvantages.

Table 2: The advantages and disadvantages of the techniques used in post combustion carbon capture [13] [11] [12]

Technique	Advantages	Disadvantages
Absorption by chemical solvents	• High purity product • Providing high absorption capacity at lower partial pressures • Mature technology • High recovery up to 95% • Commercial scale production	• Limited CO_2 loadings • High regeneration energy requirement • Solvent losses • Large equipment for circulating large volumes of regenerated solvent, so high CAPEX • Corrosion • Energy losses
Adsorption by solid solvents	• High capacity at low CO_2 partial pressures • High selectivity • Fast kinetics • Low energy consumption	• Thermal and oxidative degradation • Degradation due to impurities
Membrane absorption	• Easy operation • High recovery • Requiring no chemical process	• High membrane and production costs • Poor membrane resistance • Membrane contamination, • Pressure drop of flue gas through the membrane
Cryogenic separation	• High capture efficiency (up till 99.9%) • Low corrosion • Pure CO_2 recovery in the liquid form which allows for easier transportation an reduces extra liquefaction costs	• Not suitable for large scale carbon capture from flue gases • Blockage caused by solid CO_2 or H_2O • High energy requirement for compression and refrigeration

The advantages and disadvantages of PCC techniques are summarized in Table 2. Absorption by chemical solvents is the most mature, and commonly used capture technique which provides high purity product, high absorption capacity even at low partial pressures and high recovery. However, high regeneration requirement, solvent losses, limited loadings, high CAPEX and energy losses are the drawbacks of it. Adsorption by solid solvents provide high capacity, has high selectivity and fast kinetics, and low energy consumption. Nevertheless, due to the high degradation of the solvent it is not used very commonly. Membrane absorption on the other hand, provides easy operation with high recovery, and requires no chemicals. Yet, high production costs, membrane contamination, pressure drop, and low membrane resistance are the disadvantages. Cryogenic separation has high capture efficiency, low corrosion, and allows for easy CO_2 transportation as the product is in liquid form. However, it is not suitable for big scale commercial production, the blockage by CO_2 or H_2O limits the process, and it requires high energy for refrigeration.

The final decision has been made based on these advantages and disadvantages. Many advantages and disadvantages are similar among the techniques, but the selection was made mostly based on the availability for bigger scale production and high purity of the captured CO_2. As absorption by chemical solvents is more suitable for big scale production, the most mature technology, has high absorption capacity up to 95%, and gives high purity product it has been selected for this work.

3 Post Combustion Carbon Capture with Absorption

This section of the report explains the post combustion carbon capture (PCC) in more details. Information about the process, modifications for the process improvement, the solvents used, the chemistry of the system, and the rate-based modelling will be discussed to better understand the process.

3.1 Process description

Figure 4 represents the process of absorption-based post combustion carbon capture. The process consists of two main equipment, absorber and a desorber/stripper. Flue gas from an energy intensive plant, mostly fossil fuel-fired power plant, is pre-treated before entering the absorption unit [6]. Generally, the flue gas composition of fossil fuel fired plants is around 12-15 mol% in dry content which depends on the working principle of the plant and which fuel is being used [6] [15]. In the power plants operating around atmospheric pressure, CO_2 concentration is relatively lower than the ones operating at higher pressures, so as CO_2 partial pressure [6]. For better absorption, flue gas is cooled to 35-50^oC and fed to absorber which operates around atmospheric pressure [15]. Pre-treated flue gas is saturated with steam and sent to absorber from the bottom of absorber. Amine-based solvent flows from the top of absorber in countercurrent flow to the flue gas. CO_2 is absorbed into the amine solvent by exothermic reactive absorption. The carbon rich solvent which is called rich amine exits the absorber from the bottom, while the treated gas leaves the absorber column from the top after passing through the water washing section [15]. This section ensures the water balance and solvent concentration in the system is maintained for better absorption, also it helps remove the impurities by washing them off [15]. The treated gas has CO_2 content around 1-2 mol% which corresponds to 90% of capture [15].

Later, rich amine is pressure adjusted and routed to the lean/rich heat exchanger prior to the stripper. The rich amine is heated to around 99^oC in the lean/rich heat exchanger for getting it prepared for the endothermic desorption process in the stripper. Then, the heated rich amine is separated from carbon in desorber/stripper round 120 ^oC. The energy required for the regeneration is supplied by the reboiler which uses intermediate or low-pressure (LP) steam from steam turbines. Due to this reason, the main energy penalty arises from the steam requirement in the reboiler. The regenerated solvent, called lean amine, is pressure adjusted and recycled back to the absorber after it is cooled in the lean/rich heat exchanger. The make-up solvent is generally added before the lean amine is fed to the absorber column [15].

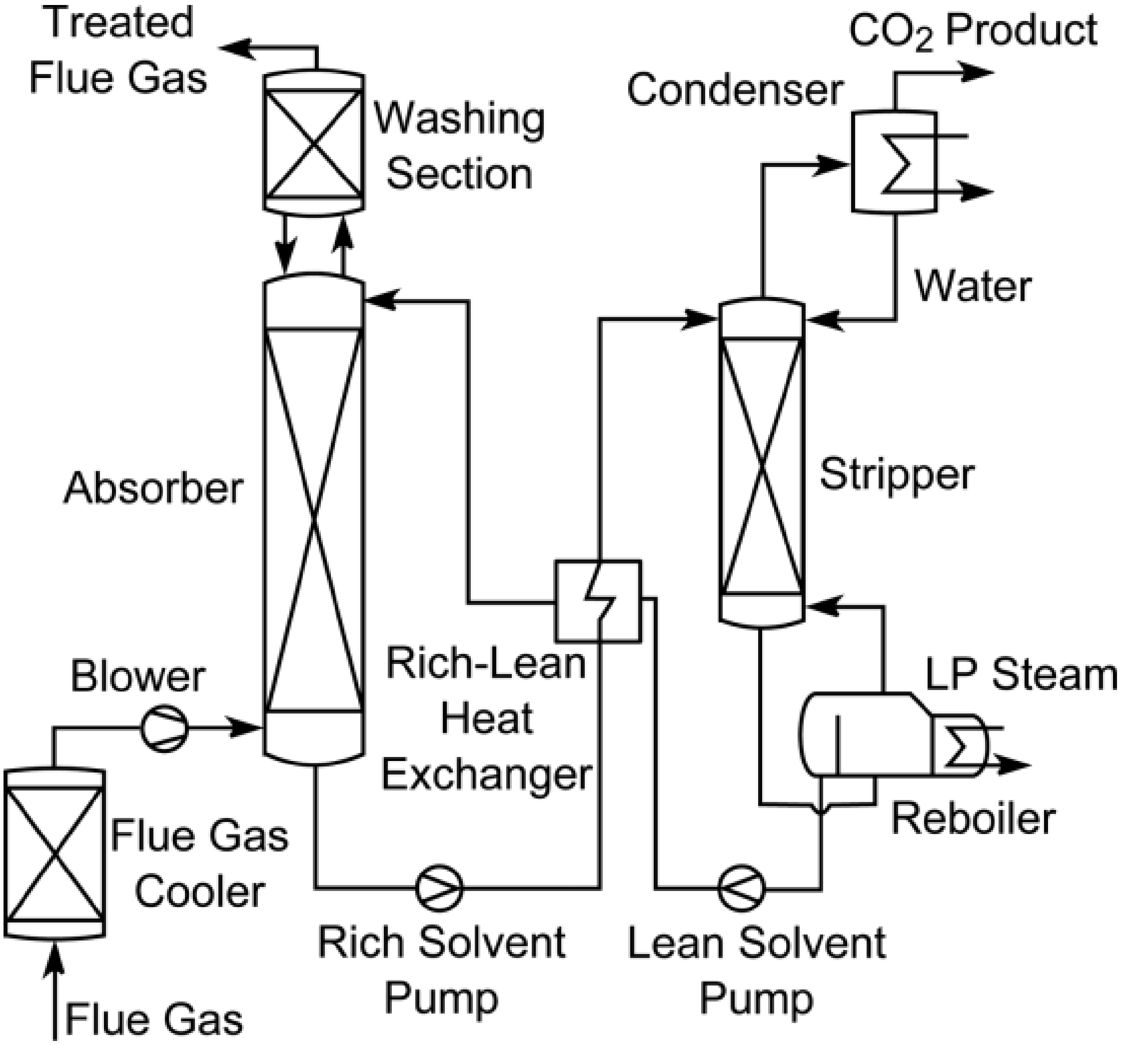

Figure 4: Process flow diagram of absorption-based post combustion carbon capture [15]

In post combustion carbon capture, absorber and desorber mostly consist of packings. Packings are generally preferred over trays due to their lower pressure drops and high mass transfer rates. Packings could be random, or structured. Random packings are randomly distributed in the column. On the other hand, structured packings come in metal sheets or wire mesh. The cost, pressure drop, mass transfer area, corrosion resistance and the strength are the defining features when choosing the packing type. In carbon capture, Mellapak structured packing, and IMTP random packing are commonly used ones [16].

3.2 Absorber Intercooling (AIC)

To decrease the reboiler duty and CAPEX, some process modifications are commonly applied in carbon capture studies. One of them is implementing absorber intercooling (AIC). In this modification, a part of the absorber's liquid flow is split, cooled to a temperature generally ranging from 20-60^{o}C and reinjected to the absorber which would cool the temperature inside the absorber and increase the absorption rate [17, 18, 19]. This efficient modification increases the capacity of the solvent, and as a result decreases the required regeneration energy by decreasing the needed solvent recirculation [19]. Hence, lower solvent recirculation will help reduce the size of the equipment. The process modification is shown in Figure 5.

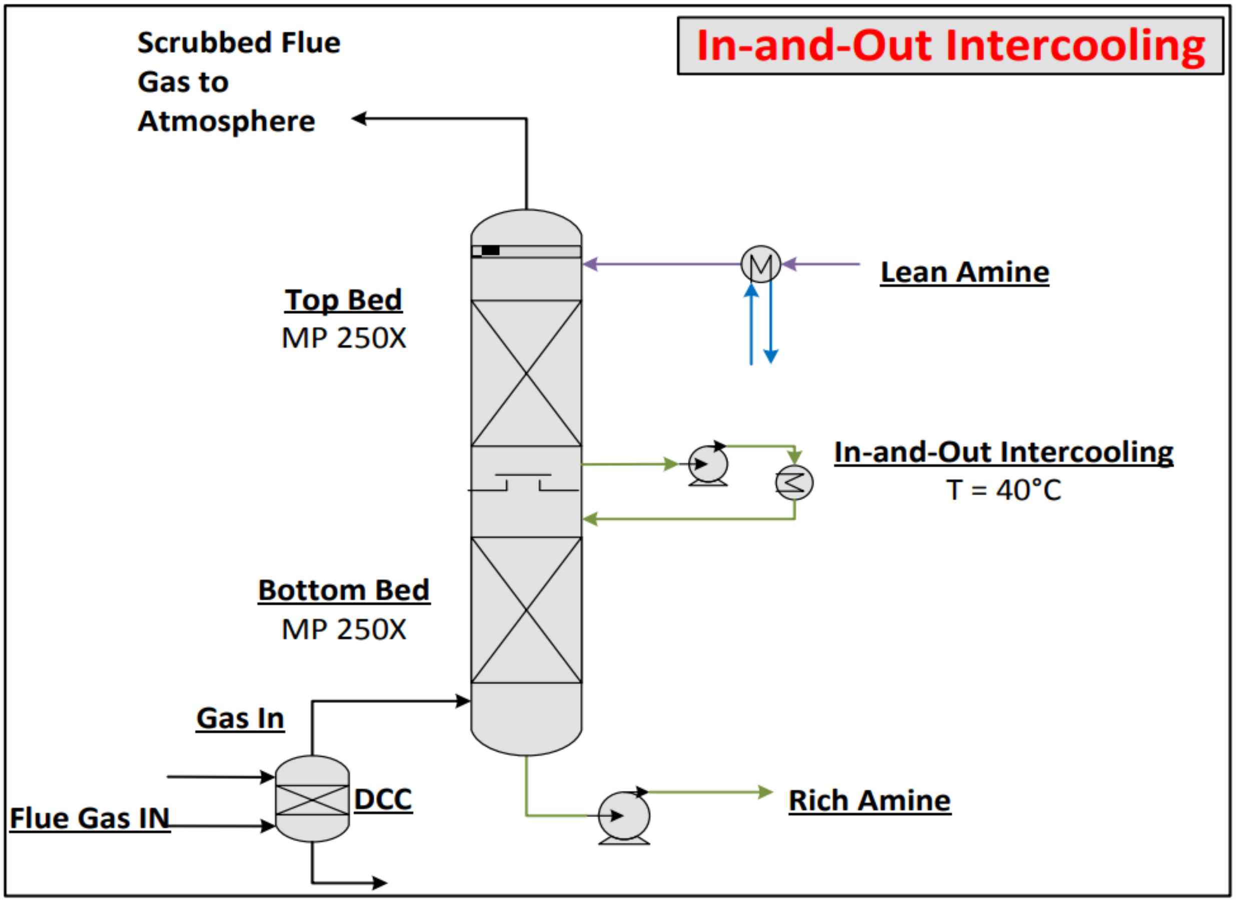

Figure 5: Absorber intercooler [19]

3.3 Lean Vapor Recompression (LVC)

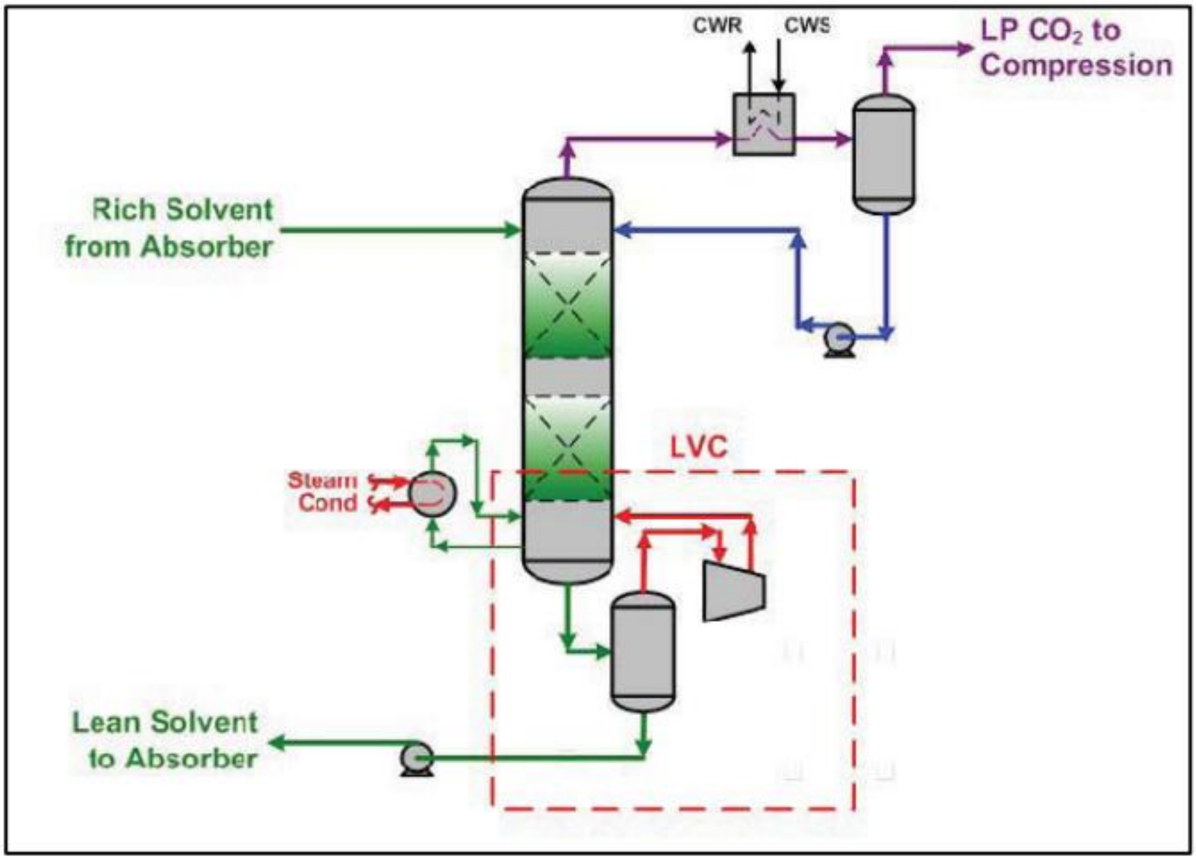

Figure 6: Lean vapor recompression [20]

Lean vapor recompression shown in figure Figure 6, is the other commonly used energy and cost reduction modification. The principle here is to flash the lean amine in the flash vessel at low pressures, then recompress this hot vapor to the stripper pressure as a process steam from the bottom of the stripper. The flashed liquid lean amine is sent to the lean pump for pressure adjustment before being fed to the lean/rich heat exchanger. The vapor mostly consists of H_2O and CO_2 [21]. As the recompressed vapor is at high temperature, it benefits the endothermic desorption process and reduces the reboiler duty and so SRD. However, the energy needed for compression should be considered to be able to make a comparison with the conventional case. This extra energy requirement is taken into account by presenting a new term called equivalent work. Equivalent work is calculated by the following formula [22];

$$W_{eq} = 0.75.\,Q_{reb}.\frac{(T_i + 10\ K - T_{sink})}{(T_i + 10\ K)} + W_{comp} \qquad 3.\ 1$$

To consider the increasing value of the steam, Carnot efficiency is used here. T_i refers to the reboiler temperature (K), Q_{reb} is the specific reboiler duty (GJ/t CO_2), T_{sink} is the Carnot engine's cold temperature which is set to 313 K, and W_{comp} is the compressor duty (GJ/t CO_2) [22].

3.4 Regeneration energy

Regeneration energy, shown by the correlation below, is defined as the sum of sensible heat, heat of desorption, and heat of vaporization.

$$Q_{reg} = \Delta H_{des} + Q_{sen} + Q_{vap} \qquad 3.\ 2$$

Heat of desorption, which is the same as heat of absorption in magnitude, is the amount of heat needed to decompose the byproducts of CO_2 – Amine reaction. Usually, the heat of absorption for the amines having the similar size and structure is in the order of primary amines>secondary amines> tertiary amines. Sensible heat is the heat required to change the temperature the solution without any phase change. Low specific heat capacity and density, and high cyclic capacity of the amine solution led to reduced sensible heat. The amount of energy required to provide stripping vapor by vaporizing the water in CO_2 rich solution is called heat of vaporization. Higher concentration of amine reduces the heat of vaporization however, the viscosity will increase. [6]

3.5 Amine solvents

Numerous organic and inorganic aqueous solvents are available for absorption-based PCC [23]. Nevertheless, mainly used solvents are the amine-based ones where the amine reacts selectively with the CO_2 [24]. Main properties a good absorption solvent should present are listed below [6]:

- Having high absorption capacity and reactivity with CO_2
- High CO_2 selectivity
- Should be easily regenerated
- Low corrosivity
- Low viscosity

- Intermediate boiling point and low vapor pressure
- Low melting point
- Chemical and thermal stability
- Low cost and high availability
- Low environmental impact

Solvent concentration depends on the viscosity and corrosivity of the solvent as well as the absorption capacity between the solvent and CO_2 [23].

Amine based solvents have been widely used both in pilot plants and in commercial processes [25]. They have been used in gas sweetening processes [6]. Their popularity comes from the fast reaction kinetics between amine and CO_2, high CO_2 absorption capacity, and easy regeneration [26]. Amines are Nitrogen containing organic molecules derived from Ammonia (NH_3),and depending on the number of Hydrogen atoms connected to the ammonia molecule, they can classified as primary, secondary and tertiary amines [6]. If one Hydrogen atom is replaced by and organic group, primary amine is formed RNH_2. If two and three are replaced then it is called secondary amine and tertiary amine, respectively [27]. Mono-ethanolamine (MEA) is the most widely used and studied organic aqueous solvent for absorption-based PCC. Besides that, 2-amino-2-methyl-1-propanol (AMP), (AMP), Piperazine (PZ), blends of AMP and PZ, Methyl-diethanol-amine (MDEA), Ethylene-diamine (EDA), and Diethanol-amine (DEA) are also being used. The properties of some amines are given in the below table.

Table 3:Properties of MEA [28] [29] [30]

Properties	**MEA**	**AMP**	**PZ**
Amine type	primary	primary	cyclic/secondary
Molar mass (g/mol)	61.08	89.13	86.14
Density (g/cm^3)	1.012	0.950	1.142
Solubility in water	soluble	insoluble	soluble

While selecting the amine solvent, compromise between CO_2 loading (will be explained in the following chapters) capacity, and reactivity should be considered. Primary amines are known as their fast reaction kinetics, but low CO_2 loading capacities limited by the stochiometric ratios [6] [25]. Tertiary amines, on the other hand, are characterized by their high CO_2 loading capacities but slow reaction rates leading to need of high absorber columns [6].Primary, secondary and tertiary amines have a significant heat of absorption which is a part of energy needed for regeneration of the solvent. Energy requirement for the solvent regeneration can be minimized by using solvent that have high heat of absorption by considering some parameters like stripper pressure [6]. Mixing different amines is another way to decrease the regeneration energy requirement [6].

3.5.1 Amine loadings

In amine-based post combustion carbon capture, amine loadings re important parameters as they represent the ratio of absorber carbon per moles of solvent. In carbon capture, two different amine loadings can be defined, lean loading and rich loading. The amine solvent which has been in contact with the CO_2 becomes rich in CO_2 and is called rich amine. It leaves the absorber from the bottom and the rich loading refers to the ratio of moles of CO_2 to the moles of amine in the rich amine stream. Similarly, the regenerated amine solvent leaving the stripper from bottom is called lean amine as it is lean in CO_2, and the lean loading refers to the ratio of moles of CO_2 to the moles of amine in the lean amine stream. Amine loadings are calculated from the formula given below.

$$\alpha = \frac{moles\ of\ CO_2}{moles\ of\ amine} \qquad 3.\ 3$$

The amine loadings depend on the stoichiometry of the reactive system. Primary amines, such as MEA, have lower amine loadings than secondary and tertiary amines. It is limited to 0.5 mol of CO_2 per mol of primary amine [31]. Secondary and tertiary amines can have loadings up to 1 mol of CO_2 per mol of amine [31]. As the rich loading indicates the amount of CO_2 absorbed by the amine, it is important to have as high amine loading as possible. Lean loading on the other hand, should be low as it represents the loading of CO_2 per mole of amine after the regeneration step.

3.5.2 Cyclic capacity

Cyclic capacity is one of the factors strongly affecting the energy demand. It is defined as the difference between the rich and lean loadings.

$$\Delta\alpha = \alpha_{rich} - \alpha_{lean} \qquad 3.\ 4$$

High cyclic capacity is important to achieve lower the sensible heat loss [32]. For good absorption and desorption of the desired product, the cyclic capacity of the solvent should be as high as possible. Having high cyclic capacity also plays an important role in the cost of the plant as smaller equipment will be needed with the solvent having high cyclic capacity. A study tested the cyclic capacities of different amines including different AMP+PZ blends, and MEA. Author tested the cyclic capacities of 30 wt% MEA, 30wt% AMP, 25 wt% AMP + 10 wt% PZ, and 25 wt% AMP + 10 wt% PZ at 3 kPa and 10 kPa. At both pressures, cyclic capacity of 30 wt% MEA was lower than AMP+PZ blends. [33]

Table 4: Cyclic capacities of MEA and CESAR-1 [33]

Cyclic capacity	30 wt% MEA	30wt% AMP	25 wt% AMP + 10 wt% PZ	25 wt% AMP + 10 wt% PZ
3 kPa	0.16	0.32	0.29	0.30
10 kPa	0.20	0.48	0.44	0.42

3.5.3 Monoethanolamine (MEA)

Monoethanolamine (MEA) is a primary alkanolamine with one alcohol and one primary amine group. MEA is a colorless to yellow liquid having mild ammonia-like smell [34]. It is known as 2-Aminoethanol with the chemical formula C_2H_7NO. Table 3 lists the properties of liquid MEA. MEA has been used in gas sweetening and gas cleaning processes for a long time due to its high availability and affordable cost [6]. As mentioned before, as MEA is a primary amine, it has fast reaction kinetics with CO_2 and, but its CO_2 loading capacity is limited to around 0.5 [6].

Although MEA is the most used solvent, it has some disadvantages. It is prone to thermal and oxidative degradation, and salt formation, and at high concentrations, it leads to corrosion [35]. Other disadvantages of MEA are the high regeneration energy requirement which has been reported to be in the range of 3.0-4.5 GJ/ton CO_2, accounting for 80% of the total energy consumption [35]. Thus, finding an alternative solution to overcome these problems is of great importance. Using improved/advanced solvents is one way of decreasing the possibility of these drawbacks.

3.5.4 Amino-2-methyl-1-propanol and Piperazine

Primary amine AMP (Amino-2-methyl-1-propanol) and secondary amine PZ (Piperazine) are the solvents used in carbon capture. Unlike MEA, AMP and PZ are often being used in blends with either each other or with other amine solvents such as MEA, MDEA, DEA.

CESAR-1 solvent has been developed under the European CESAR project. It has been found to show superior performance compared to MEA in terms of energy requirement, degradation rate, solubility, and corrosion [36] [37]. It is a mixture of sterically hindered amine AMP(Amino-2-methyl-1-propanol) and cyclic diamine PZ (Piperazine). Several blending ratios have been used in different studies. More detailed information about the literature studies done on blending ratio will be explained later.

Study done by Hasse et al [37] tested the solubility of CO_2 in CESAR-1 and MEA solvents at two different temperatures and represented it in partial pressure of CO_2 vs CO_2 loading plot. Figure 5 shows that CESAR-1 showed to have larger distance between the equilibrium curves meaning that the magnitude of desorption enthalpy is greater which will lead to need of lower regeneration energy and the solvent flow. Also, the solvent was found to capture the same amount of carbon with requiring lower SRD and lower L/G which is a way of indicating the amount of solvent used [37] .

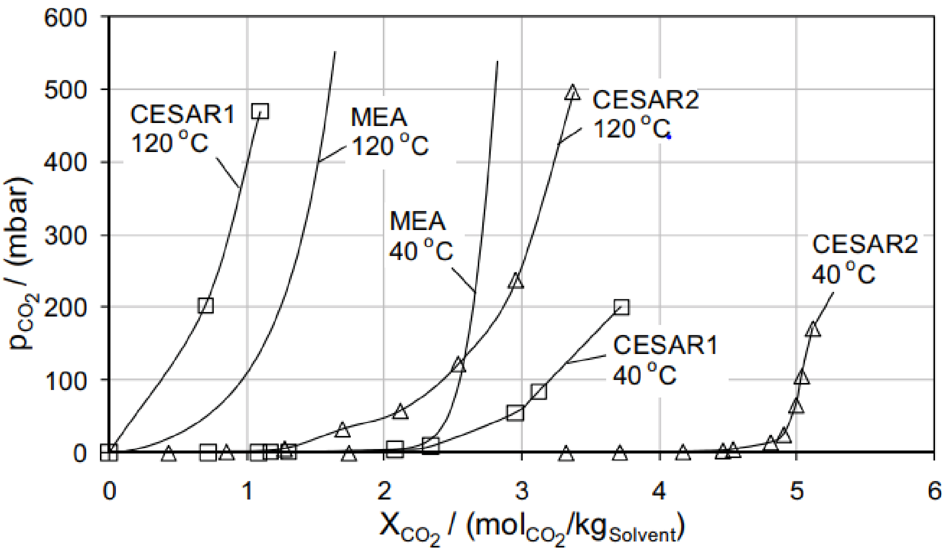

Figure 7:Calculated equilibrium data of CO2 solubility at different temperatures [37]

3.5.5 AMP + PZ blend ratio

As it has been already mentioned, CESAR solvent consists of AMP and PZ blend in different ratios. AMP is a sterically hindered amine having good absorption capacity, higher stability, and less energy requirement than MEA. However, its main disadvantage is the lower absorption capacity towards CO_2 [38] [39][4]. PZ is another promising solvent in CO_2 capture thanks to its fast kinetics with CO_2, less corrosivity, high absorption capacity [40]. On the other hand, its relatively small CO_2 loading range is its drawback and at lean loadings PZ hexahydrate is formed, and at rich loadings PZ carbamate hydrate is formed [40]. Nevertheless, combining g AMP and PZ has been found to improve AMP's CO_2 absorption performance [40]. In a study done by D.Tong et al, solubility study of CO_2 in different blend ration of AMP and PZ has been studied and compared to 30wt % MEA. In the study, 30wt % MEA, 30w t% AMP, 25wt % AMP + 5wt % PZ, 20 wt% AMP + 10wt % PZ have been compared [33]. Results showed that at 10 kPa, reducing AMP concentration from 30wt % to 25wt % by replacing it with 5wt % PZ reduced the cyclic capacity around 8% [33]. Even further replacing it with 5wt % more PZ (to 20 wt% AMP + 10wt % PZ), further reduced the cyclic capacity by 4.5wt %, yet it has been found to be higher than that of 30 wt% MEA [33] which indicates that the solubility of CO_2 and the absorption capacity of the solvent decrease with higher concentrations of PZ in the solution [33]. Dash et al. studied the CO_2 absorption in AMP + PZ blend and found that the solvent capacity of 25wt % AMP + 5wt % PZ is 0.623 at 313 K whereas that of 35wt % AMP + 5wt % PZ is 0.902 at the same temperature again indicating CO_2 solubility is affected by the PZ amount in the solution, and the higher concentrations of PZ gives smaller CO_2 solubility [41]. The same authors studied the enhancement factor for absorption of CO_2 and the absorption rate of CO_2. Results showed that enhancement factors for 40 wt% AMP, 2 wt% PZ + 38 wt% AMP, 5 wt% PZ +35 wt% AMP and 8 wt% PZ+32 wt% AMP have been found to be 83.0, 201.7, 290.3 and 347.9, respectively [41]. From these results, it could be concluded that the solubility of CO_2 decreases as the PZ amount increased at the solution however, enhancement factor increases with increasing concentration.

3.5.6 Degradation of amines

The absorber sump, cross heat exchanger, reboiler, and reclaimer are the primary regions where degradation occurs for any amine during post-combustion CO2 capture. This degradation is caused by thermal factors resulting from the high process temperature and oxidative factors due to dissolved oxygen and free radicals [42].

Degradation of MEA leads to foaming and corrosion which adds on the OPEX and make up costs [43]. At high stripper temperatures (above 200^0C) MEA experiences thermal degradation where carbamate polymerization is the main process [6] [43]. Irreversible reactions with CO_2 are also enhanced at elevated temperatures [6]. To prevent thermal degradation, low pressure steam is used so that the reboiler temperature is limited to maximum 135^0C [6]. Oxidative degradation, by which ammonia, organic salts, CO_2 and aldehydes are produced, occurs when O_2 is present in the flue gas [6]. Presence of organic acids in the solvent leads to irreversible ion formation known as heat stables salts (HSS) [6].

Even though the degradation products CESAR-1 solvent have not been extensively studied, numerous research studies have focused on proposing and assessing the degradation mechanisms of PZ and AMP independently in the literature. M. Campbell et al. [44] found that the degradation products of CESAR-1 are mainly 2,4-lutidine, DMOZD - 4,4-dimethyl-2-oxazolidinone, MNPZ - N-methylpiperazine, OPZ - 2-oxopiperazine, and Organic acids and heat stable salts. The same study compared the degradation products and degradation rates of MEA and CESAR-1, the results are shown in the figure below.

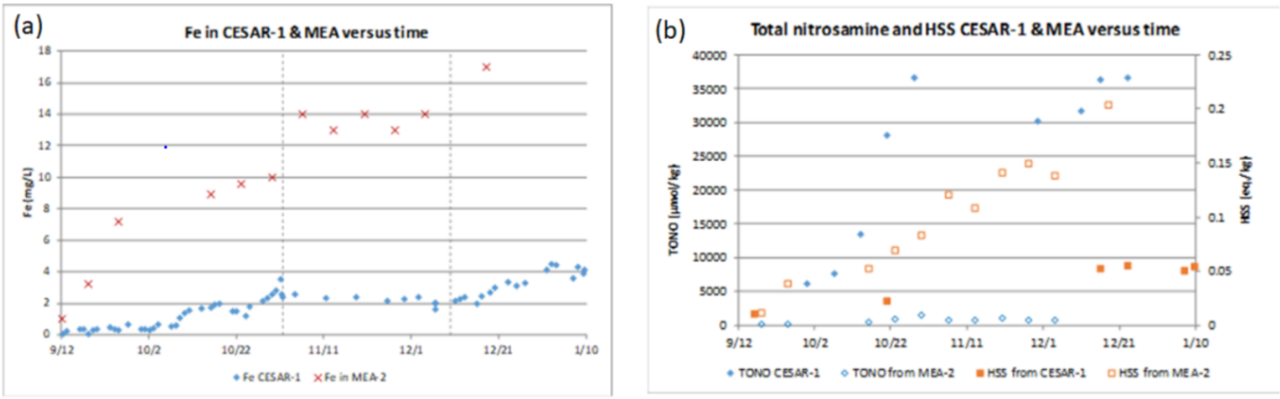

Figure 8: a) Iron concentration for CESAR1 and MEA and (b) Total nitrosamine and HSS for CESAR1 and MEA [44].

From figure 4 a) The authors discovered that CESAR-1 has a notably lower Fe concentration than MEA, which suggests that CESAR-1 undergoes less amine degradation due to oxidative and thermal factors [44].

The findings from figure 4 b) indicate that MEA undergoes considerably more degradation to heat stable salts than CESAR1, while the opposite trend is observed for total nitrosamines. In CESAR-1, the piperazine component functions as a secondary amine, making it highly susceptible to nitrosamine formation in the presence of NO_2. In contrast, MEA is a primary amine, resulting in a substantially lower rate of nitrosamine [44].

Piperazine and AMP are more stable than MEA. The solvent losses due to degradation of MEA is known to be around 1.5 kg per ton of CO_2. AMP has around 0.5 kg per ton of CO_2 degradation rate and that for PZ is around 0.05 kg/t CO_2 [45].

3.6 Chemistry of reactive system

Many studies have been done towards understanding the complex reaction mechanism between the amines and the CO_2 in carbon capture. Especially, the mechanism for MEA-CO_2-H_2O has been widely studied and three reaction mechanisms have been proposed. Zwitterion mechanism involves reaction of primary and secondary amines with carbon to produce zwitterion followed by carbamate formation by instantaneous neutralization of the intermediate by the base like amine, water, or hydroxyl group. A study by G. Hwang et al. [46] found that absorption and desorption of CO_2 reaction mechanism of involves two-step mechanism zwitterion formation [23]. The same study also found that interaction of zwitterion by the nearby water molecules strongly affect the relative probability between the carbamate formation and solvent regeneration [47]. Proposed mechanism is given by the below reactions.

$$CO_2 + RNH_2 \leftrightarrow RNH_2^+COO^- \qquad 3.5$$

$$RNH_2^+COO^- + RNH_2 \leftrightarrow RNH_3{}^+ + RNHCOO^- \qquad 3.6$$

The second proposal for this complex reaction mechanism. E. Silva et al. [48] found that zwitterion formation is through a third order single step reaction mechanism is more compatible for the reaction between given species, yet no stable zwitterion species has been formed. However, in this mechanism proton accepting species is the water molecule rather than MEA. Proposed mechanism is given by the following reaction. [48]

$$CO_2 + RNH_2 \ldots B \leftrightarrow RNHCOO^- \ldots BH^+ \qquad 3.7$$

Nevertheless, it is known that MEA in an aqueous solution has second order reaction rate [47]. The last proposed mechanism involves carbamic acid formation where one MEA molecule reacts with CO_2 to form carbamic acid, then carbamate is formed by further catalyzing the produced carbamic acid by another MEA molecule.

$$CO_2 + RNH_2 \leftrightarrow RNHCOOH \qquad 3.8$$

$$RNHCOOH + RNH_2 \leftrightarrow {RNH_3}^+ + RNHCOO^- \qquad 3.9$$

Among these proposed three mechanisms, the one with zwitterion formation is the most widely accepted one. A recent study found that the reaction between MEA and CO_2 changes by the loading. At low loadings, carbamate formation takes place by reversible reactions of MEA and CO_2, then $HCO_3^- \ or \ CO_3^{2-}$ are formed by hydration of CO_2 followed by carbamate hydrolysis at high loadings. [47]

Fast exothermic reaction between MEA and CO_2, shown by reaction 3.8 takes place at the low loadings where the absorption capacity of MEA is reported to be around 0.4 mol CO_2 /mol MEA. The same authors reported that as the pH decreased while the absorption capacity went up leading to higher CO_2 loading which led to CO_2 hydration.

$$CO_2 + H_2O \leftrightarrow H^+ + HCO_3^- \qquad 3.10$$

$$CO_2 + H_2O \leftrightarrow 2H^+ + CO_3^{2-} \qquad 3.11$$

The species present at the solution at high loadings would easily influence the carbamate and it is formed by either reaction of MEA and CO_2 or the reaction of MEA and HCO_3^-.

$$HCO_3^- + RNH_2 \leftrightarrow RNHCOO^- + H_2O \qquad 3.12$$

Another possibility at this point is the hydrolyzation of CO_3^{2-} into HCO_3^- followed by reaction with MEA to produce carbamate.

$$CO_3^{2-} + H^+ + RNH_2 \leftrightarrow RNHCOO^- + H_2O \qquad 3.13$$

It has been observed that the pH value of the solution decreased drastically at high loadings which lead to HCO_3^- formation by the reaction of carbamate with H^+.

$$RNHCOO^- + H^+ + H_2O \leftrightarrow HCO_3^- + RNH_2H^+ \qquad 3.14$$

The conclusion was that at very low pH and MEA concentration, the reverse reaction between MEA and CO_2 would be quite weak where carbamate would quickly degrade into carbamic acid by H^+.

Regeneration of the solvent is the reverse of absorption reaction which we have just discussed. This is done to desorb CO_2 from CO_2 rich MEA solution to recover the solvent. It is an endothermic process and heat must be supplied for desorption to happen. Firstly, carbamate is formed by heating the solution.

$$2H^+ + CO_3^{2-} \leftrightarrow CO_2(g) + H_2O \qquad 3.15$$

$$H^+ + HCO_3^- \leftrightarrow CO_2(g) + H_2O \qquad 3.16$$

$$2HCO_3^- + RNH_3{}^+ \leftrightarrow RNHCOO^- + 2H_2O + CO_2(g) \qquad 3.17$$

In the last step, MEA and CO_2 are produced by the decomposition of carbamate under thermolysis.

$$RNHCOO^- + H^+ \leftrightarrow CO_2(g) + RNH_2 \qquad 3.18$$

On the other hand, AMP and PZ blend is a novel solvent, and its the reaction mechanism is very complex with many reactions and species involved. AMP is a sterically hindered secondary amine which has unstable reversible carbamate formation. The proposed reaction mechanism with CO_2 is the same zwitterion mechanism accepted for primary amines [49].

$$CO_2 + AMP \leftrightarrow AMP^+COO^- \qquad 3.19$$

$$AMP^+COO^- + B \leftrightarrow AMP^+COO^- + BH^+ \qquad 3.20$$

$$CO_2 + 2AMP \leftrightarrow AMP^+COO^- + AMPH^+ \qquad 3.21$$

$$CO_2 + H^- \leftrightarrow +HCO_3^- \qquad 3.22$$

$$H_2O + AMP \leftrightarrow AMPH^+ + OH^- \qquad 3.23$$

The instability of the carbamate is associated with the steric effect of amine. Due to the instability of the carbamate formation, required regeneration energy is less [50].

A relatively new cyclic diamine and absorbent, PZ, is being used as a rate activator with AMP and with other widely used absorbents [51]. The reactions taking place between PZ and CO_2 are carbamate and bicarbamate formation which are listed below where B could be PZ, $PZCOO^-$ or PZH^+ [52].

$$CO_2 + PZ + B \leftrightarrow BH^+ + PZCOO^- \quad 3.24$$

$$CO_2 + PZH^+ + B \leftrightarrow PZCOO^- + BH^+ \quad 3.25$$

$$CO_2 + PZCOO^- + B \leftrightarrow BH^+ + PZ(COO^-)_2 \quad 3.26$$

3.7 <u>Rate based simulation</u>

Many process simulators have been used for modeling CO_2 capture process including Aspen HYSYS, Aspen Plus, COSIM, ProMax, Pro/II. These simulations use rate-based approach meaning that the separation is calculated based on heat and mass transfer equations coupled with reaction kinetics [53]. Two-film theory, proposed by Whitman and Lewis [54] is used to explain the mass transfer at steady state. Graphical representation of the two-film theory is shown in the following figure [55].

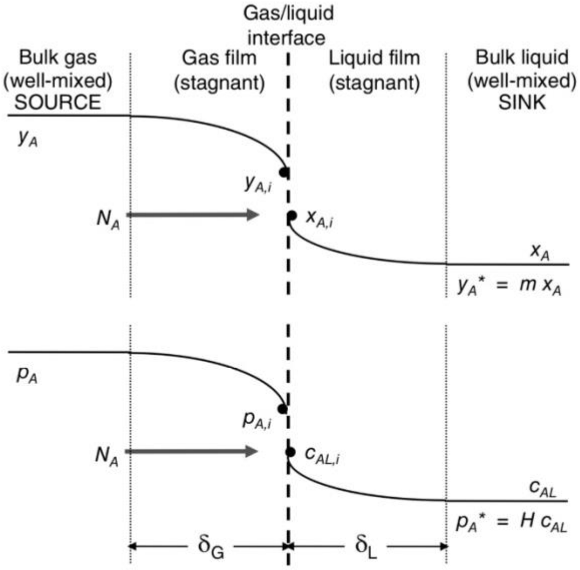

Figure 9: Two-film theory [55]

This theory assumes that the liquid and the gas phases are divided into two distinct regions, bulk and the film. Two main assumptions are accepted by this theory: (1) the rate of diffusion is controlling the mass transfer through each phases, (2) the diffusing component diffuses without any resistance. The driving force for the mass transfer is the concentration difference of the bulk gas and liquid phase. Also, there is the partial pressure gradient from the gas bulk phase to the interface as well as the concentration gradient from the liquid bulk phase to the interface. Based on the second assumption gas and liquid phases are assumed to be in equilibrium at the interface as no resistance to the mass transfer is assumed [55].

If a gas mixture carrying solute A (A is CO_2 in carbon capture) and a liquid phase containing dissolved solute A is assumed, the mass transfer flux through the film is explained bythe following equations at the steady state [55];

$$N_A = k_G.(p_A - p_{A,i}) \text{ in the gas film and} \tag{3. 27}$$

$$N_A = k_L.(C_{AL,i} - C_{AL}) \text{ in the liquid film} \tag{3. 28}$$

where k_G $(\frac{moles\ of\ A\ transferred}{time * interfacial\ area * pressure})$ and $k_L$$(\frac{moles\ of\ A\ transferred}{time * interfacial\ area * concentration})$ stand for the convective mass transfer coefficients in the gas phase and in the liquid phase, respectively.

As mentioned before, the driving force for the mass transfer in the gas phase is the partial pressure gradient. Concentration difference in the liquid phase allows mass transfer to continue from the liquid interface to liquid bulk phase. These driving forces are shown in the figure below by the short arrows. Mass transfer from gas to liquid is represented by the part above the equilibrium line, whereas from liquid to gas phase is represented by the part below the equilibrium line [55].

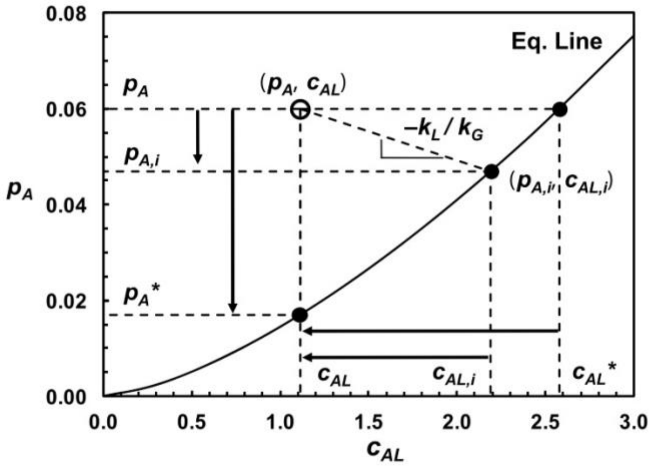

Figure 10: Mass transfer driving forces in terms of partial pressures and concentrations [55]

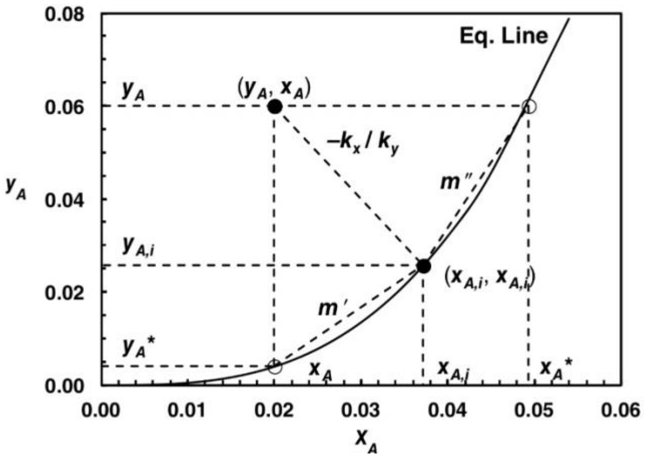

Figure 11: Mass transfer driving forces in terms of mole fractions [55]

At the steady state, the mass transfer fluxes from each phase should be equal. Hence, the following equation is obtained.

$$N_A = k_G.\left(p_A - p_{AL,i}\right) = -k_L.\left(C_{A,L} - C_{AL,i}\right) \quad 3.29$$

And the following mass transfer coefficient ratio is obtained;

$$-\frac{k_L}{k_G} = \frac{p_A - p_{AL,i}}{C_{A,L} - C_{AL,i}} \quad 3.30$$

Fluxes can also be written in the form of mole fractions.

$$N_A = k_y.\left(y_A - y_{A,i}\right) \quad 3.31$$

$$N_A = k_x.\left(x_{A,i} - x_A\right) \quad 3.32$$

At the steady state;

$$N_A = k_y.\left(y_A - y_{A,i}\right) = k_x.\left(x_{A,i} - x_A\right) \quad 3.33$$

And the mass transfer coefficients ratio would be;

$$-\frac{k_x}{k_y} = \frac{y_A - y_{A,i}}{x_A - x_{A,i}} \quad 3.34$$

Interrelationship between the mass transfer fluxes then can be obtained:

$$N_A = k_y.\left(y_A - y_{A,i}\right) = k_G.\left(y_A - y_{AL,i}\right) = k_G P.\left(y_A - y_{AL,i}\right) \quad 3.35$$

$$N_A = k_c.\left(C_A - C_{A,i}\right) = k_y.G\left(y_A - y_{A,i}\right) = k_y \frac{P}{RT}.\left(y_A - y_{A,i}\right) \quad 3.36$$

At low concentrations Henry's law can be used to express the linear equilibrium.

$$p_A = H.C_{AL}^{*} \quad 3.37$$

$$p_A{}^{*} = H.C_{AL} \quad 3.38$$

Flux can also be written in the form of mole fractions at the gas and liquid phases

$$N_A = K_y.\left(y_A - y_A^{*}\right) \quad 3.39$$

$$N_A = K_x.\left(x_A^{*} - x_A\right) \quad 3.40$$

4 Literature study

This section will mainly focus on the studies done on carbon capture to give an overview about the status of PCC, and the important parameters affecting the capture rate, capture efficiency, specific reboiler duty, and CAPEX. Although there are many different factors affecting those properties, based on deep literature study the studied parameters are found to be the major ones. These parameters are;

- Liquid to gas ratio (L/G); SRD and CAPEX are expected to decrease by increasing L/G.
- Absorber feed temperature; SRD and CAPEX are expected to increase by increasing temperature
- Stripper pressure; SRD and CAPEX are expected to decrease by increasing stripper pressure.
- Minimum temperature difference in the lean/rich heat exchanger; SRD and CAPEX are expected to increase by increasing minimum temperature difference.
- Absorber and stripper height; SRD and CAPEX are expected to decrease by increasing absorber and stripper height.

4.1 Specific reboiler duty (SRD)

Specific reboiler duty is one of the most important parameters in carbon capture. It is defined as the energy required to capture a specific amount of carbon, and generally is it formulated as:

$$SRD = \frac{reboiler\ duty}{\dot{m}_{CO_2,inlet} * capture\ rate} \qquad 4.\ 1$$

Where $\dot{m}_{CO_2,inlet}$ stands for the mass flow rate of CO_2 in the inlet flue gas in *tons/h*, reboiler duty is measured in *GJ/h* ,and the capture rate is the percentage of carbon captured from the flue gas, therefore SRD is represented in GJ/t CO_2. Representation in different units is also possible such as GJ/t CO_2, MJ/kg CO_2, and kJ/kg CO_2. As mentioned before, high SRD is a major problem associated with PCC. There have been studies done to minimize the duty whilst maximizing or remaining with same the efficiency and the capture rate.

E. Sanchez [45] made a comparative study between novel solvent 23 wt% AMP + 12 wt% PZ (CESAR-1) and conventional MEA. The process was modelled in Aspen Plus, with 1.1 bar absorber pressure, 1.8 bar stripper pressure, and constant removal rate at 90%. She investigated the performance of these solvents for Advanced Supercritical Pulverized Coal (ASC) power plant, and Natural gas Combined Cycle (NGCC) power plant in technical, thermodynamical, and economical way. Reported energy demand for ASC case is 4.16 GJ/t CO_2 to 3.07 GJ/t CO_2 with benchmarking solvent and novel CESAR-1 solvent respectively which accounts for 25% reduction. The reduction for NGCC design is reported to be 12%, from 3.36 GJ/t CO_2 to 2.94 GJ/t CO_2 by moving from MEA to CESAR-1.

Pilot plant experiments have done by H. Hasse et al. [13] where two novel solvents, namely CESAR-1 and CESAR-2 have been tested with respect to MEA which is reported to give 4.1 GJ/t CO_2 SRD. The pilot plant consisted of 4.25 m absorber, 2.55 m stripper with 0.125 m diameter for both. The details of the solvents are given in the table below. The flow rate of the flue gas varied from 30 to 110 kg/h with CO_2 partial pressure ranging from 35-135 mbar at a constant removal rate of 90%. At optimum solvent flowrate and flue gas flow rate, new solvents showed improvements in the SRD reduction, CESAR-1 giving 3.3 GJ/t CO_2, and CESAR-2 giving 3.3 GJ/t CO_2.

Table 5: Details of the solvents [13]

Solvent	Composition
MEA	30 wt% MEA, 70wt % water
CESAR-1	28wt% AMP, 17wt% PZ, 55 wt% water
CESAR-2	32 wt% EDA, 68 wt% water

W. Zhang et al. [18] studied the performance of a novel solvent blend of AMP + PZ for PCC from coal fired power plant, and the process modeling was made in Aspen Plus. They found that the reboiler duty could be lowered by increasing the stripper pressure, decreasing the capture rate, and increasing the AMP amount in the solvent. The lowest reboiler duty of 3.18 GJ/t CO_2 was achieved with 23 wt% AMP + 17wt% PZ at 90% removal rate. They have also implemented process modifications such as absorber intercooling (ICA), lean vapor compression (LVC), and rich solvent split (RSS). By these implementations, they reported decrease in the reboiler energy demand of 0.497 GJ/t CO_2 at 40ºC cooling temperature, 0.521 GJ/t CO_2 at 1.5 atm flash pressure, and 0.488 GJ/t CO_2 at 0.3 split fraction. Respectively, these accounted for 6.7%, 2.7%, and 8.5% reduction in reboiler energy demand [18]. Increasing the concentration of AMP will influence the reaction rate resulting in increased cyclic capacity of the solvent [51]. Hence, the required reboiler duty will be lower as a result of lower sensible heat requirement of the desorber [51].

4.2 Liquid to gas ratio (L/G)

Liquid to gas ratio is the indication of required solvent recirculation for the desired capture rate. It is most often defined as the total mass flowrate of the solvent divided by the total mass flowrate of flue gas being fed to the absorber. It has a direct effect on the reboiler duty, however, the optimum L/G ratio depends on the used solvent, design properties such as the capture efficiency, and [56] the flue gas properties. H. Hasse [13] has compared the L/G ratios for CESAR solvents and MEA in the range of 0.94-3.5. At high partial pressures of CO_2, optimum L/G ratio for CESAR have been found to be 1.4 corresponding to regeneration energy of 3.3 GJ/tCO_2, and for MEA L/G=2.5 with 4.1 GJ/tCO_2 [13]. Tönnies et al. [57] have found that the optimum L/G for CESAR-1 is around 2.3 with around 3 GJ/tCO_2 energy demand, and for MEA those are around 3.3 and 3.6 GJ/tCO_2 respectively. Another study done by J.Knudsen et al. [17] under CESAR project to reduce the carbon capture cost compared different L/G ratios for the same solvents in the range of 1.5-4.0. The authors reported the optimum L/G ratio for CESAR-1 to be 2.0 with 3.05 GJ/tCO_2, for CESAR-2 to be around 2.25 with 3.5 GJ/tCO_2 and those for MEA to be around 2.7 and 3.60 GJ/tCO_2 respectively.

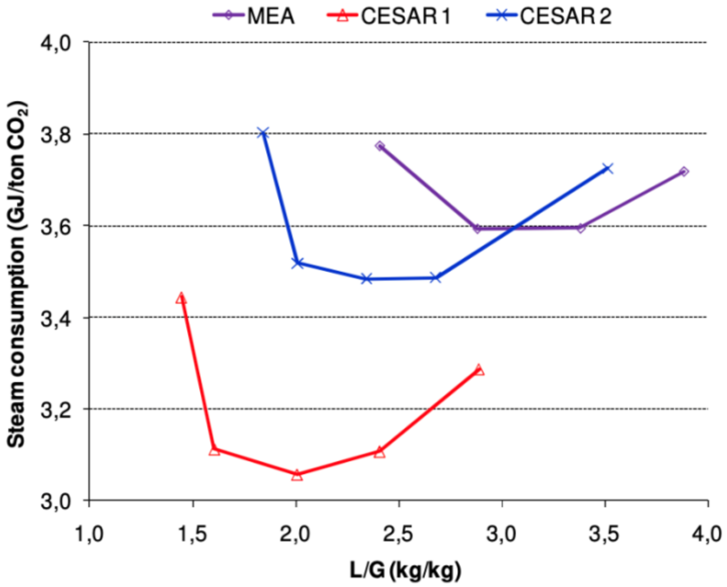

Figure 12: Steam consumption for different solvents vs L/G [17]

The same authors investigated the effect of lean vapor compression and absorber intercooling. The results indicated that with lean vapor compression, the reboiler duty of the conventional 30 wt% MEA process could be reduced from 3.6 to 2.8 GJ/t CO_2. Applying absorber intercooling at 25°C allows saving 0.2 GJ/t CO_2 which accounts for saving 7% of steam consumption [17].

S. Manjare et al. [58] investigated the effect of L/G ratio on the overall carbon absorption for PCC. The simulation studies were performed with 30 wt% MEA at different CO_2 concentrations in the flue gas ranging from 0.85 to 0.95 with 318K flue gas temperature with 30 theoretical stages. Table below summarizes the effect of L/G on overall carbon absorption.

Table 6:Effect of L/G on overall carbon capture [58]

L/G ratio	Inlet CO_2 concentration	Outlet CO_2 concentration
2.0	0.95	0.31
4.5	0.95	0.185
8.5	0.92	0.039

As the L/G is increased from 2.0 to 8.5, overall carbon absorption also increases, resulting in reduction of outlet CO_2 concentration from 0.31 to 0.039 at the absorber outlet. Similarly, W. Zhang et al. [18] reported optimum L/G ratios giving the lowest SRD by optimizing the effect of L/G ratio for different AMP + PZ blends. The optimum L/G ratios for different amine blends lie in the range of 1.5 to 2.5 giving required SRD ranging from 2.75 to 3.25 GJ/t CO_2. From the figure below, as the PZ concentration increases, the SRD at optimum L/G ratio increases, too. The reason for that is the loading capacity of AMP being higher than that of PZ. Therefore, using more PZ would increase the regeneration energy needed 28 wt% AMP + 17 wt% PZ.

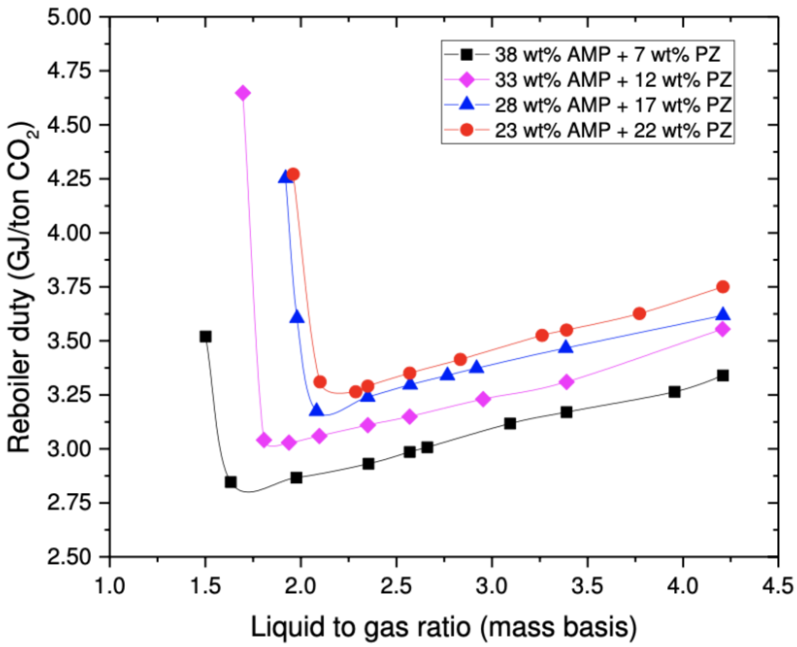

Figure 13: Different blends of AMP + PZ and optimum L/G ratio

4.3 Flue gas temperature/ Absorber inlet temperature

Flue gas temperature is an important parameter affecting the capture efficiency and capture process. The process where the amines are used as solvent medium, lower temperature are more effective than higher. Amines have high affinity towards CO_2 at low temperatures. As the absorption reaction of CO_2 in amines is exothermic, better results are obtained at lower temperatures, please see the reaction below [59].

$$2R - NH_2 + CO_2 \rightarrow R - NH_3^+ + R - NHCOO^- + Heat \qquad 4.\,2$$

$$R - NH_2 + CO_2 + H_2O \rightarrow HCO_3^- + R - NH_3^+ + Heat \qquad 4.\,3$$

These reactions will cause the absorber temperature to rise up to 340 K [59]. Also, higher temperatures will lower the viscosity of the fluid and limit the mass transfer as the fluid will flow faster through the absorber column, resulting in shorter contact time with the flue gas.

Due to the high temperatures in the absorber, emissions could take place in the form of gas-phase emissions or aerosols. Gas phase emissions depend on the volatility of the solvent, and as the temperature increases, volatility increases too. These can be prevented by implementing a water wash system. On the other hand, aerosols are harder to capture due to their sizes. Therefore, they have been a major problem related to temperature increase in the columns [60].

A. Andreasen (Andreasen, Optimisation of carbon capture from flue gas from a Waste- to-Energy plant using surrogate modelling and global optimisation , 2021) has optimized the parameters affecting the performance of a Carbon Capture from flue gas with MEA from Waste to Energy plant. He has investigated the performance in the flue gas range of 40-50ºC and has found 40 ºC to be the optimum (Andreasen, Optimisation of carbon capture from flue gas from a Waste- to-Energy plant using surrogate modelling and global optimisation , 2021). G. Leonard [62] reported the absorption temperature of CO_2 to be in the range of 40-60 ºC [62]. H. Hasse et al. [13] made a comparative study between amine-based solvents, MEA, CESAR-1, and CESAR-2, at the absorber temperature of 47 ºC at a constant removal rate of 90%.

4.4 **Stripper pressure**

Operating pressure of a stripper has a direct effect on the reboiler duty and the reboiler temperature [22]. Regeneration process is the reverse reaction of absorption reaction(s), meaning that the higher temperature will favor the reaction and will require less heating input from reboiler. An increase in the absorber pressure results in a higher temperature in the reboiler, thus lowering the reboiler duty [6]. However, as temperatures higher than 135ºC will cause solvent thermal degradation, and due to the higher temperature in the reboiler, high pressure steam would be needed to supply the heat demand [6, 22]. Therefore, a compromise should be made to find the optimum operating pressure [6].

Xue at al. [22] investigated the stripper pressure effect on the reboiler duty in the range of 0.7-2.2 bar and found higher pressures being more beneficial for saving total energy requirement. From lower end to upper end, reboiler duty was reduced by 0.05 GJ/t CO_2 [22]. A. Andreasen (Andreasen, Optimisation of carbon capture from flue gas from a Waste- to-Energy plant using surrogate modelling and global optimisation , 2021) found the optimum value based on his investigations on the stripper pressure in range of 1.5-3.0 bar. Stripper pressure around 1.83-1.85 bar was found to be the optimal range for post combustion carbon capture from flue gas from waste to energy plant. S. Warudkar et al. [63] has studied the influence of stripper pressure on the process of PCC with amine solvent in the pressure range of 1.5-3.0 bar in ProMax. It was reported that bigger stripper columns are needed at lower pressures, which would increase CAPEX. This is due to the increased steam volumetric flow rate coupled with the increase in the ratio of partial pressure of water to that of CO_2 would lead to the need of larger diameter in the stripper column [63]. C. Nwaohaa et al. [64] performed a techno-economic evaluation on PCC from a cement plant with AMP-PZ-MEA blend with in ProMax v 4.0 1.7 bar stripper pressure. For 90% capture rate, the reboiler duty was found to be 3.86 GJ/t CO_2 with 128 million US $$ CAPEX [64]. W. Zhang et al. [18] investigated the stripper pressure effect on the performance of AMP+PZ blends in 0.75-3.0 atm pressure range and found that the reboiler duty decreases with increasing stripper pressure.

4.5 Absorber and stripper packing height

Absorber and stripper packing height or total height of the absorber and stripper columns have effect on the mass transfer thus on the carbon capture rate and reboiler duty. Bigger columns allow for more residence time in the column, therefore it could be beneficial for the mass transfer. However, weeping possibility should also be kept in mind as the bigger columns might result in weeping if the vapor flow is less than adequate. As the absorber height decreases, the solvent flow rate increases in the absorber. This increased solvent flow affects the size of the lean/rich heat exchanger due to the change of the amine flow rate [65].

X. Luo et al. [66] reported that the packing height of absorber ranges in 13.6m to 30.5m, that for stripper ranges in 7.6 m to 28.15 m in carbon capture. O. Kallevik performed sensitivity analysis to see the effect of absorber height on the cost and reboiler duty. The analysis was performed in the 14-23 m range for 90% removal rate. Although the smallest reboiler duty, 3.5 GJ/t CO_2 was obtained at the higher end, with 19 m the optimum NPV is achieved [67]. In another study done by S. Shirdel, the optimum absorber height was found as 19 m for the flue gas having 7.5 mol% CO_2.The sensitivity analysis was performed in 18-24 m range with EDF and Power Law methods, and the lowest cost was obtained at 19 m 37.3 EUR/t CO_2 and 37.1 EUR/t CO_2, respectively. The lowest reboiler duty of 3.48 GJ/t CO_2 was obtained at 24 m [65]. C. Nwaohaa et al. [64] used a stripper with Melapak 250 Y packings and height of 15.85 m to capture carbon from a cement plant flue gas with 90% capture efficiency with MEA. To capture the same amount of carbon with AMP-PZ-MEA blend, required the stripper height was 9.14 m. Calculated total cost for MEA design was estimated as 147 Million $$ whereas that of AMP-PZ-MEA was estimated as 128 Million $$ [64]. U. Arachchige et al. [68] varied the stripper height for the carbon capture, from 500 MW gas -fired power plant, from 14 m to 22 m and observed that the reboiler duty is slightly decreasing as the stripper height increases. The decrease is around 0.02 GJ/t CO_2 from the upper end to the lower end [68].

4.6 Minimum end temperature approach

Minimum end temperature approach in the lean/rich heat exchanger is found to influence the reboiler duty and the cost of the plant as it has a direct effect on the heat transfer area. Heat transfer area is calculated by the heat transfer coefficient, log mean temperature difference, and the heat duty of the heat exchanger [69]. Smaller minimum temperature difference will minimize the utility cost but the area needed for the same amount of heat to be transferred would be bigger. Therefore, bigger heat exchanger would be needed for smaller minimum temperature difference [69]. S. Shirdel et al. [65] conducted a sensitivity and cost analysis in Aspen HYSYS to find the optimum minimum temperature approach for MEA based carbon capture process with two different methods, namely Power Law method and Enhanced Detailed Factor method. The used minimum temperature approach range was 5.5-15 ^oC, and the results showed that the minimum cost was obtained at $\Delta T_{min} = 15^oC$ [65] in both methods. Another study done by A. Andreasen found the optimized value for minimum temperature approach in the range of 5-15 ^oC. At 2.2 L/G ratio, and 1.85 bar desorber pressure, the optimum minimum temperature difference was found as 5^oC (Andreasen, Optimisation of carbon capture from flue gas from a Waste- to-Energy plant using surrogate modelling and global optimisation , 2021). E. Fernandez [45] found that at $\Delta T_{min} = 5^oC$, the reboiler duty of PCC with MEA is 4.16 GJ/t CO_2 with 163 million Euro of total cost, while the same with CESAR-1 is 3.07 GJ/t CO_2 with 146 million Euro of total cost of the plant. S. A. Aromada et al [69] studied the optimum type of heat exchangers for PCC capturing simulated in Aspen HYSYS to capture 85%. Based on their findings, the minimum CAPEX is obtained at $\Delta T_{min} = 15^oC$ for plate heat exchangers, and at $\Delta T_{min} = 20^oC$ for shell and tube heat exchangers with 65 million Euros and 80 million Euros, respectively.

4.7 Summary

To sum up all what has been discussed, L/G ratio, absorber inlet temperature, stripper pressure, minimum temperature difference in the lean/rich heat exchanger, absorber and stripper height are main parameters affecting the reboiler duty and the cost of carbon capture. Specific reboiler duty of MEA has been reported in 3.0-4.5 GJ/t CO_2 range, whereas that for AMP+PZ blends is reported in a lower range from 2.5-3.5 GJ/t CO_2. Higher L/G ratio has a positive effect in the energy and cost savings but too high ratio might lead to a higher reboiler duty. Therefore, the optimum range for MEA and AMP+PZ blends should be around 1.5-4.0. Absorber feed temperature around 40-50^{o}C seems to be suitable for the absorption as anything higher would favor the backwards reactions, also thermal degradation and aerosol emission would be in question. Most studies reported minimum temperature difference to be effective in decreasing the lean /heat exchanger to decrease the reboiler duty. Nevertheless, higher CAPEX will be the problem with too low temperature difference bigger size equipment would be needed as the heat transfer area required will be higher. Thus, the effect of ΔT_{min} should be investigated in the range of 5-15 ^{o}C. Stripper pressure in the range 1.5-3.0 bar is reported to be the suitable range for desorption process. Very high pressures will cause absorber temperature to rise, and high pressure steam would be required to satisfy the steam requirement. And finally, absorber and stripper height in the range of 10-30 m would be a suitable range for the capture process.

5 Problem Statement

Carbon capture is not an entirely brand-new technology, it has been in research and operation in pilot scale since 1938, and the first commercial large scale carbon capture plant was built in Norway in 1996 [70]. However, some challenges associated with large scale carbon capture plants such as high regeneration energy requirement, high CAPEX, solvent loss, degradation of solvent and environmental impacts are the main concerns. Due to these concerns, carbon capture is currently not applied to the fossil fuel fired and energy intensive industries in big scales. Among the current technologies, post-combustion carbon capture is the most promising and the most studied one. It involves capturing the carbon from flue gas in the absorber by using amine-based solvent. Then, the rich solvent is regenerated in the stripper where extensive amount of energy is needed for the regeneration of the solvent. Regenerated solvent is sent back to the absorber after it is blended with make-up solvent. Currently, research has been going on in order to decrease the reboiler duty, one way of doing this is using improved solvents. Monoethanolamine (MEA) is the most commonly used state-of-art solvent in absorption bases carbon capture. Process with aqueous solution of 30 wt% MEA is reported to require around 4.2 GJ/tCO_2 energy input [13]. Being prone to thermal and oxidative degradation, and solvent losses are other major disadvantages of MEA. During CESAR project promising, novel solvents have been developed [71]. CESAR-1 solvent is an aqueous solution of 2-amino-2-methyl-propanol (AMP) and piperazine (PZ). Based on many studies, it can be concluded that the AMP+PZ, namely CESAR-1 solvent, is a promising solvent to overcome these drawbacks of MEA. Then, one can ask the following question:

In which operating conditions, and specifications will CESAR-1 solvent with respect to MEA give the lowest reboiler duty and the cost while capturing 90% of CO_2 from flue gas from coal fired power plant?

The objective of this master thesis is to evaluate the performance of CESAR-1 solvent (19 wt% AMP + 9 wt% PZ) in technical and economical point of view with respect to simple MEA solvent. Absorption based post combustion carbon capture process has been studied and the process will be modelled in commercial process simulation software ProMax$^{®}$ V6 by Bryan Research and Engineering. As preliminary studies, the performance of CESAR-1 in pilot plant scale will be evaluated. Energy and cost reduction modifications, absorber intercooling, and lean vapor recompression will be implemented, and the results will be validated by Esbjerg PCC Pilot Plant.

The results from MEA case and CESAR-1 case will then be analyzed and compared. Then, while scaling up, real flue gas data from a coal fired power plant will be used. Sensitivity analysis with 6 different process parameters which include mass-based L/G ratio, absorber feed temperature, stripper pressure, minimum temperature approach, absorber height, and stripper height will be conducted. Scenario tool feature of ProMax will be used for sensitivity analysis. CAPEX and OPEX for each case in the sensitivity analysis will be estimated. For the CAPEX estimation, CAPEX tool provided by Rambøll will be used, and based on CAPEX, OPEX estimations will be made. All the results from sensitivity analysis and cost analysis will be investigated and compared between MEA and CESAR-1 case.

6 Esbjerg Post-combustion Carbon Capture Pilot Plant

Under EU FP7 CESAR (CO_2 Enhanced Separation And Recovery) project, CO_2 capture has been studied to investigate the low-cost post combustion CO_2 capture. Esbjerg pilot plant receives flue gas by slip stream from 400 W pulverized Coal-fired power plant where it is located at [72]. Power plant is owned by Dong Energy Generation. The conventional amine-based absorbing/desorbing process is used at the pilot plant. In the first year of the plant, 2006, two 1000 h campaigns were conducted with simple 30 wt% MEA solvent [72]. Flow diagram of Esbjerg Post Combustion Carbon Capture (PCC) pilot plant is shown in the Figure 14. Flue gas is taken by the slipstream right after SO_2 scrubbing without any pre-treatment. Flue gas information is given in table Table 7. Flue gas is saturated with steam and fed to the absorber at 47^0C and 1.01325 bar from the bottom of the absorber, and it gets into contact with the amine solvent in counter current flow. Absorber consists of four packed bed each having 4.25 m packing height filled with Mellapak 2X structured packing, and 1.1 m section diameter. Before each bed, a liquid distributor plate is placed to maintain even liquid flow. There is a fan placed at the bottom of the absorber to ensure absorber operates at slightly above the atmospheric pressure. Samples are taken from the bottom of the absorber to monitor the CO_2 content. Absorber has a 3 meter water wash bed filled with Mellapak 250Y. Liquid for water wash is collect from the bed right below the water wash bed, and it is cooled down by water-cooler before it is recycled back to the wash bed. Amine build-up is control by adding make up water. [72]

Table 7: ESV Flue Gas Characteristics [73]

Parameter	Design value
Flue gas composition	<10 ppm SO_2, <65 ppm NO_x, <10 mg/Nm^3 dust, N_2: 76 mol%, CO_2: 13 mol%, O_2: 11 mol%
Temperature (^{0}C)	47
Flue gas flow (Nm^3/h)	5000 (0.5% of Esbjergvaerket flue gas)

Table 8: Esbjerg Pilot Plant Characteristics [72] [73]

Parameter	Design value	Unit
CO_2 Capture	1000	kg/h
Removal Rate	90%	
Maximum Solvent Flow	40	m^3/h
Solvent	30% MEA	wt
	19% AMP & 9% PZ	wt

Treated gas leaves the absorber from the top while CO_2 rich amine leaves the absorber as bottom product and is pumped to the counter current plate heat exchanger through two parallel mechanical filters to be heated by the lean amine. The stripper consists of two sections each 5 m in height, having 1.1 m diameter, and filled with IMTP 50 random packing. A pressure regulation valve is used to set the pressure of the stripper. A water wash bed is installed to the stripper with 0.8 m diameter, 3 m height, and IMTP 50 random packing. Reboiler operates with 2.5 bar(g) saturated steam which is supplied by Esbjergvaerket (ESV). Separated CO_2 and vapor are collected from the top of the tower and cooled in water cooled condenser before they are further separated in in liquid/gas separator. Almost pure CO_2 is sent back to ESV flue gas duct while the separated liquid is recycled back to the stripper wash section. Bottom product of the stripper, lean amine, is cooled in counter current plate heat exchanger, where the cold stream is rich amine, before being recycled back to the absorber. [72]

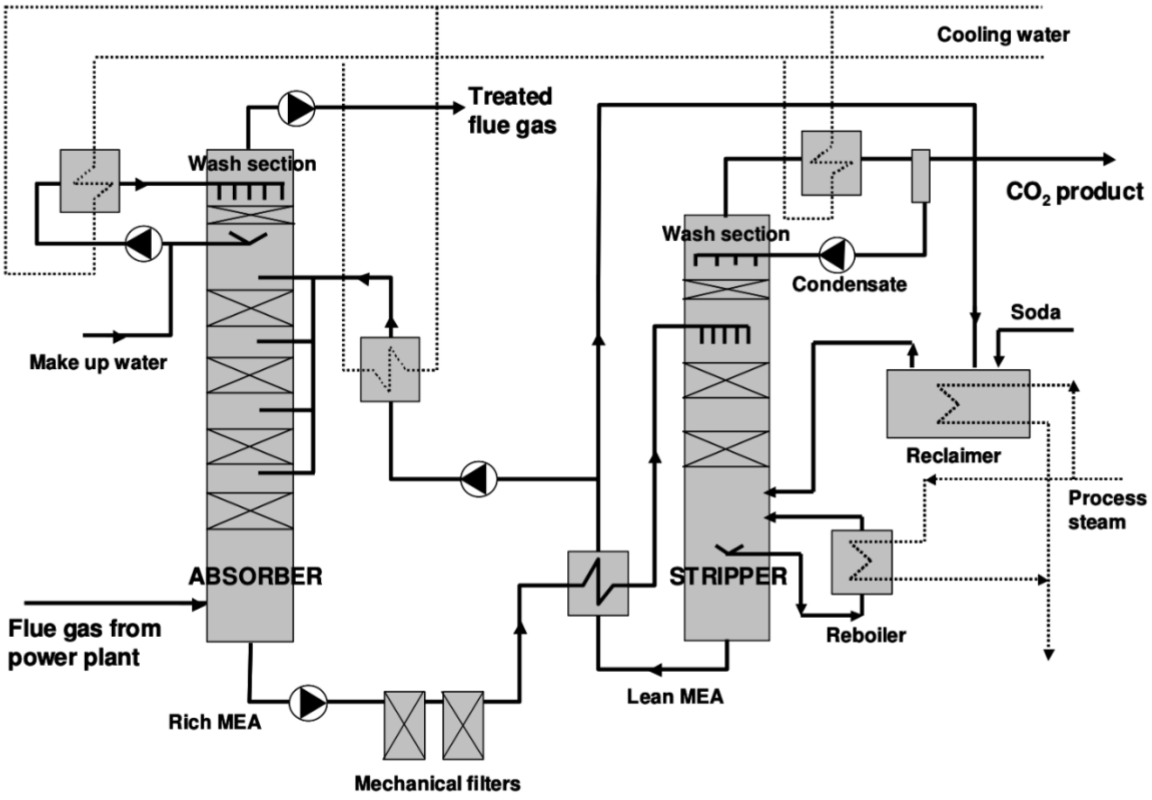

Figure 14: Process flow diagram of Esbjerg Pilot Plant [72]

As a part of CESAR project, some design modifications have been made to decrease the reboiler duty and cost. Implementation of lean vapor compression and absorber inter-cooling and improving heat exchanger and absorber were the modifications had been applied. [17]

Absorber packing was used to be IMTP 50 random packing, after the campaign, it was changed to Mellapak 2X structured packing. Liquid distributors were replaced with new ones, and bubble cap tray was installed on top of the water wash section. Absorber pressure was reported to decrease from 600 to 300 mm H_2O at normal volumetric flowrate of 5000 Nm^3/h. [17]

Plate heat exchanger which is used to heat up the cold rich amine, and cool down the lean amine is replaced with new one having increased capacity. Heat transfer area was increased by 35%. As a result, pinch side temperature approach was decreased from 7-8 ^{0}C to 4-4.3^{0}C by which it was observed to recover 0.2-0.3 GJ/ton CO_2 sensible heat. [17] Absorber inter-cooling and lean vapor recompression have been implemented. Process flow diagram of the improved process design is shown in Figure 15.

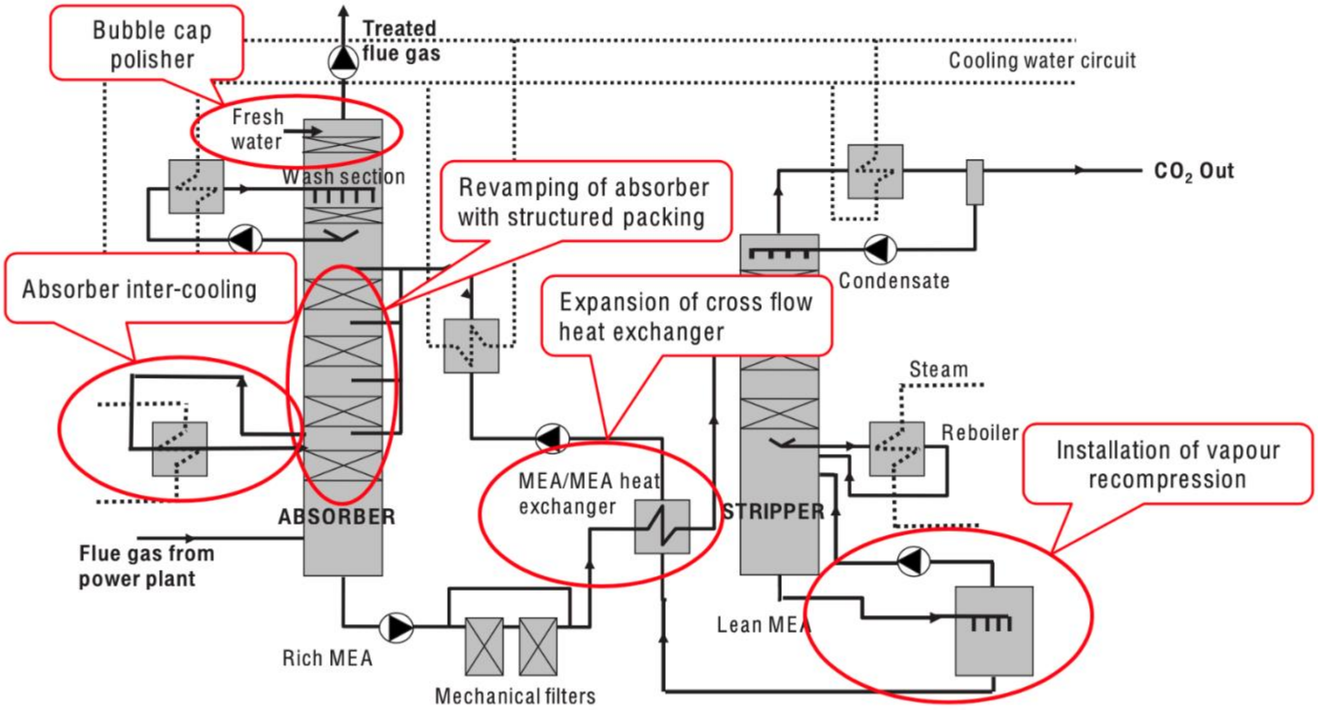

Figure 15: Improved process design in Esbjerg Pilot Plant [17]

Under CESAR EU project, three test campaigns took place between 2008 and 2011. 30 wt% MEA was used as benchmark solvent, and two novel solvents have been tested. CESAR-1 solvent, aqueous solution of AMP & piperazine, was run for more than 1000 hours. Afterwards, the second novel solvent, CESAR-2 (30 wt% EDA) was run for 200 hours. After the third campaign, the specific reboiler duty seemed to decrease significantly. [17]

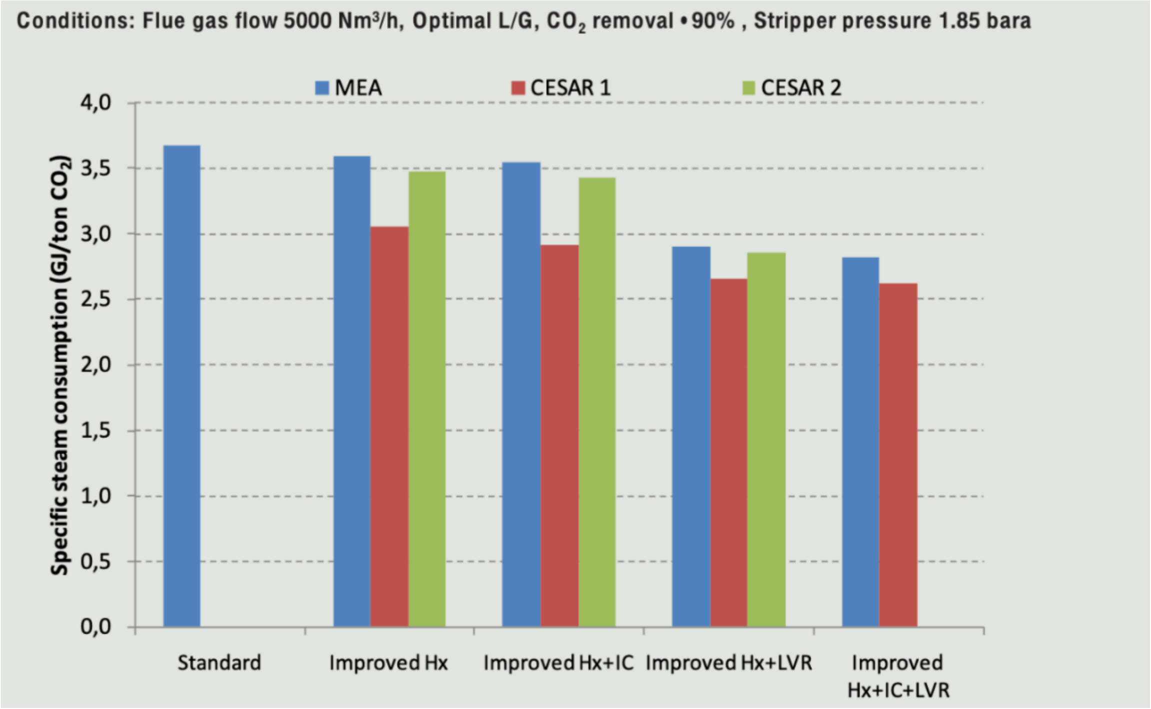

Figure 16: Improvements with process modifications at Esbjerg Pilot Plant [17]

The best performance was observed by CESAR-1 solvent. CESAR-1 solvent showed to have good energy efficiency, low corrosivity, and high CO_2 cyclic capacity. With process modifications, reboiler duty could be reduced from 3.05 to 2.60 GJ/ton CO_2 [17]. Based on the literature research, these results are expected. For example, using heat exchanger with lower minimum approach would decrease the SRD by allowing more heat transfer from the hot lean to the cold rich amine. Thereby, the stripper feed would be at higher temperature which benefits the desorption process. Applying absorber intercooling cools down the part of solvent in the absorber, which increases the absorption capacity of the solvent, thus decreases the SRD. Applying lean vapor recompression provides more heating in the form of compressed process steam which also benefits the desorption process and decreases the SRD.

7 Process Modelling

In this part, the methodology followed in the simulation studies will be explained in detail. For easier understanding, the methodology is also presented as a flow chart in Figure 17and Figure 18.

7.1 Methodology

Process modelling for this thesis includes two main sections; pilot plant studies, and the real plant studies. For the pilot plant studies, Esbjerg Pilot plant has been chosen as reference, and the same operating conditions and the equipment sizes have been used. The capture rate has been set to 90% by adjusting the reboiler duty by using a Simple Solver in ProMax. After the very basic design is made and validated by Esbjerg Pilot Plant, lean vapor compression (LVC) and absorber intercooling (AIC) have been implemented. Then, validation by the reported Esbjerg Pilot Plant data has been made. The validation for each case will be discussed in a separate section. Pilot plant studies needed for checking if the design is a good reflection of experimental data, and if it can be used for bigger scale studies.

The second part of the process modeling includes the scaling up to the real size plant. The flue gas data from coal-fired Advanced Super-Critical (ASC) Power Plant is used for the flue gas properties. The temperature and the pressure of the used flue gas are assumed to be adjusted before arriving to the capture plant. Solvent compositions were adjusted based on the reference design from E. Fernandez [45]. The first trial was done by keeping all operating conditions the same as Esbjerg Pilot Plant. As the equipment sizes were not suitable for the real flue gas flow rate, the sizing of the columns has been deleted and the flooding rate in the columns has been set to 80% so that the simulation calculated the diameter of the columns. Packing height and the number of stages were set based on the literature data. After the base case was developed, the optimum L/G ratio has been found and the conditions for sensitivity analysis were set. Six parameters have been defined for the sensitivity analysis:

1. Mass-based L/G ratio
2. Absorber feed temperature
3. Minimum temperature difference in the lean/rich heat exchanger
4. Stripper pressure
5. Stripper height
6. Absorber height

The ranges for the sensitivity analysis were chosen based on the literature research. Ten points were set for each sensitivity analysis; however, simulation did not converge at some of the data points. Therefore, those data points have been removed from the range and the number of data points were reduced. Schematics of the methodology is shown in Figure 17and Figure 18;

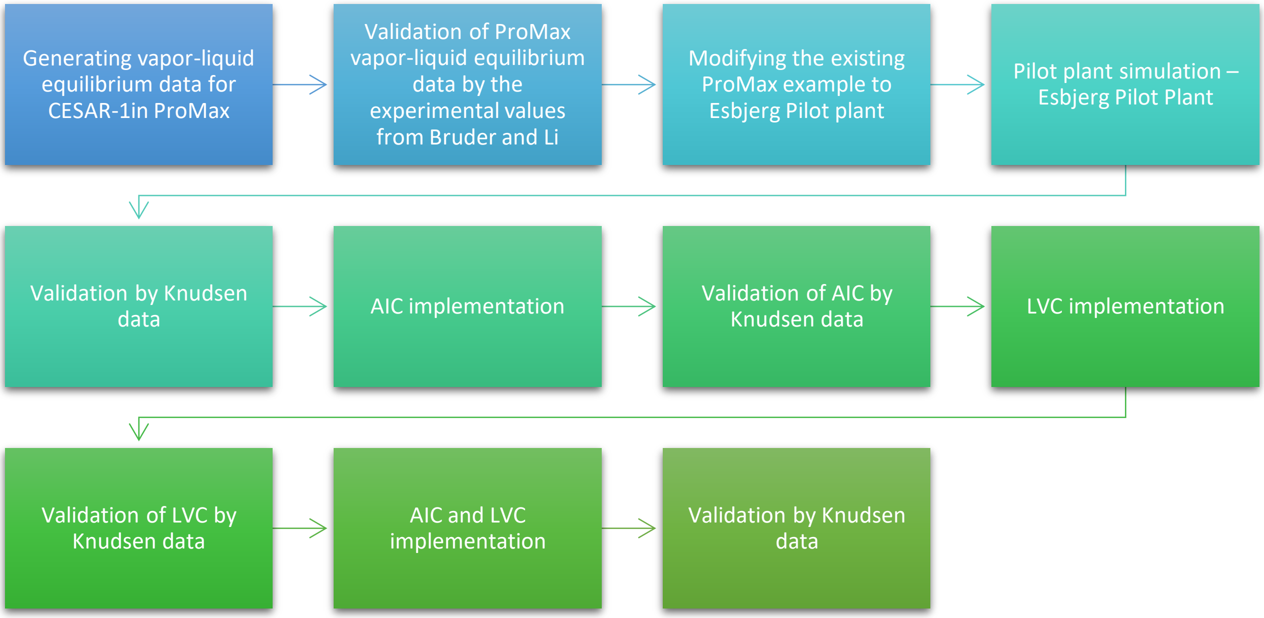

Figure 17: Pilot plant simulations methodology

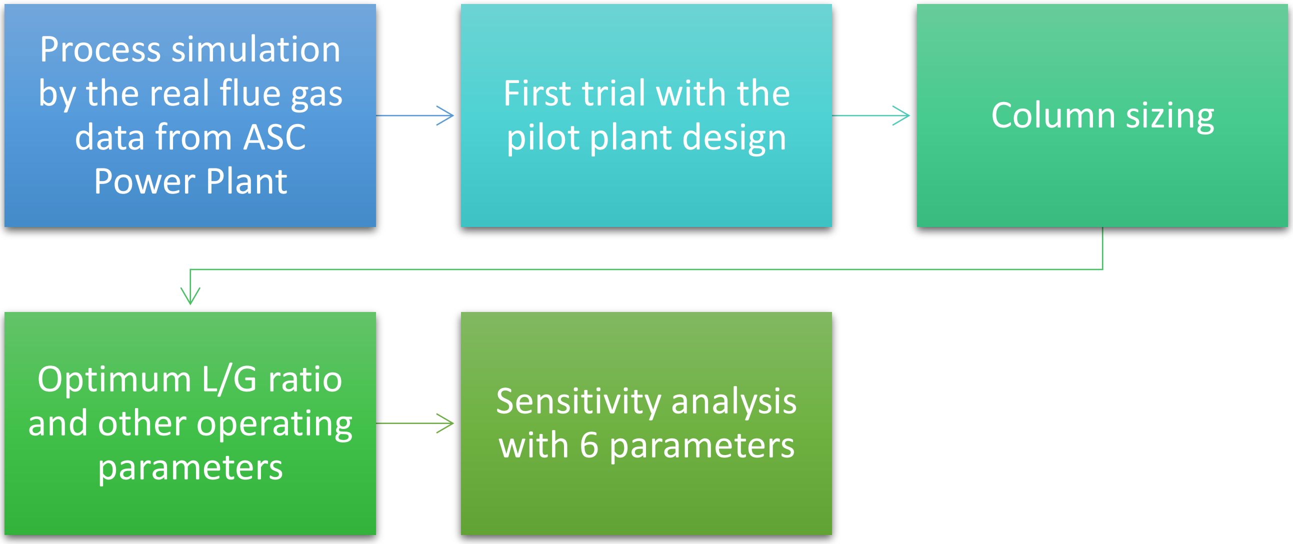

Figure 18: Real plant simulation methodology

7.1 Validation of vapor-liquid equilibrium data for CESAR-1

To overcome the problems associated with MEA, performance of CESAR-1 solvent is tested in techno-economical point of view with respect to MEA. ProMax® V6 software includes Amine Sweetening Packages for the thermodynamic calculation methods based on PR, PR Polar, SRK, and SRK Polar equations of states. Partial pressure of CO_2 vs loading at two different temperatures for CESAR-1 has been created in ProMax. This has been done to see if the software is able to predict the vapor-liquid equilibrium data of AMP&PZ-CO_2-water system as this is a complex system. The results have been compared with the experimental data provided by P. Bruder et al. [74] and H. Li et al. [75]. Comparison of the ProMax results and the experimental results are shown in the plot below.

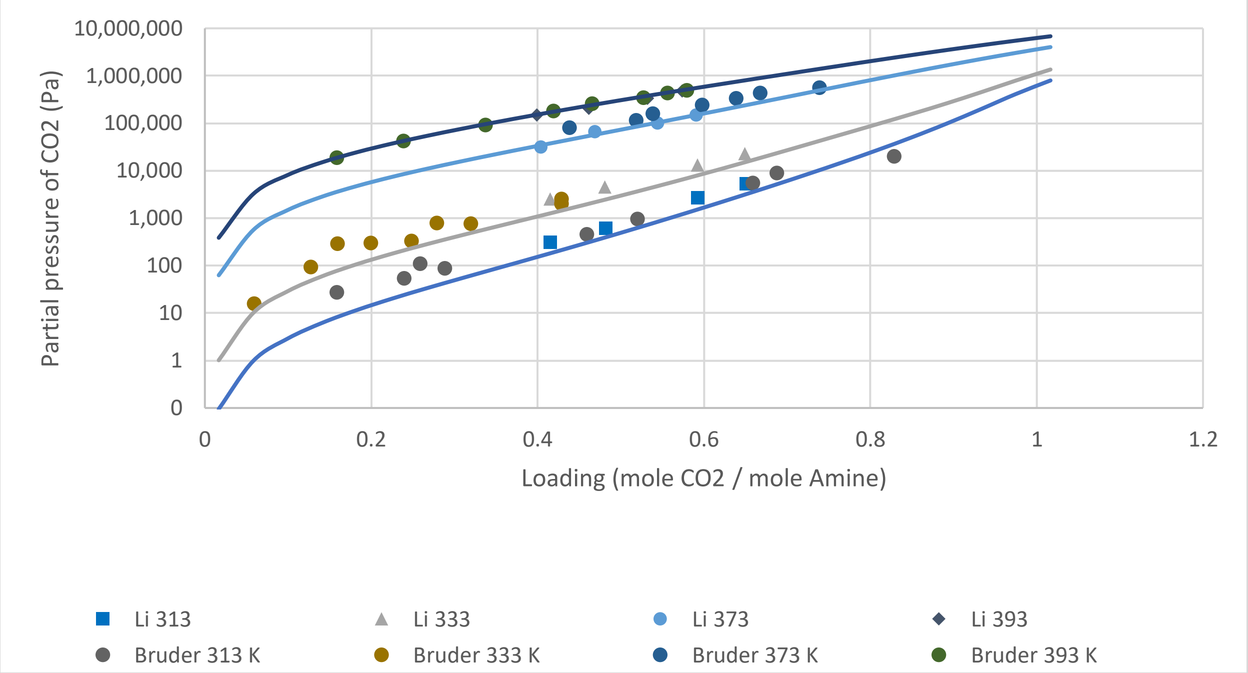

Figure 19: Simulation results vs experimental data by Bruder [74] and Li [75] for CESAR (AMP+PZ) system

Simulation results seem to align with reported experimental data by Bruder [74] very well while they show slight difference from Li [75], meaning that thermodynamic data of AMP+PZ system is well represented by ProMax. The differences from the experimental data could be result of the fluid package, assumptions, or the input data given to the simulation. These result show that we can go ahead and start the simulation of absorption-based carbon capture.

7.2 Pilot plant simulation studies

For both systems, MEA and CESAR-1, four cases have been made. Base case, case with lean vapor compression (LVC), case with absorber inter-cooling (AC), and case with both LVC and AC have been modelled. The same designs have been used for MEA and CESAR.

7.2.1 Base Case

ProMax existing Amine Sweetening with MEA model was modified for building the base case scenario. Flue gas information was taken from Esbjerg pilot plant. As mentioned before, flue gas is received by slip stream from pulverized Coal-fired power plant in Esbjerg [72]. The flow diagram of the base case is shown in Figure 20 and the design parameters are shown in Table 9.

Table 9: Base case properties

Parameter	Value
Flue gas flow rate (N m^3/h)	5000
Flue gas temperature (^oC)	47
Flue gas pressure (bar)	1.01325
Flue gas composition (mol%)	N_2: 76, CO_2: 13, O_2: 11
Solvent MEA	30 wt%
Solvent CESAR-1	19 wt% AMP + 9 wt% PZ
Absorber packing height (m)	4*4.25
Absorber diameter (m)	1.1
Absorber packing	Mellapak 2X
Rich pump pressure change (bar)	0.51
Lean/rich minimum temperature difference (cold in/hot out) (^oC)	4.5
Stripper operating pressure (bar)	1.85
Stripper packing height (m)	10*1
Stripper diameter (m)	1
Stripper packing	IMTP 50
Condenser temperature (^oC)	40
Lean pump pressure difference (bar)	0.51

Lean cooler temperature (ºC)	30
Circulation pump pressure difference (bar)	0.05

Cooled flue gas is fed to the absorber at 47^{0}C and 1.01325 bar with maximum of 5000 Nm^{3}/h. In the original Esbjerg Pilot Plant design. The absorber consists of four 4.25 m stages. The first trial has been run by this; however, the simulation did not converge. Therefore, absorber design has been modified until the simulation converged. During this process, more beds summing up to 17 m packing height have been used instead of four 4.25 m beds with 1.1 m section diameter filled with Mellapak 2X structured packing. Absorber top product, treated gas, leaves at 1.85 bar and 100^{0}C, while the bottom product which is rich in carbon is pumped to the plate heat exchanger to be heated for further separation from amine in the stripper. The minimum temperature difference in the lean/rich heat exchanger is 4.5ºC, and the pressure drop in the hot side of the plate heat exchanger is set to be 0.51 bar. Rich amine is heated up to around 100^{0}C by lean amine before it is fed to the stripper. The stripper operates at 1.85 bar(a) and around 100^{0}C without any pressure drop across the sections. Stripper has been modified just as absorber. 10 sections each 1 m in height, having 1.1 m diameter, is used instead of using 2 sections with 5 m packing height. IMTP 50 random packing is used. Reboiler operates with steam, and the reboiler duty has been set by a simple specifier so that it captures 90% capture. Lean amine leaves the stripper at 1.85 bar and is pumped to plate heat exchanger by booster pump to be cooled down by carbon rich amine. Minimum temperature approach is set to be 4.3^{0}C in the plate heat exchanger. Recycled rich amine is further cooled by water-cooler before it mixes with additional solvent in the make-up block. Make-up block is used to ensure adequate solvent flow and concentration for each run. Mixed rich amine and the solvent is pressure adjusted by booster pump and sent back to the absorber from the first stage. Only difference between the designs is the used solvent. In the MEA case, 30 wt% MEA was used whereas in CESAR-1 case 19 wt% AMP + 9 wt% PZ was used. [17] [72]

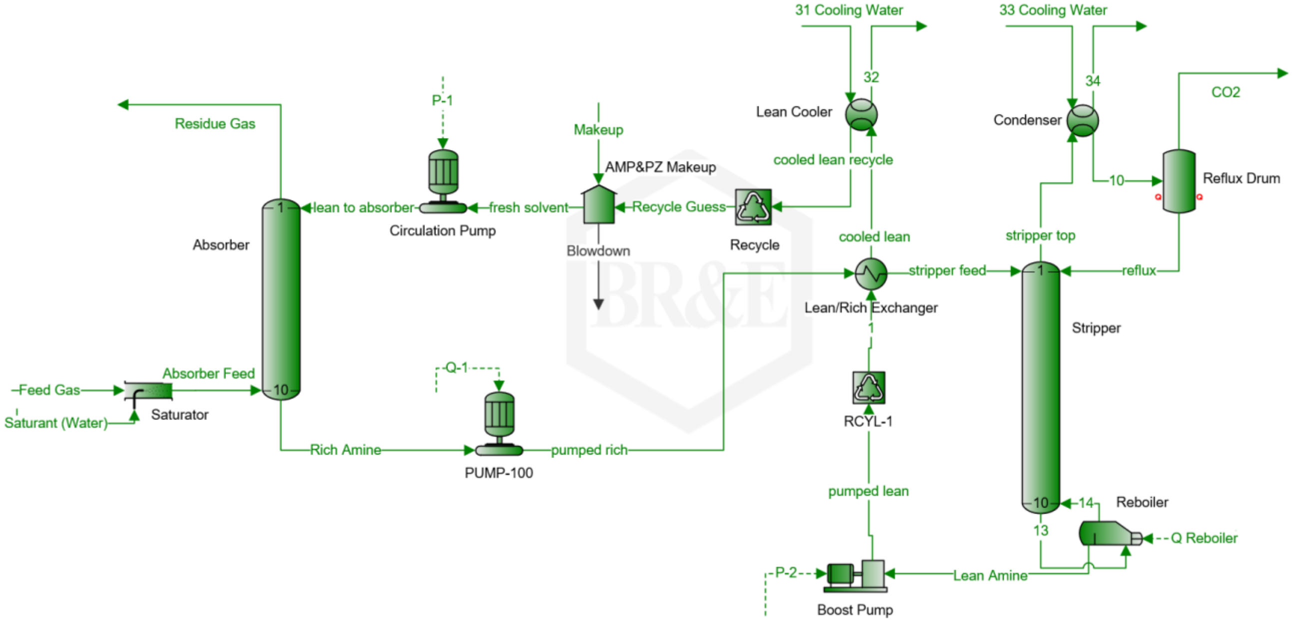

Figure 20: Base case flow diagram

7.2.2 Implementation of Absorber Intercooling (AIC)

As the absorption reaction is an exothermic one, it will increase the temperature in the column. However, this will limit the loading capacity of the solvent and the absorption’s thermodynamic driving force [22, 19]. In return, this might end up increasing the packing requirement of the absorber and decreasing the energy performance of the stripper both of which will have direct effect on the plant cost and SRD [19].

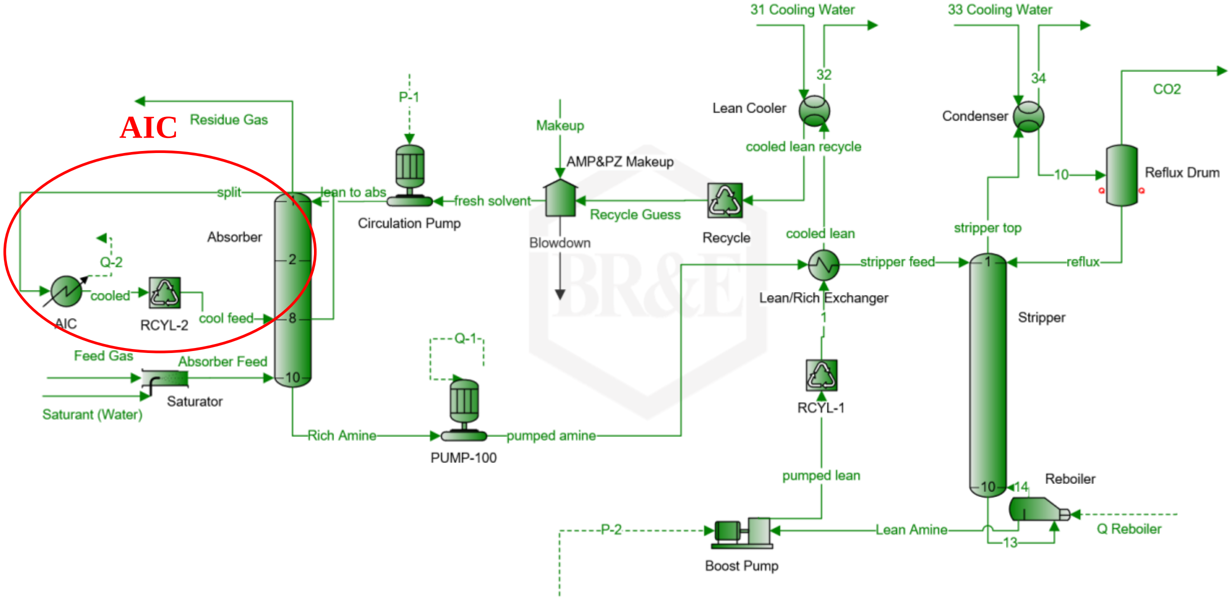

Figure 21: Absorber inter cooling flow diagram (AIC)

Absorber intercooling modification is implemented to reduce the reboiler duty for capture process, as depicted in Figure 21. As discussed earlier, this modification involves diverting a portion of the absorber's liquid flow, cooling it to a temperature generally ranging from 20-60°C and reinjecting it to the absorber which would cool the temperature inside the absorber and increase the absorption rate [17, 18, 19]. This efficient modification increases solvent the capacity, thereby reducing the required regeneration energy through a decrease in the solvent recirculation [19]. Consequently, lower solvent recirculation helps minimize the size of the equipment. In this work, absorber intercooling effect has been investigated in the range of 20-45 °C with a split fraction 30%.

7.2.3 Lean vapor recompression (LVC)

Another very common cost and energy reduction implementation is the lean vapor recompression (LVC) shown in Figure 22.

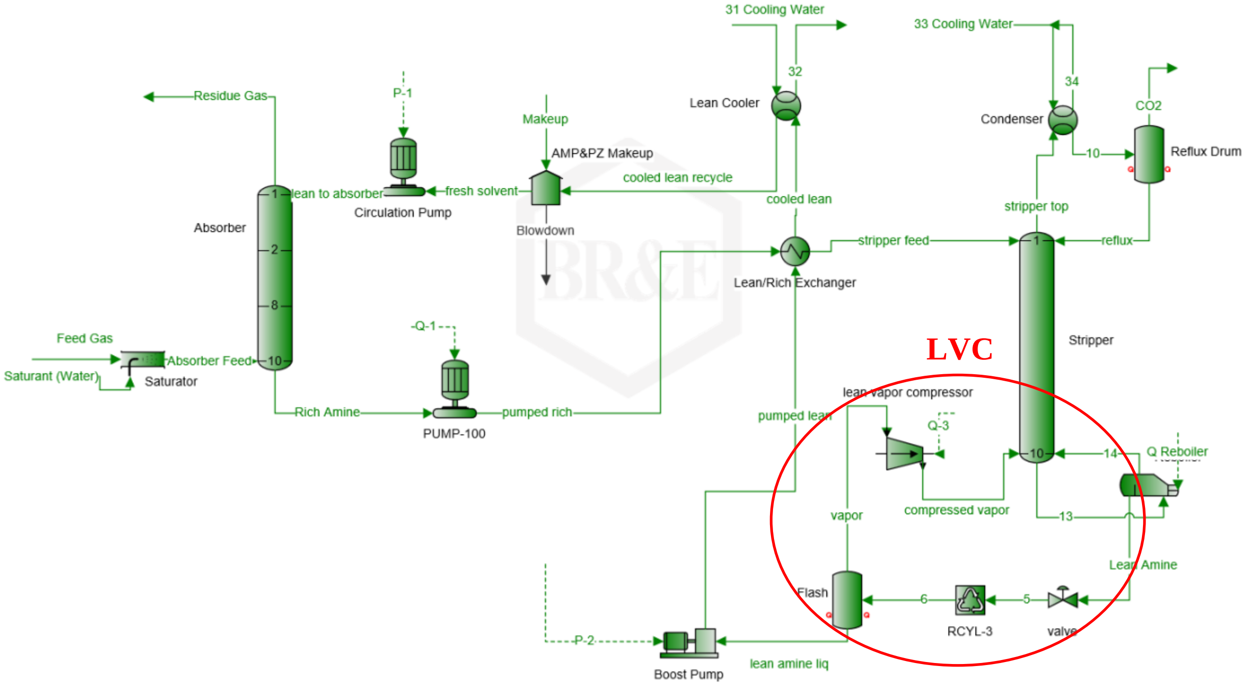

Figure 22: Lean Vapor Recompression (LVC) flow chart

As discussed in the earlier sections, the concept employed in this process involves flashing the lean amine in the flash vessel at low pressures, then recompressing the resulting hot vapor to the stripper pressure. This compressed vapor is utilized as a process steam and fed from the bottom of the stripper. The flashed liquid lean amine is sent to the lean pump for pressure adjustment before being fed to the lean/rich heat exchanger. The vapor mostly consists of H_2O and CO_2 [21]. Since the recompressed vapor is at high temperature, it benefits the endothermic desorption process, thereby reducing the reboiler duty and the SRD. However, it is essential to consider the energy needed for compression to be able to make a fair comparison with the conventional case. To account for this extra energy requirement, a new term called equivalent work is introduced. Equivalent work is calculated by the following formula [22];

$$W_{eq} = 0.75.\,Q_{reb}.\frac{(T_i + 10\,K - T_{sink})}{(T_i + 10\,K)} + W_{comp} \tag{7.1}$$

To consider the increasing value of the steam, Carnot efficiency is used here. T_i refers to the reboiler temperature (K), Q_{reb} is the specific reboiler duty (GJ/t CO_2), T_{sink} is the Carnot engine's cold temperature which is set to 313 K, and W_{comp} is the compressor duty (GJ/t CO_2) [22].

In most studies, the flash pressure is generally varied from 0 to 0.8 bar(g) [17, 76]. Knudsen et al. [17] observed 20% energy reduction by applying LVC for MEA, and 13% reduction by applying LVC to CESAR-1. The effect of LVC has been tested in the pressure range of 0-0.8 bar(g).

7.2.4 Final Case

After implementing the cost and energy reduction modifications separately, to further reduce the cost and energy, both LVC and AIC have been implemented, and the effect of L/G ratio has been investigated in the final case. Please find the flow diagram of the final case below.

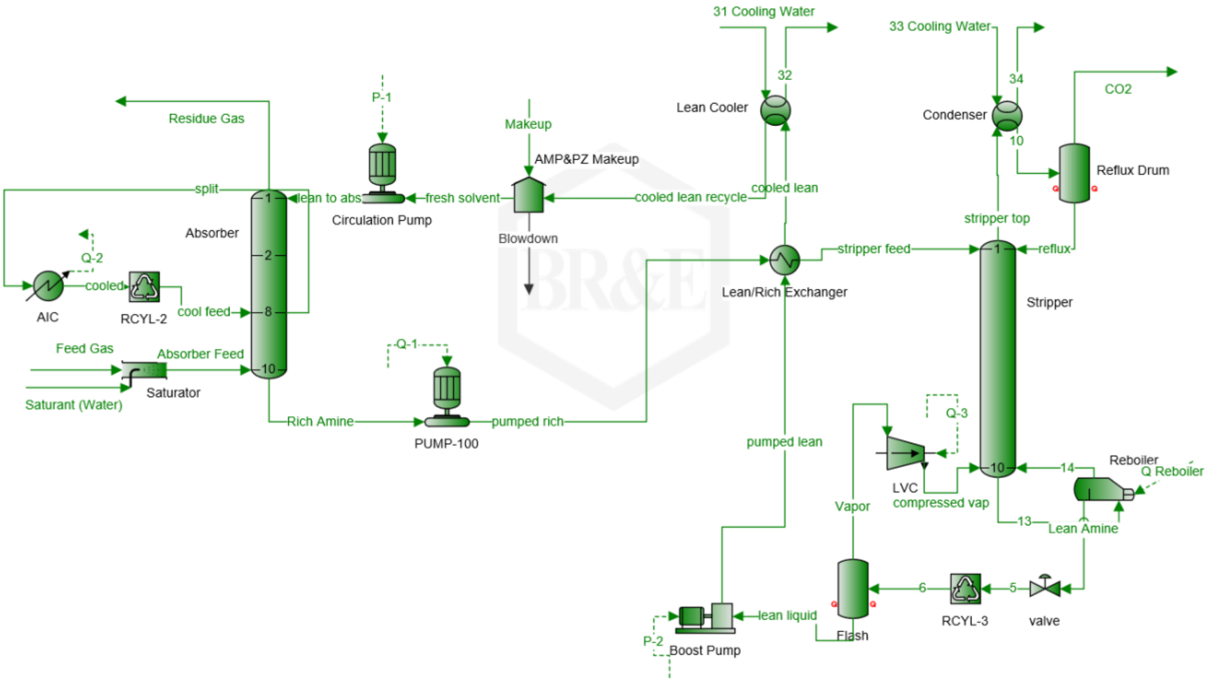

Figure 23: Flow diagram of the final case with AIC and LVC

7.3 Scaling up

To be able to test the plant efficiency at a big scale power plant, scaling up is needed. The same design approach used in the pilot plant studies was followed. The absorber and the stripper sizing have been adapted to capture 90% carbon from a real coal-fired Advanced Super Critical (ASC) power plant. The flue gas properties from ASC power plant are given in the table below. The flue gas is assumed to be temperature and pressure adjusted.

Table 10: Flue gas properties from ASC power plant

Parameter	Value
Flue gas flow rat (kg/s)	782.0
Composition (mol%)	Ar: 0.9, N_2: 72.0, O_2: 3.7, CO_2: 13.7, H_2O: 9.7
Temperature (^oC)	44
Pressure (atm)	1.01
Solvent MEA	30 wt%
Solvent CESAR-1	19 wt% AMP + 9 wt% PZ
Absorber height (m)	25 (MEA), 18 (CESAR)
Absorber packing	Mellapak 2X
Absorber number of stages	25 (MEA), 15 (CESAR)
Rich pump pressure change (bar)	0.51
Lean/rich minimum temperature difference (cold in/hot out) (^oC)	5.0
Stripper operating pressure (bar)	1.85
Stripper height (m)	13.5 (MEA), 12 (CESAR)
Stripper packing	IMTP 50
Stripper number of stages	15 (MEA), 10 (CESAR)
Condenser temperature (^oC)	40
Lean pump pressure difference (bar)	0.51
Lean cooler temperature (^oC)	30
Circulation pump pressure difference (bar)	0.05

The same design as the pilot plant design has been used, but to account for the higher flow rate, the absorber and the stripper column dimensions have been changed. As the simulation did not converge with the given dimension from the reference paper, columns dimensions for both designs have been changed based on the literature values. S. Uhre [60] used 25 m absorber height, and 15 m stripper height for capturing 90% of carbon. N. Sipöcz et al. [77] used absorber with 26.9 m height and 9.6 m diameter, and a stripper of 23.5 m height and 5.5 m diameter for a commercial scale carbon capture plant with MEA. E. O. Agbonghae et al. [78] studied carbon capture from

Ultra-supercritical coal-fired power plant by using 2.68 L/G ratio with a capture rate of 90%. They used 16.92 m diameter with 23.74 m height in absorber column, and 13.89 m diameter with 25.36 m height in stripper. W. Zhang et al. [18] studied carbon capture with CESAR-1 at a commercial scale and made the modeling in Aspen Plus. The reported diameter and the height of the absorber is 20.8 m, and 30 m, the reported stripper diameter and the height is 12.1 m, and 30 m, respectively.

As a starting point, 15 m total absorber height and 10 m total height for stripper was used in the MEA design. In CESAR-1 design, as a first trial, 10 m total absorber height and 10 m total stripper height was used. However, with these dimensions, simulations did not converge with higher L/G ratios. Therefore, they have been increased until they converged with all L/G ratios in the sensitivity analysis. The final dimensions set for the columns are given in Table 10.

7.4 Sensitivity analysis

Sensitivity analysis is a way of testing how sensitive your design is to the certain parameters, which would help in finding the optimum operating conditions. As mentioned before, high reboiler duty and CAPEX are the major problems associated with carbon capture plants. Finding the optimum operating parameters would strongly help reduce the reboiler duty, so as the CAPEX. Sensitivity analyses were performed to find the best operating conditions for the design. Six different parameters were varied in the intervals having 10 data points. The parameters and the intervals were selected based on what author authors reported in the literature. The parameters and the data intervals are shown in Table 11.

Table 11: Sensitivity analyses parameters and boundaries

Parameter	Lower bound	Upper bound
L/G (kg/kg)	8.0	21.0
Absorber temperature (ºC)	40	49
Minimum temperature difference in lean/rich heat exchanger	4	13
Stripper pressure (bar)	1.3	2.2
Stripper height (m)	7.5 (MEA) 10.0 (CESAR)	21.0 (MEA) 19.0 (CESAR)
Absorber height (m)	12	39

8 Economic Evaluation

In the previous sections, technical part of the design has been discussed. The main focus was finding the operating parameters giving the lowest specific reboiler duty. However, the design with the lowest specific reboiler duty is not always economically best, and the most profitable design. Therefore, CAPEX and OPEX calculations should be made to evaluate the best design technical design parameter giving the lowest cost.

8.1 Capital expenditures

There are different cost calculation methodologies in the literature but in this work, Bottom-up method will be used. This method is based on using the mass and energy balance, stream information, and equipment information. It relies on calculating cost of each equipment by the available economic models, or software tools. The schematic of the cost estimation method is represented in the following flow chart [45].

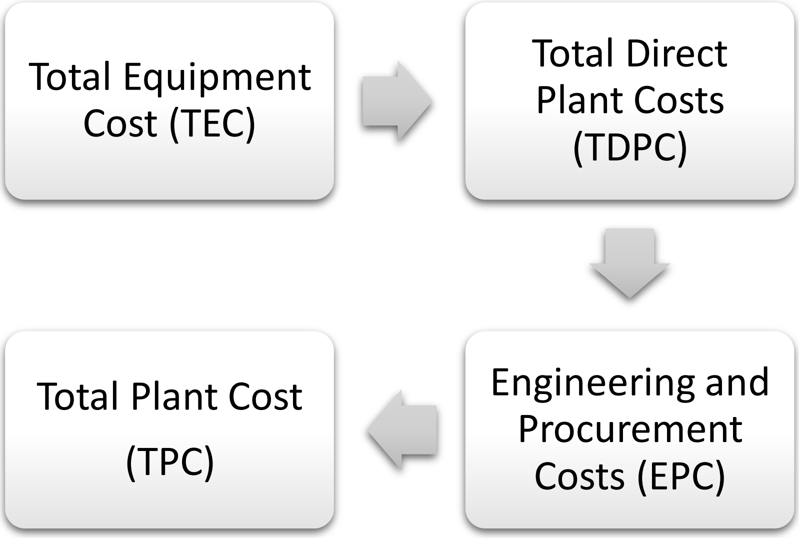

Figure 24: Methodology of CAPEX

After calculating the cost of each individual equipment, the further cost factors such as installation, erection, civil, structural, instrumentation, piping factors need to be calculated as a certain percentage of the equipment cost. These factors depend on the type of the equipment and are different in each type [45].

$$TEC = \sum \sigma_k(r_k) \tag{8. 1}$$

Where σ_k is the cost of individual equipment and r_k is the equipment performance rate. Total Equipment Cost, erection, instrumentation and controls, piping, electrical equipment and materials, civil works, and solvent inventory make up the Total Direct costs of the plant [45].

$$TDPC = TEC.(1 + I_k) \tag{8. 2}$$

Indirect costs, on the other hand, include yard improvements, service facilities, engineering and supervision, and building costs. The sum of Total Direct Plant Cost and Total Indirect Plant Cost gives the Engineering and Procurement cost [45].

$$EPC = TDPC + TIPC = TDPC.(1 + IC) \tag{8. 3}$$

Where Indirect Cost (IC) is calculated based on a percentage of TDPC. Total Plant Cost, then, is calculated from the equation below where β is the Contingency and Owner's cost [45].

$$TPC = EPC.(1 + \beta) \tag{8. 4}$$

This process is the general and not detailed methodology of CAPEC estimation. In this thesis, CAPEX estimation tool provided by Engineering Consultant company Rambøll has been used. This tool uses Wood's method proposed for estimating equipment costs [79, 80]. This method calculates the cost with Carbon Steel material and CEPCI index of 1000 which in the tool is converted into $CEPCI_{2022}$ =816 [79, 80].

$$Cost\ in\ year\ A = Cost\ in\ year\ B\ .(\frac{CEPCI_A}{CEPCI_B}) \tag{8. 5}$$

A base cost for the most equipment is given with a reference capacity which could be flow rate, heat transfer area, heat duty etc. and this is then scaled to the actual capacity by a sizing exponent (n);

$$C_{eq,CS} = C_{eq,CS,reference}(\frac{Capacity}{Capacity_{reference}})^n \tag{8. 6}$$

The detailed method is given in [79]. As an example, the sizing parameters for some equipment are given in Table 12.

Table 12: Sizing parameters for some equipment

Equipment	Sizing parameter
Columns	Total height (mm), column diameter (mm)
Heat exchanger	U value (W/m^2 K), LMTD, heat duty
Pump	Flow rate (m^3/h)

If the sizing parameter is higher than the upper limit for a specific equipment, multiple equipment summing up to the same size is assumed. After calculating the base equipment cost, required the total installed equipment cost is calculated by Enhanced Detailed Factor (EDF) method is applied [81]. In this method, the installation costs depend on the cost of the equipment rather than the type [80]. The installation cost for each equipment in Carbon Steel is calculated by using the installation factors given in Table 13.

Table 13: Installation factors in EDF method in 2020 [80] [81]

Equipment cost (k€)	Installation factor
0-10	14.98
10-20	10.12
20-40	8.54
40-80	7.22
80-160	5.89
160-320	4.92
320-640	4.19
640-1280	3.63
1280-2560	3.19
2560-5120	2.84
5120-	2.56

The price correction is done by using CEPCI correlations of 2020 and 2022. Then, the total installed cost of equipment is obtained by summing up all the equipment costs [80] (Andreasen, Optimisation of carbon capture from flue gas from a Waste- to-Energy plant using surrogate modelling and global optimisation , 2021).

8.2 Operational expenditures

Operational expenditures are the costs for running the plant. For calculating OPEX, plant is assumed to be operating 8000 hours per year.

OPEX includes Fixed Operating and Maintenance Cost (Fixed O&M), and Variable Operating and Maintenance Cost (Variable O&M). Fixed O&M Costs consist of Maintenance and Repairs (MR), Operating Labor (OL), laboratory charges, operating supplies, insurance, and plant overhead costs. Fixed costs are estimated based on the percentages of Total Plant Cost [45].

$$MR = 2.5\% \ of \ TPC \tag{8. 7}$$

$$Laboratory \ charges = 10\% \ of \ OL \tag{8. 8}$$

$$Insurance = 1.5\% \ of \ TPC \tag{8. 9}$$

$$Plant \ overhead \ cost = 60\% \ of \ (M + OL) \tag{8. 10}$$

Variable OPEX includes the raw materials which are the solvent make-up, and process water in our case, and the utilities which are the cooling water, low pressure steam, and electricity. Solvent losses occur due to the degradation, evaporation, salt formation etc. In many studies, the overall solvent loss estimated for MEA, AMP and PZ [45];

- MEA: 1.5 kg/ t CO_2
- AMP: 0.5 kg/ t CO2
- PZ: 0.05 kg/ t CO_2

Table 14 shows the costs used for estimating variable OPEX. CEPCI correction was applied to bring the costs to 2022 prices.

Table 14: Cost of variables

Parameter	Cost	Year
LP steam	1.83 €/kg [82]	2002

Cooling water	0.35 €/m^3 [45]	2011
Process water	0,9 €/m^3 [82]	2002
Electricity	0.094 €/kWh [82]	2011
MEA	1.042 €/kg [45]	2011
AMP	8 €/kg [45]	2011
PZ	6 €/kg [45]	2011

The summation of the variable OPEX and the fixed OPEX gives the Total Annual OPEX of the plant.

$$Total\ Annual\ OPEX = Total\ Variable\ OPEX + Total\ Fixed\ OPEX \tag{8. 11}$$

The cost of operating supplies was assumed to be the same as the reference case, 0.8 million € for MEA, and 0.68 million € for CESAR [45].

9 Results and discussion

In this part of the report all the results from pilot plant studies to the real size plant will be shown and discussed. Then the results will be compared between MEA and CESAR and the literature.

9.1 Pilot plant studies

Pilot plant studies included the conventional carbon capture design, AIC implementation, LVC implementation, and both AIC + LVC implementation.

9.1.1 Base case

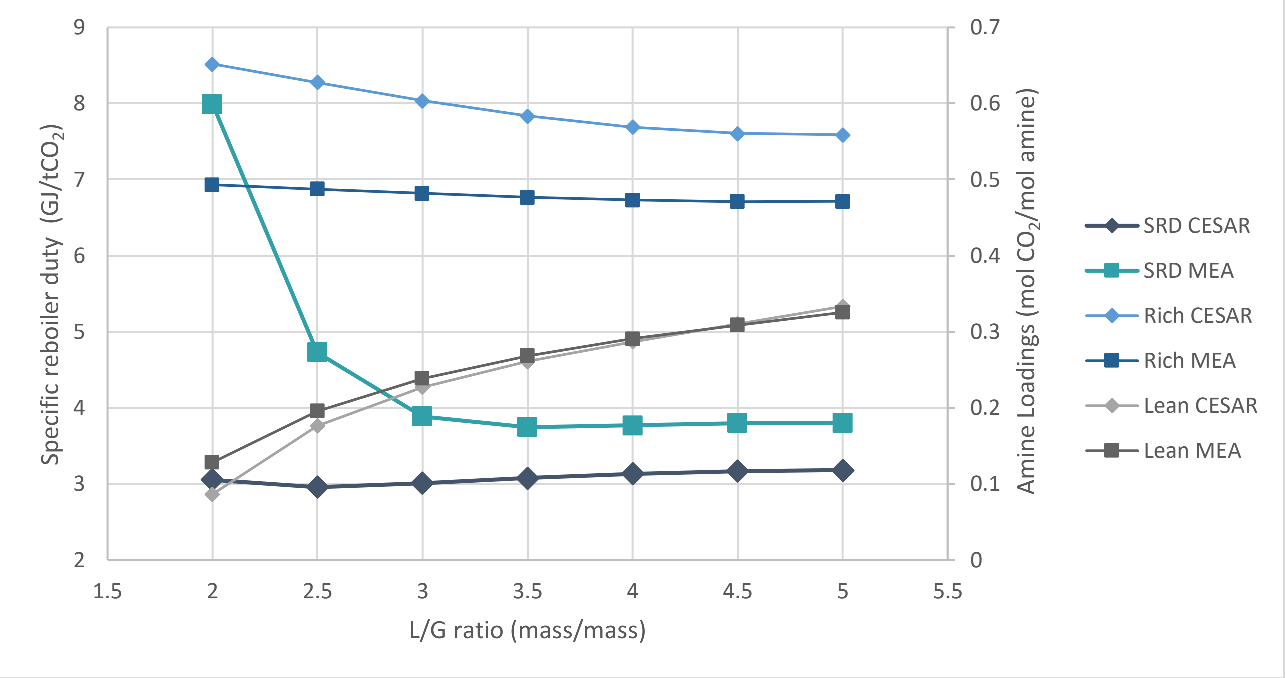

Figure 25:Comparison of MEA and CESAR-1 for conventional pilot plant study

Figure 25 compares the results for the base case for MEA and CESAR-1. The L/G ratios has been varied in the range of 2.0- 5.0 to find the best ratio for both designs. When looking at the figure, we can see that the SRD for both designs decrease by increasing L/G ratio. The reason for this is that the more amine solvent circulates through the system, and the regeneration requirement decreases as the amount of available amine solvent gets more by increasing L/G ratio. L/G has big effect on the MEA case while its effect on the CESAR-1 case is not as significant as the MEA case. Yet, the SRD obtained by CESAR-1 case is always smaller than that of MEA. For the MEA, case SRD decreases dramatically from L/G=2.0 to L/G=3.5 and almost stabilizes around that value indicating that this might be the optimum L/G for MEA case. SRD of CESAR-1 case, on the other hand, finds a minimum at L/G=2.5 and starts to increase by further increasing the L/G. Thus, 2.5 could be accepted as the optimum L/G for CESAR-1 case. Lean loadings for both designs increase by increasing L/G ratio while rich loading decreases slightly compared to the lean loading. However, high lean loading is not beneficial for the system as it means the regenerated solvent still carries relatively more CO_2 and the difference between the rich loading and lean loading gets smaller. Smaller difference decreases the cyclic capacity of the system which in return reduces the energy performance of the design. Therefore, although higher L/G ratio gives smaller SRD, it is not always the best for the system to be operated at higher L/G ratios.

The optimum L/G ratio for MEA is around 3.5 corresponding to 3.74 GJ/ t CO_2. In the case of CESAR-1, this ratio is at 2.5 with 2.97 GJ/ t CO_2. The optimum L/G ratio was around 2.5 for MEA in the reference case, and the obtained SRD is around 3.60 GJ/ t CO_2. For CESAR-1, optimum L/G is 2.0 with 2.90 GJ/ t CO_2. The results mostly align with the reference case (Esbjerg PCC Pilot Plant), with little differences but still are acceptable.

9.1.2 Absorber intercooling

The effect of absorber intercooling has been investigated in 25-60°C range and with the optimum L/G ratio. From the figure below, it is obvious that the SRD increases by the increasing intercooling temperature. As lower temperatures would shift the absorption reaction to right (forward reaction) and would result in increased solvent capacity as well as rich loading. Cyclic capacity increases by increased rich loading and less energy is required for regeneration [72]. By applying 25°C, SRD reduction from 3.74 GJ/ t CO_2 to 3.58 GJ/ t CO_2 can be obtained with MEA, from 2.96 to 2.79 can be obtained with CESAR-1 which account for 0.04 GJ/ t CO_2 and 0.06 GJ/ t CO_2 savings, respectively. In the reference case, at 25°C intercooling, 3.55 GJ/ t CO_2 SRD was obtained by MEA, and 2.80 GJ/ t CO_2 was obtained by CESAR-1 [72]. These results are almost the same as what has been found in this study which validates the results.

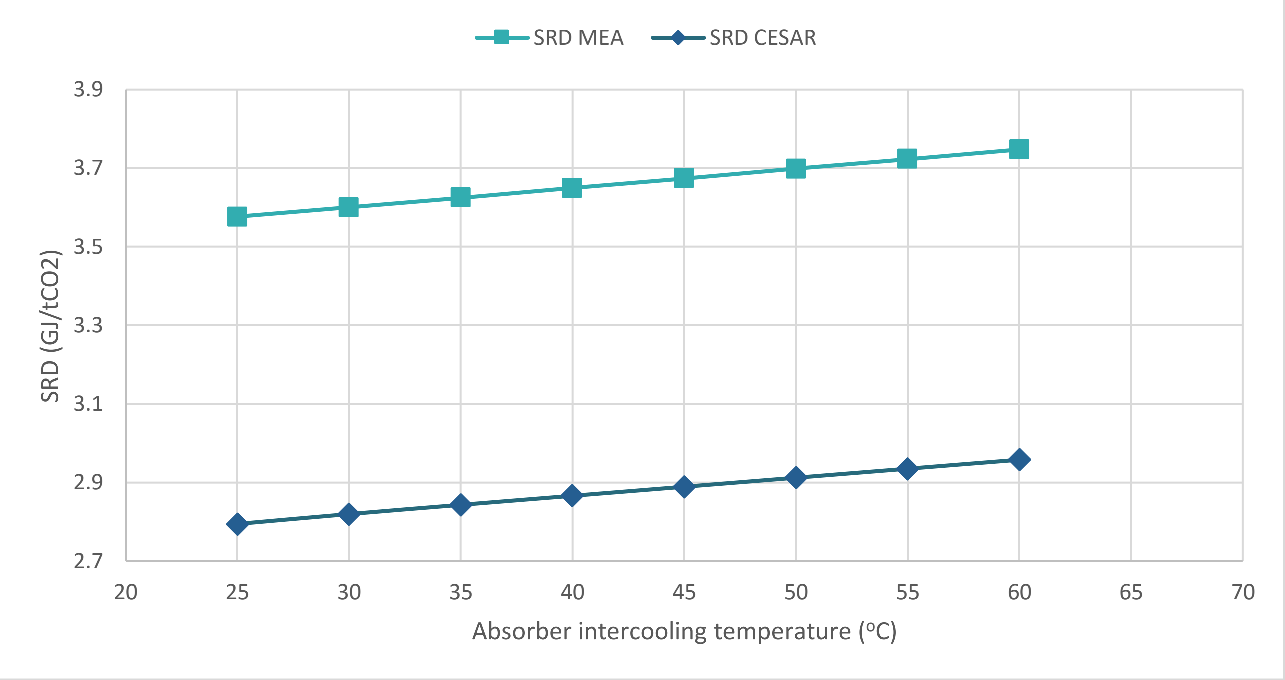

Figure 26: Comparison between MEA and CESAR-1 for absorber intercooling

9.1.3 Implementation of Lean Vapor Recompression (LVC)

Lean vapor recompression has been studied in 0-0.8 bar (g) flash pressure range and with the optimum L/G ratio to see the effect on SRD. Implementation of LVC adds extra compressor work to the system; therefore, to account for the energy reduction, additional compressor work was considered by calculating equivalent work.

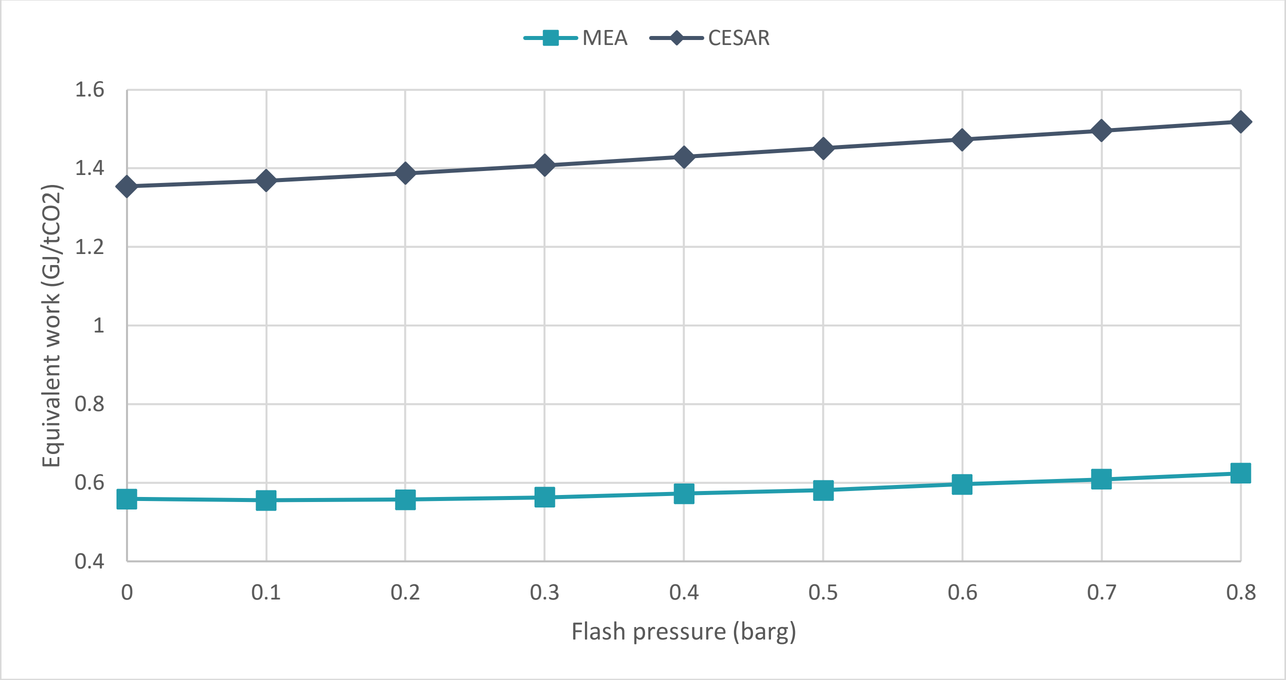

Figure 27: Equivalent work

Equivalent work in both MEA and CESAR case shows increasing trend; however, it is much higher for the CESAR case as well as the rate of increase. From the graph, it can be said that the LVC is more effective in MEA case than CESAR case. However, more results are needed to make a conclusion. The direct effect of additional compressor was also investigated by summing the reboiler duty and the compressor duty and calculating the SRD again.

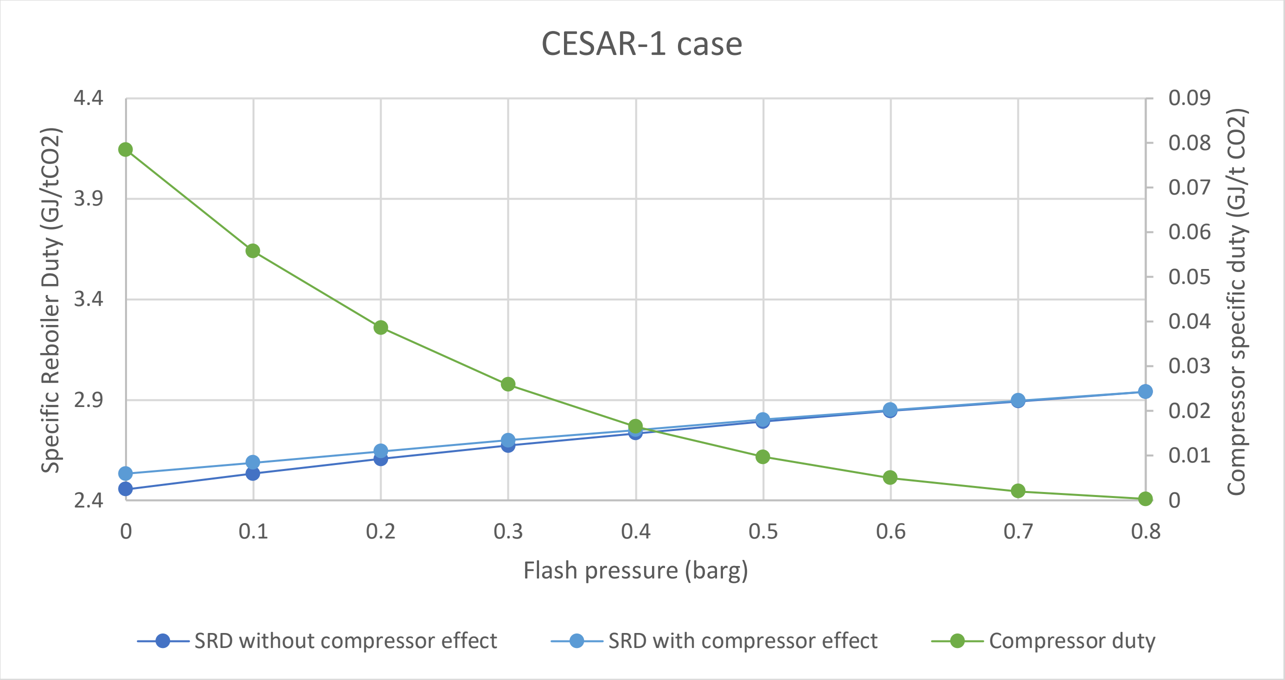

Figure 28: SRD with and without compressor effect for CESAR case

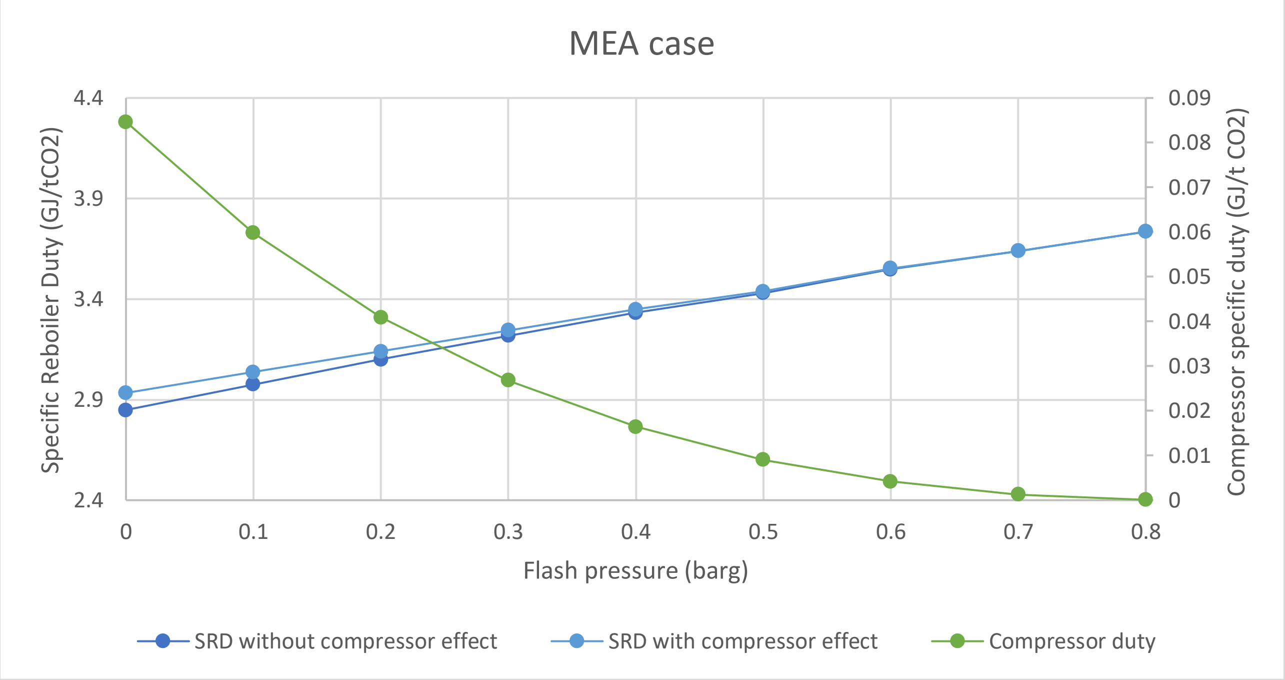

Figure 29: SRD with and without compressor effect for MEA case

Figure 28 and Figure 29 show the SRD with and without compressor effect. SRD shows increasing behavior as the flash pressure increases whereas compressor duty shows decreasing behavior. This was expected as higher the flash pressure, the closer the vapor pressure to the stripper pressure, which decreases the compression requirement. That is also the reason why the compressor effect is smaller as flash pressure increases. Like the equivalent work case, the compressor effect for CESAR-1 case is higher than that for MEA case. Thus, the same comment can be made, LVC is more effective in MEA. One more parameter was tested to make the conclusion for LVC, the steam savings. In the reference case, by applying LVC in 0.0-0.8 bar(g) flash range, SRD was reduced from 3.05 GJ/ t CO_2 to 2.65 GJ/ t CO_2 in CESAR case, from 3.60 GJ/ t CO_2 to 2.7 GJ/ t CO_2 in MEA case without compressor effect [72]. In our work, this number was 2.94 GJ/ t CO_2 to 2.45 GJ/ t CO_2 for CESAR, and from 3.73 GJ/ t CO_2 to 2.85 GJ/ t CO_2 for MEA. The values are not exactly the same as the reference but they are acceptable.

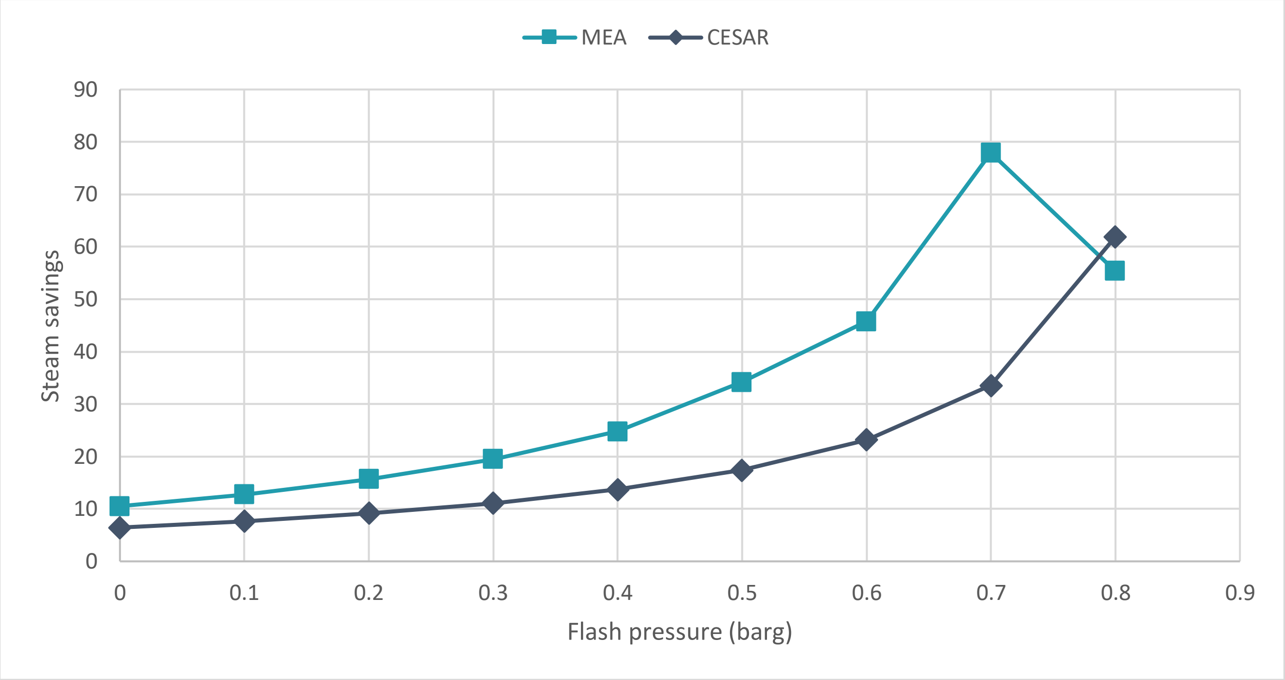

Figure 30: Steam savings

Figure 30 shows the steam savings by using LVC. Savings have been calculated as the steam saved in (kW) per power consumed by the compression (kW). Although both designs seem to save more steam as the flash pressure is increased, the savings with MEA is more than that of CESAR-1. Therefore, it can be concluded that the LVC is more effective in MEA case. It should be pointed out that last point in MEA case seems to be off the trend. The reason could be a simulation error and this point stand as an outlier, or for MEA flash pressure after 0,7 bar(g) would not be suitable.

9.1.4 Final case

In the final case, the effect of combined AIC and LVC was investigated. The optimum cooling temperature, flash pressure and L/G ratio was used, and one final case have been created. Then, the results were validated by J. K. Knudsen at al. [72].

Error! Reference source not found. shows the summary and the validation of the base case, AIC, L VC, and the implementation of both as a final case. The table below summarizes the operating parameters.

Table 15: Final case operating parameters

	MEA	**CESAR-1**
L/G (kg solvent/kg CO_2)	3.5	2.5
Absorber cooling temperature (ºC)	25	25
Flash pressure (bar(g))	0.1	0.1

By the implementation of AIC and LVC as a final case, 0.86 GJ/t CO_2 energy saving was obtained. For the CESAR-1 case, this saving was lower, 0.53 GJ/t CO_2. With the implementations, changing the solvent from MEA to CESAR-1 would give 0.78 GJ/t CO_2 savings.

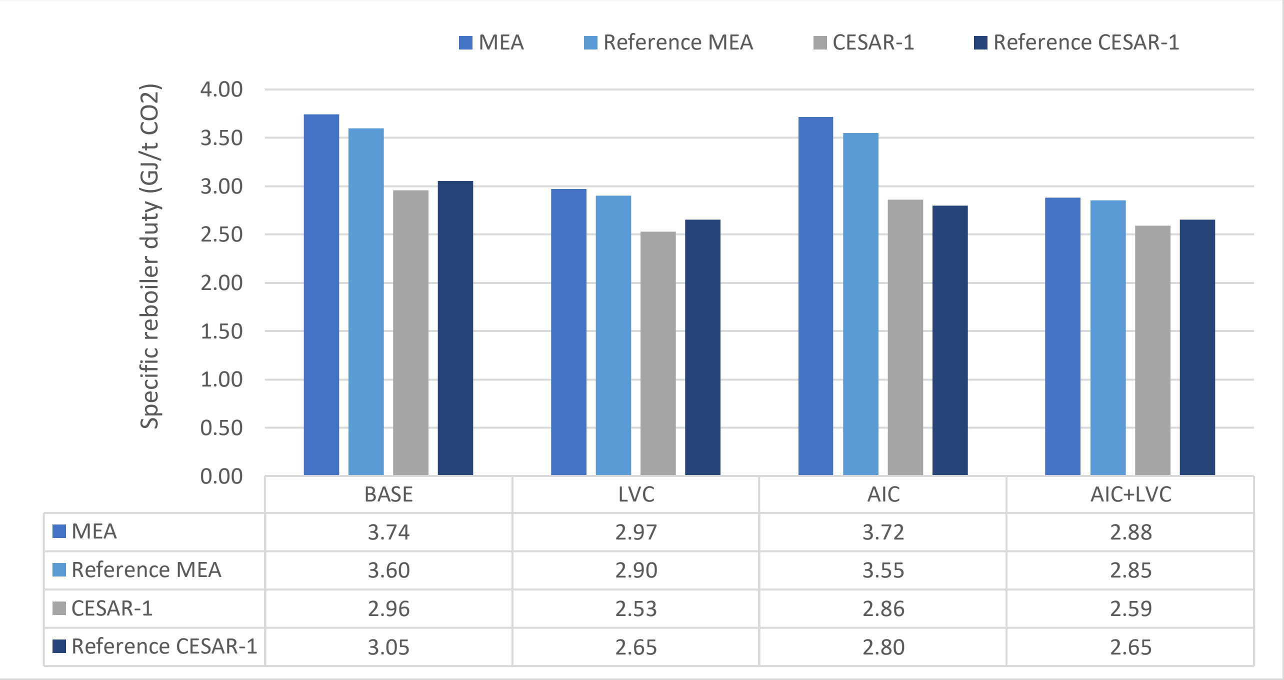

	BASE	LVC	AIC	AIC+LVC
■ MEA	3.74	2.97	3.72	2.88
■ Reference MEA	3.60	2.90	3.55	2.85
■ CESAR-1	2.96	2.53	2.86	2.59
■ Reference CESAR-1	3.05	2.65	2.80	2.65

Figure 31: Final case and the validation with the literature data

For the validation of the results, data from J. K. Knudsen at al. [72] was used. The reported data by authors is the real data from Esbjerg Pilot Plant experiments. The simulation results show to align well with the actual data except for slight variations in some values such as the CESAR-1 case in the AIC. These variations could be due to the fluid package used, or some assumptions made for the missing details in the design of the Esbjerg PCC Pilot Plant.

9.2 Summary of pilot plant studies

The base was a simple, conventional PCC pilot plant simulation where process modifications was made later. The second case included absorber intercooling (AIC), and the third case included lean vapor recompression (LVC) to see the effect of these modifications on the SRD. A final case including both AIC and LVC was simulated, and the results have been compared with the Esbjerg PCC Pilot Plant. As shown in Figure 31: Final case and the validation with the literature data the results from this study align with the results from Esbjerg PCC Pilot Plant. Therefore, we can conclude that the design and the software used in this study is a good reflection of the real/experimental data, and it is suitable for using in study of the big scale production.

9.3 Sensitivity analysis

For commercial size capture plant, sensitivity analyses with 6 parameters including L/G ratio, absorber temperature, stripper pressure, minimum temperature approach, absorber height, and stripper height have been conducted. The results are given in the following sections.

9.3.1 Liquid to gas ratio (L/G)

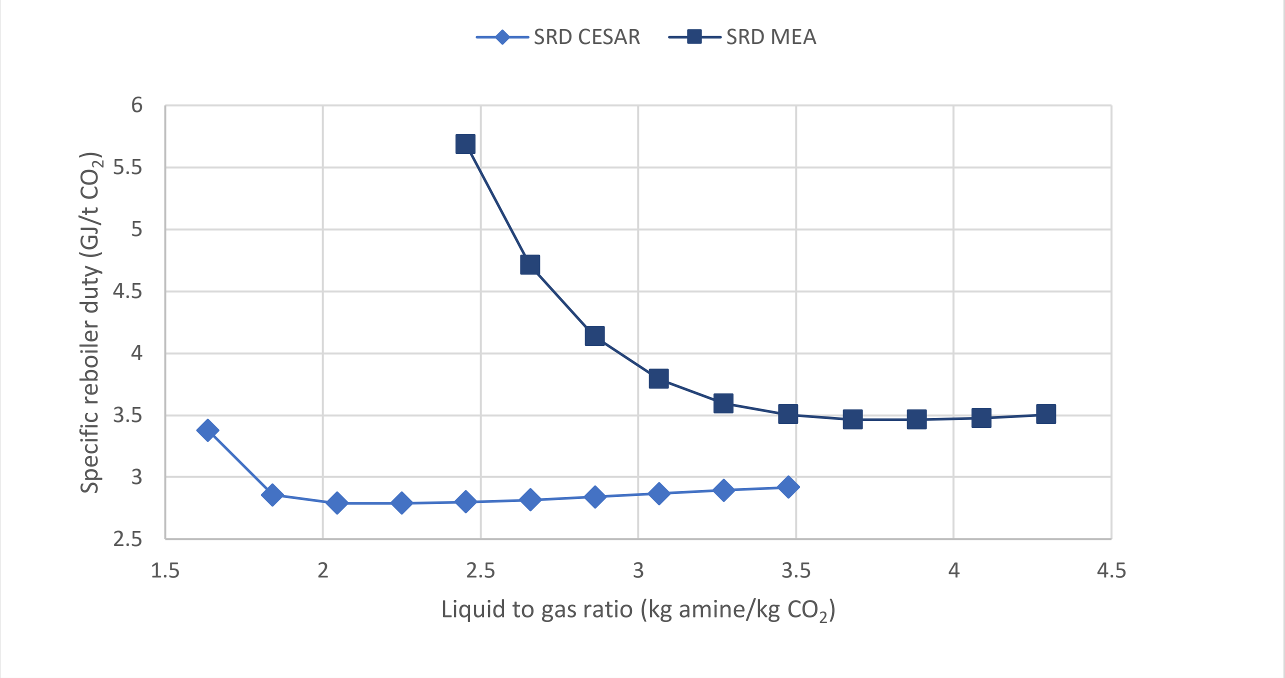

Figure 32: Sensitivity analysis with varied mass-based L/G ratio

This figure shows the sensitivity analysis done by varying the L/G ratio. The operating range for MEA and CESAR is selected differently due to the capacity of the solvent, and as the simulation did not converge with the low L/G ratios for MEA. Selected range for MEA is from 2.40 to 4.30, for CESAR-1, the range is from 1.60 to 4.50. Both MEA and CESAR designs showed similar behavior, decreasing, reaching a minimum and then starting to increase again. At each L/G ratio, CESAR-1 gives smaller SRD than MEA. The L/G ratio giving the smallest SRD, the minimum point, is taken as the optimum, and the other sensitivity analyses run by the optimum L/G. For MEA case, this value is around 3.7 corresponding to 3.5 GJ/t CO_2. For CESAR-1, the optimum L/G is smaller around 2.0 corresponding to 2.8 GJ/t CO_2. Cost of the plant should also be considered to find the optimum L/G, as the L/G ratio giving the smallest SRD might not be the cheapest option.

Many authors studied the effect of L/G in 1.5-4.0 range and found the SRD of MEA to be in the range of 3.0-4.5 GJ/t CO_2, SRD of CESAR to be in the range of 2.5-3.5 GJ/t CO_2 [13] [17] [58] [18]. The optimum L/G is in the same range but changing depending on the process parameters. Therefore, the results from this sensitivity analysis are acceptable based on the literature values.

9.3.2 Absorber feed temperature

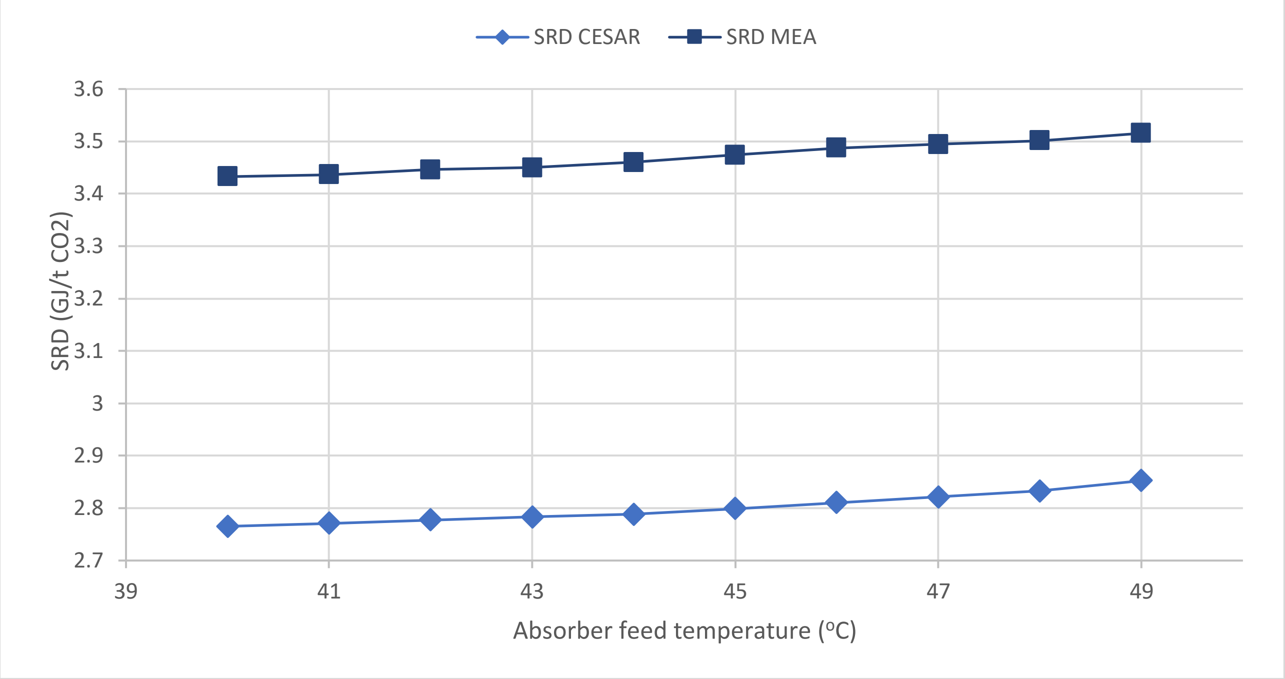

Figure 33: Sensitivity analysis with varied absorber feed temperature

Figure 33 shows how sensitive the design to the absorber feed temperature. SRD shows increasing behavior with increasing temperature in both designs. This was expected as the exothermic absorption reaction would be affected negatively by the increasing temperature. Absorption capacity of the solvent will drop, resulting in higher regeneration requirement. The best condition for both designs seem to be 40°C giving 3.43 GJ/t CO_2 for MEA and 2.76 GJ/t CO_2 for CESAR. It is obvious from the graph that the SRD of MEA is much higher than CESAR in every case.

The reference case [45] studied PCC at 40°C and obtained SRD of 4.16 GJ/t CO_2 for MEA case, and 3.07 GJ/t CO_2 for CESAR-1 case. Values slightly deviate from the reference case but are still in the acceptable range. In most studies for PCC, effect of absorber feed temperature was studied by changing the temperature from 30-60°C and found the optimum value in 40-50 °C with reboiler duties ranging from 3.0 to 4.5 GJ/t CO_2 for MEA and from 2.5 to 3.5 GJ/t CO_2 for CESAR [62] [61] [18] [17] [13]. The optimum values and the SRD are in the reported ranges.

9.3.3 Minimum temperature approach

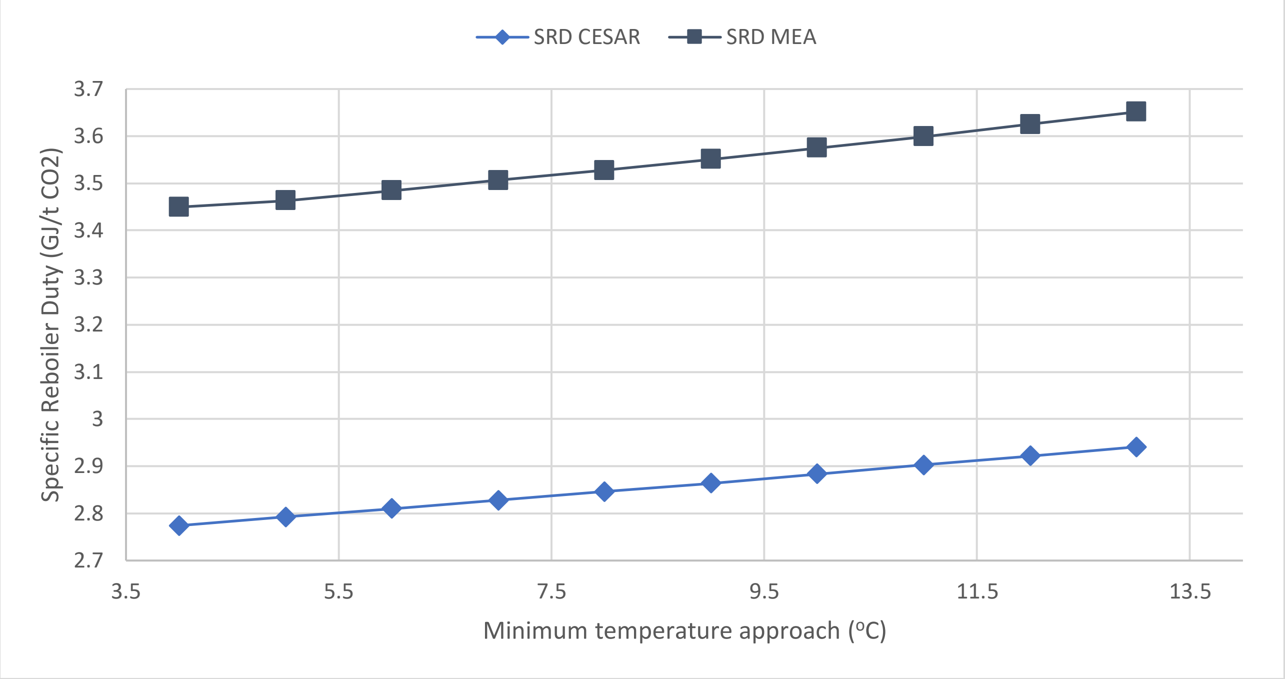

Figure 34: Sensitivity analysis with varied minimum temperature difference

Minimum temperature approach in the lean/rich heat exchanger is another important parameter to be considered. Smaller minimum temperature difference will allow for more heat transfer from ho to cold; therefore, smaller amount of heat will be required by the reboiler. The smaller minimum temperature difference will result in higher equipment as the area needed for the heat transfer would be higher. This temperature difference also influences the stripper feed temperature. Higher temperatures will favor the desorption reaction; however, thermal degradation of the solvent should be considered at high temperatures. Also, as the minimum temperature is decreased, there will be more heat transfer from the hot lean to cold rich which would influence the desorption process. The effect of minimum temperature difference was studied in 4-13°C range. Figure 34 shows the results from the sensitivity analysis. Like absorber feed temperature case, the trend of SRD vs minimum temperature difference is the same for both designs and the lowest SRD is obtained at $\Delta T_{min} = 4^{o}C$ giving 3.45 GJ/t CO_2 for MEA and 2.77 GJ/t CO_2 for CESAR. Cost analysis should also be considered to find the optimum condition for minimum temperature approach.

The reference case [45] used $\Delta T_{min} = 5^{o}C$ and obtained SRD of 4.16 GJ/t CO_2 for MEA case, and 3.07 GJ/t CO_2 for CESAR-1 case. In this study, the SRD values are a bit lower than the reference case but still in the reported range. The reason could be the usage of different process simulation software. In many studies, this effect was investigated in 4-15°C range giving with reboiler duties ranging from 3.0 to 4.5 GJ/t CO_2 for MEA and from 2.5 to 3.5 GJ/t CO_2 for CESAR [69] [65] (Andreasen, Optimisation of carbon capture from flue gas from a Waste- to-Energy plant using surrogate modelling and global optimisation , 2021). Therefore, SRDs and the optimum values found in this study are in the reported ranges.

9.3.4 Stripper pressure

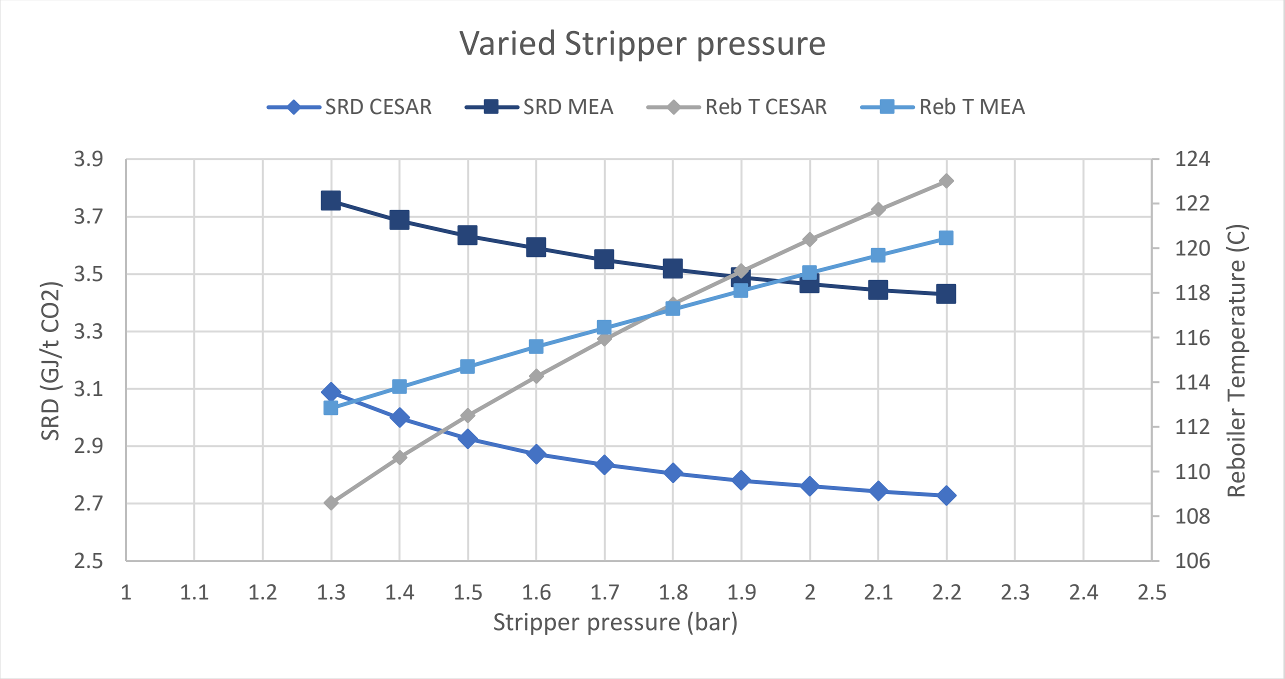

Figure 35:Sensitivity analysis with varied stripper pressure

Stripper pressure has direct effect on the reboiler temperature. The steam demand for regeneration will be lower with higher temperatures in the reboiler. The mass transfer and the reaction rate would also benefit from the higher temperatures. However, temperatures higher than 135°C will cause thermal degradation of the solvent. The effect of stripper pressure was also investigated in the range of 1.3-2.2 bar. Figure 35 shows the sensitivity analysis by varying the stripper pressure. SRD decreases by increasing stripper pressure in both designs whereas the temperature of the reboiler increases. Temperature increase by the CESAR case is more than that of MEA case. SRD could be reduced by 0.32 GJ/t CO_2 with the MEA case, and by 0.36 GJ/t CO_2 with CESAR case. Xue at al. [22] investigated the stripper pressure effect on the reboiler duty in the range of 0.7-2.2

bar and found higher pressures being more beneficial for saving total energy requirement. From lower end to upper end, reboiler duty was reduced by 0.05 GJ/t CO_2 [22].

9.3.5 Stripper height

The range has been selected based on the values used in the literature for big scale carbon capture. As stated in *Absorber and stripper packing height* section, many different stripper heights have been used, mostly in the range of 7.6-28.15 m [66]. It was decided to investigate the stripper height in this range. As a first trial, both simulations studied in the range of 7.5-21 m. However, in the process design as a rule of thumb, the column height/ column diameter ratio should either be 1 or higher [82]. Therefore, to maintain this ratio in MEA design, first 4 data points (from 7.5 m to 12 m) were discarded. In CESAR design, simulation converged starting from the stripper height of 10 m. Therefore, for CESAR design, analysis was performed in a slightly smaller range, 10-19 m. For maintaining the height/diameter ratio around 1 or higher, the first point (10m) in the CESAR design was discarded.

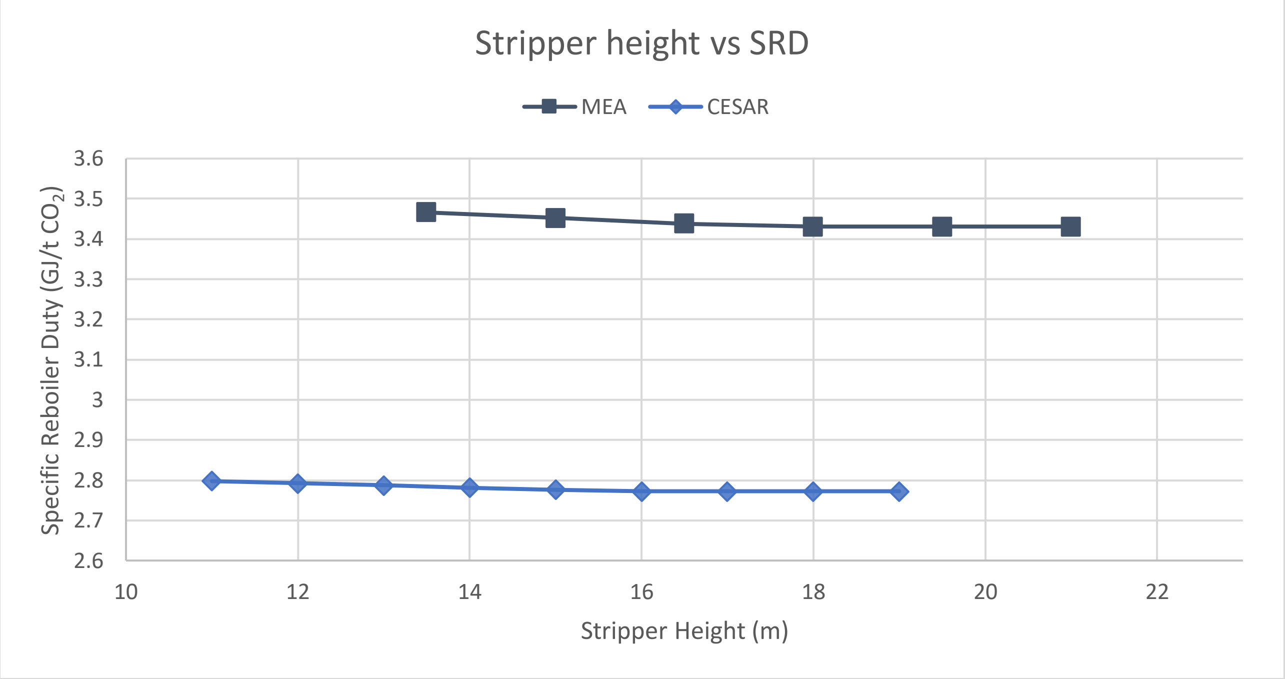

Figure 36: Sensitivity analysis with varied stripper height

Figure 36 shows how SRD is changing by varying height of the stripper column. SRD is expected to decrease by increasing the column height as with higher stripper column, more contact time would be given to the solvent and better mass transfer; therefore, better regeneration would take place. With better regeneration, less steam would be required in the reboiler.

For both designs, striper vs SRD height shows slightly decreasing trend, with being more effective in MEA case. SRD for CESAR remains being lower than MEA. In both designs the effect of stripper column is insignificant. The SRD value lies around 3.4 GJ/t CO_2 for MEA, and around 2.80 GJ/t CO_2 for CESAR. N. Thomas [83] investigated the effect of stripper height in PCC with MEA in 1.5-6.0 m range and observed a decrease from 3.6 to 3.5 GJ/t CO_2. Therefore, slightly more decrease in the SRD was expected.

9.3.6 Absorber height

For the sensitivity analysis with absorber height, the range was selected based on the literature research. It was reported by X. Luo et al. [66] that the absorber heights have been studied in 13.6-30.6 m range for PCC, also based on different studies discussed in the *Absorber and stripper packing height* section, these parameters were selected. For the analysis, absorber height was varied from 12.5 m to 30.0 m for MEA, from 12.0 m to 30.0 m for CESAR. Based on these the same approach as in stripper height has been used for column height/diameter ratio. Therefore, the first point of the MEA analysis was discarded as the diameter was bigger than the height. The same logic applies here, as the absorber height is increased, the contact time and the mass transfer will also increase which would influence the absorption capacity. Therefore, increasing the absorber height is expected to reduce the SRD.

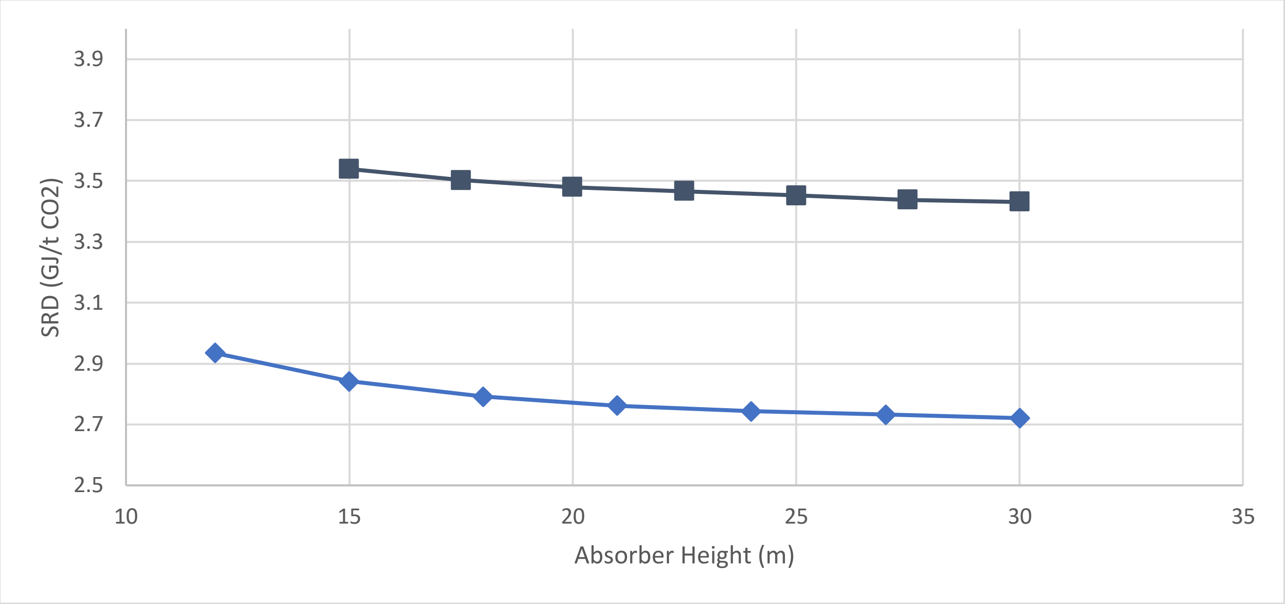

Figure 37: Sensitivity analysis with varied absorber height

Figure 37 shows the results from sensitivity analysis by varying absorber height. Both MEA and CESAR shows decreasing trend as the absorber height is increased which was expected. CESAR gives lower SRD at each data point and shows more significant decreasing trend than MEA. By increasing the absorber height from 12.5 m to 30.0 m, SRD was reduced from 3.59 GJ/t CO_2 to 3.43 GJ/t CO_2 in MEA case, more decrease was observed. By increasing absorber height from 12.0 m to 30.0 m, SRD was reduced from 2.93 GJ/t CO_2 to 2.72 GJ/t CO_2. S. Shirdel et al. [65] varied the absorber height from 18 m to 24 m and observed an SRD decrease from 4.02 GJ/t CO_2 to 3.48 GJ/t CO_2. In their study with PCC with MEA, M. Biermann et al. [84] increased the packing height of the absorber from 11.0 m to 18.0 m and observed 0.1 GJ/t CO_2 decrease in SRD from 3.82 to 3.72 GJ/t CO_2., Based on these values, more decrease was expected in MEA case, yet the results are still meaningful. However, due to the lack of sources studying the effect absorber height for CESAR, validation by literature data could not be done. However, considering the SRD difference between MEA and CESAR, these results for CESAR seem reasonable.

10 Process Economy

In this part of the report, the process economy of the cases in the sensitivity analysis will be discussed. However, due to the amount of data, only the most important results will be highlighted. For the rest of the results, please refer to Appendix.

10.1 Liquid to gas ratio

CAPEX and the total costs of the cases in sensitivity analysis were calculated to have a better overview on the best design parameter in techno-economic way. Figure 38 shows the CAPEX calculated for each case in the sensitivity analysis done by varying the solvent recirculation rate. In each case, CESAR-1 has lower CAPEX than MEA. However, the cost does not have a specific trend over different L/G ratios, but it is obvious that at higher L/G ratios, the cost is higher. The reason for that might be the requirement for bigger equipment due to higher solvent flow. For the CESAR case, the minimum CAPEX was obtained when the L/G was 1.84, with 172.25 million €. This is not the same optimum selected only by looking at the SRD, but it is very close. MEA case shows the same behavior, giving the minimum CAPEX at a lower L/G = 2.66.

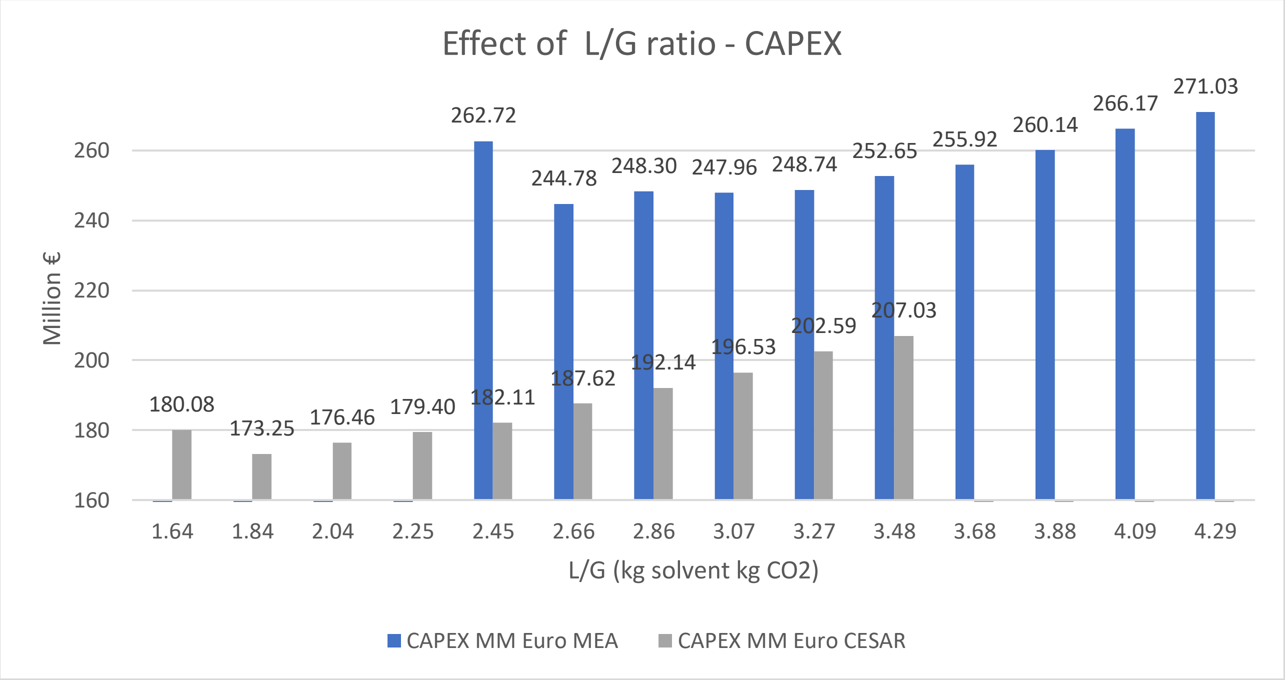

Figure 38: CAPEX – L/G ratio effect

In Figure 39, the OPEX estimations for the different L/G ratios are shown. The trend is the same as CAPEX but the costs are closer to each other compared to CAPEX.. As the L/G ratio increases, the reboiler duty decreases. Therefore, the steam requirement will be lower which lowers the OPEX. However, increasing the L/G ratio more than adequate would result in increase in the OPEX as more solvent will be recirculating in the system which would increase the electricity requirement of the pumps and the cooling water requirement. Also, it should be considered that the OPEX is calculated based on CAPEX, and as CAPEX increases, OPEX would increase too. However, design with lower OPEX would be more logical in the long term as the payback time would probably be smaller with lower OPEX although the CAPEX not the smallest for that specific case. For example, operating at L/G=3.48 for MEA will be more logical in the long run as it gives the smallest OPEX.

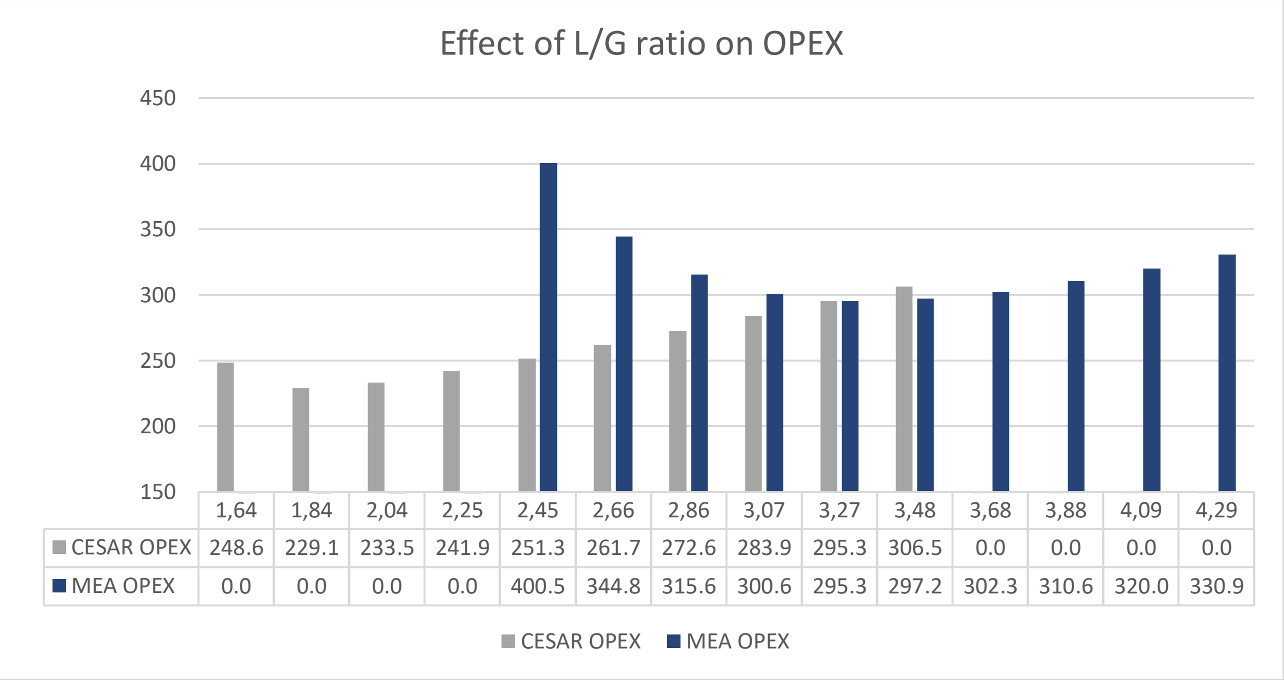

	1,64	1,84	2,04	2,25	2,45	2,66	2,86	3,07	3,27	3,48	3,68	3,88	4,09	4,29
■ CESAR OPEX	248.6	229.1	233.5	241.9	251.3	261.7	272.6	283.9	295.3	306.5	0.0	0.0	0.0	0.0
■ MEA OPEX	0.0	0.0	0.0	0.0	400.5	344.8	315.6	300.6	295.3	297.2	302.3	310.6	320.0	330.9

Figure 39:OPEX – L/G ratio effect

Figure 40 and Figure 41 show the OPEX distribution for CESAR and MEA, respectively. The three biggest contributors for the OPEX in both designs are solvent make-up, cooling water, and the LP steam for reboiler. Solvent make-up in the CESAR design makes up 39% of the total OPEX, while in MEA design this is 11%. The reason for that difference is the higher cost of AMP and PZ which are the components of CESAR solvent. LP steam requirement for the reboiler accounts for the 17% of OPEX for CESAR, and 29% of OPEX for MEA. This was expected as the SRD required in for MEA is higher than CESAR, therefore, more steam would be needed in the reboiler. The cooling water requirement is extremely high, it accounts for the 39% of OPEX of CESAR, and 48% of OPEX of MEA. This was unexpected and the reason is not known, and the optimization is definitely needed.

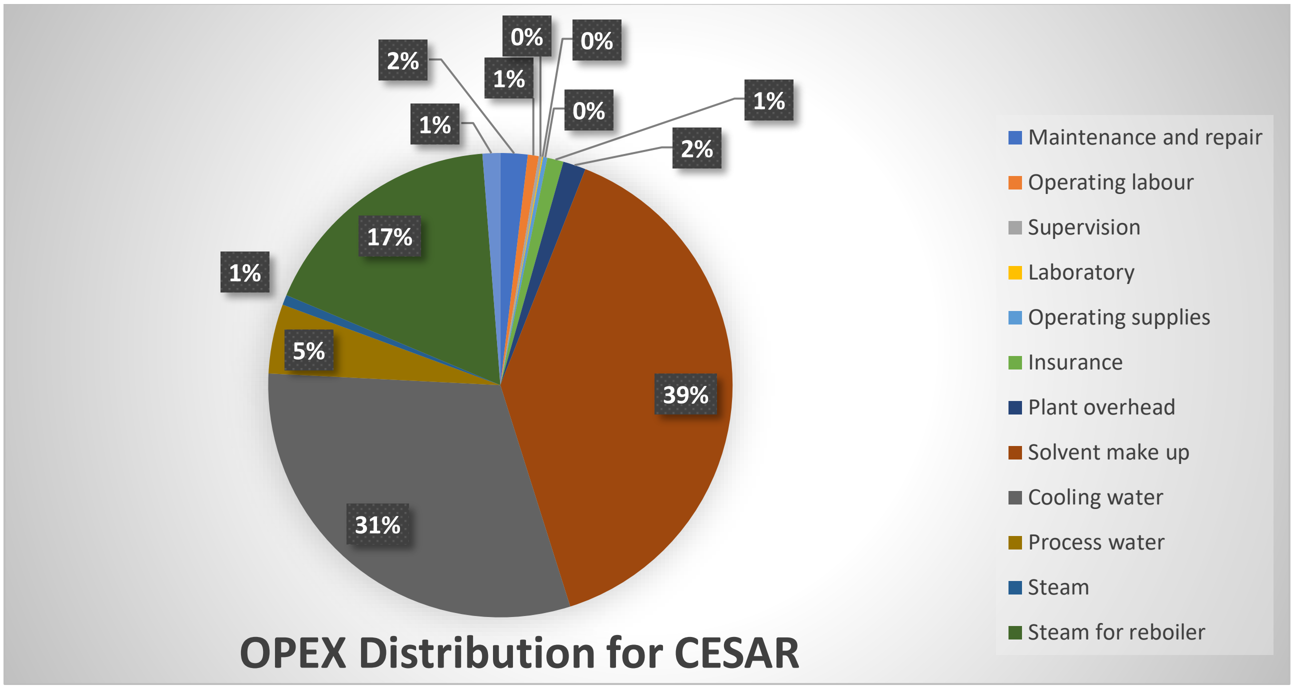

Figure 40: OPEX distribution for CESAR with varied L/G

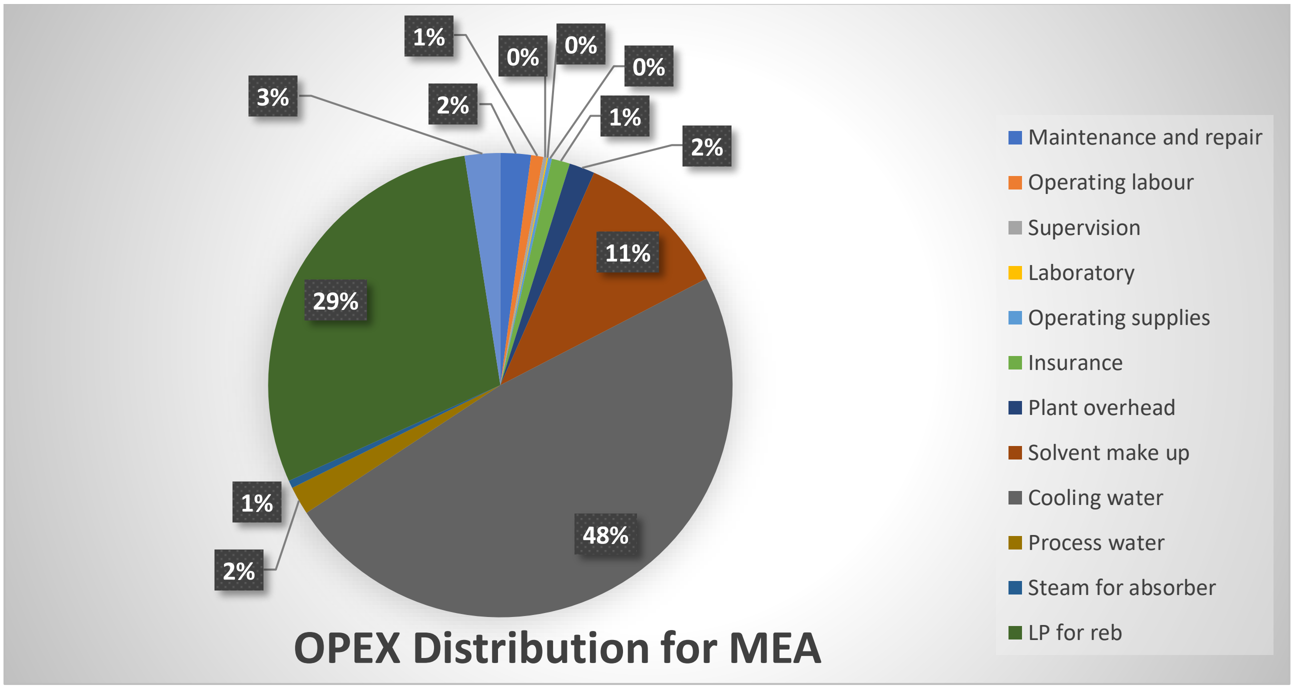

Figure 41: OPEX distribution for MEA with varied L/G

Figure 42 shows the total investment for both designs. The trend is the same as CAPEX and OPEX, and the lowest total investment is obtained at L/G=1.84 for CESAR case, and at 3.27 for MEA case. As mentioned before, the lowest OPEX is more beneficial in the long term. Thus, smallest total investment might not be the optimum choice.

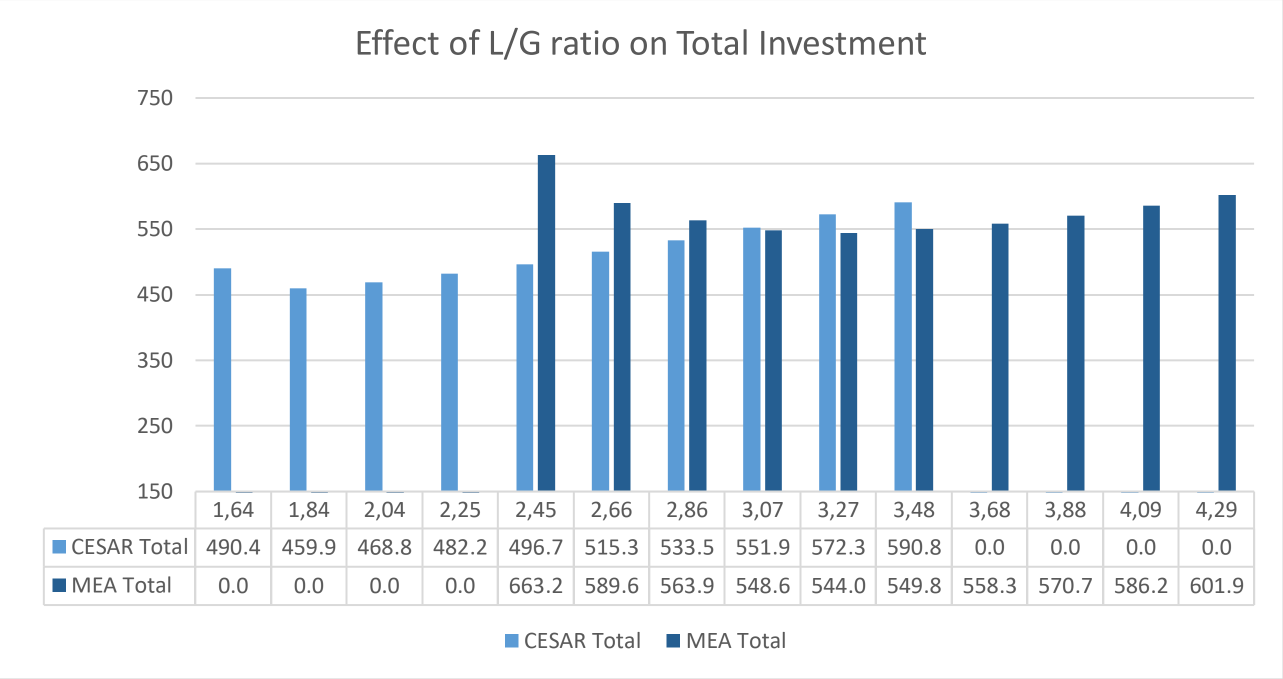

	1,64	1,84	2,04	2,25	2,45	2,66	2,86	3,07	3,27	3,48	3,68	3,88	4,09	4,29
■ CESAR Total	490.4	459.9	468.8	482.2	496.7	515.3	533.5	551.9	572.3	590.8	0.0	0.0	0.0	0.0
■ MEA Total	0.0	0.0	0.0	0.0	663.2	589.6	563.9	548.6	544.0	549.8	558.3	570.7	586.2	601.9

Figure 42: Effect of L/G ratio on total investment

10.2 Minimum temperature difference/approach

Another parameter that has a significant impact on the cost is minimum temperature difference in the lean/rich heat exchanger. As the minimum temperature difference between the cold inlet and hot outlet decreases, the heat exchanger area required for the heat transfer increases, therefore, we should expect to see an increase in the CAPEX. The results from the CAPEX estimation are shown in Figure 43. As expected, CAPEX for both designs decreases by increasing minimum temperature approach. Around 48 million €, and 18 million € saving could be possible by decreasing the minimum temperature difference from 13^{o}C to 4^{o}C in the case of MEA and CESAR, respectively. S. Shirdel et al. [65] investigated the effect of minimum temperature approach on the CAPEX in 5.5-15 ^{o}C range and observed reduction from 31.41 €/t CO_2 to 30.29 €/t CO_2.

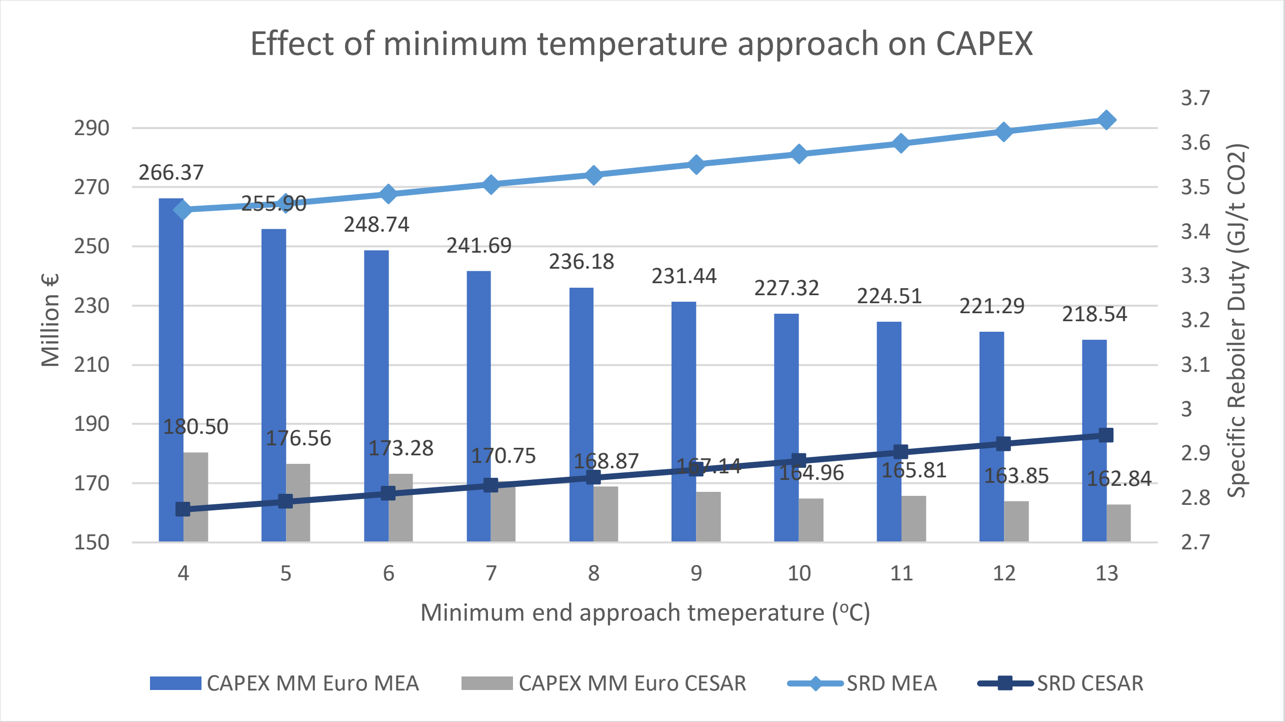

Figure 43: Effect of minimum temperature difference on CAPEX

In Figure 44 the effect of minimum temperature difference on OPEX is shown. For both MEA and CESAR, the minimum OPEX was obtained at 4 °C. The same trend was observed in both designs, OPEX decreases by decreasing minimum temperature approach. This was expected as the minimum temperature difference decreases, reboiler duty decreases which would result in less steam requirement. This is due to the more heat transfer from hot to cold at lower minimum temperatures differences.

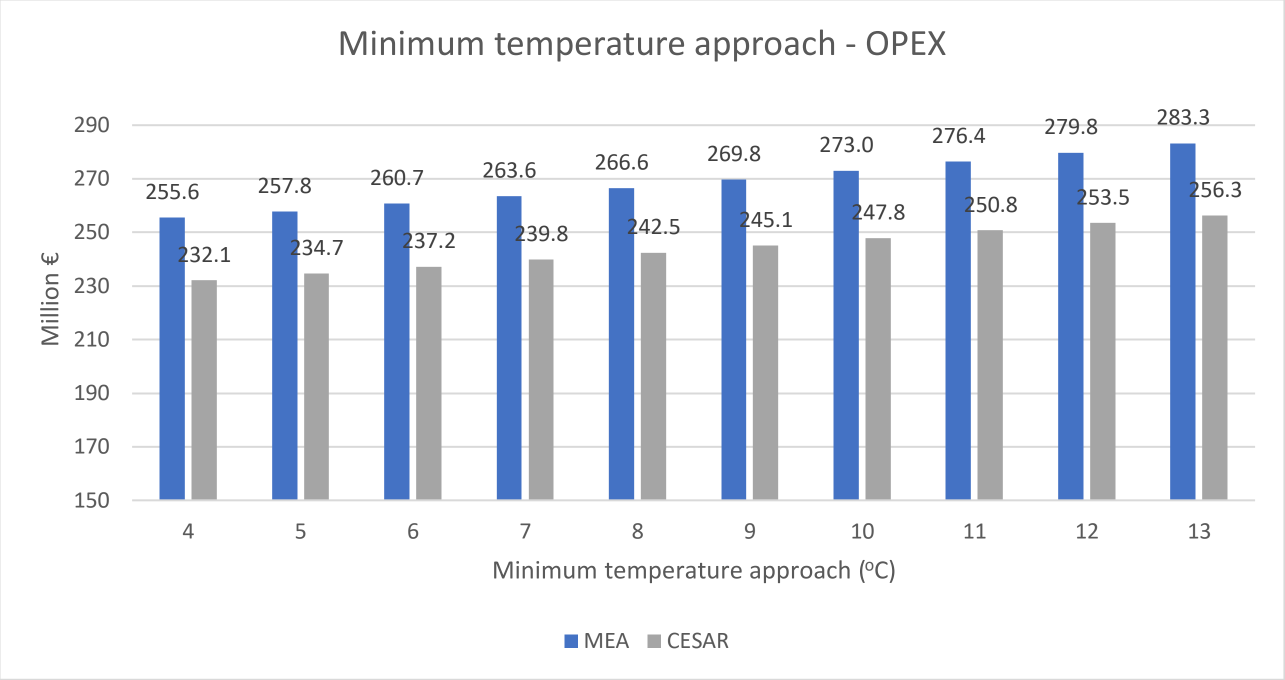

Figure 44: Effect of minimum temperature difference on OPEX

Figure 45 and Figure 46 show the break down of the OPEX. The same distribution as in is observed as sensitivity analysis with L/G is observed here, too. As discussed before, LP steam requirement will be higher at higher minimum temperature differences which would influence the OPEX. Figure 47 shows the total investment for both designs. Total investment for CESAR shows slightly increasing trend with increasing minimum temperature difference whereas that for MEA shows decreasing trend. This is due to the higher CAPEX difference in the lower and upper end for MEA design. Total investment does not change significantly at different temperature approaches. As discussed before, even though the total investment for greater temperature approach is smaller, in the long-term choosing the value with low OPEX will benefit more.

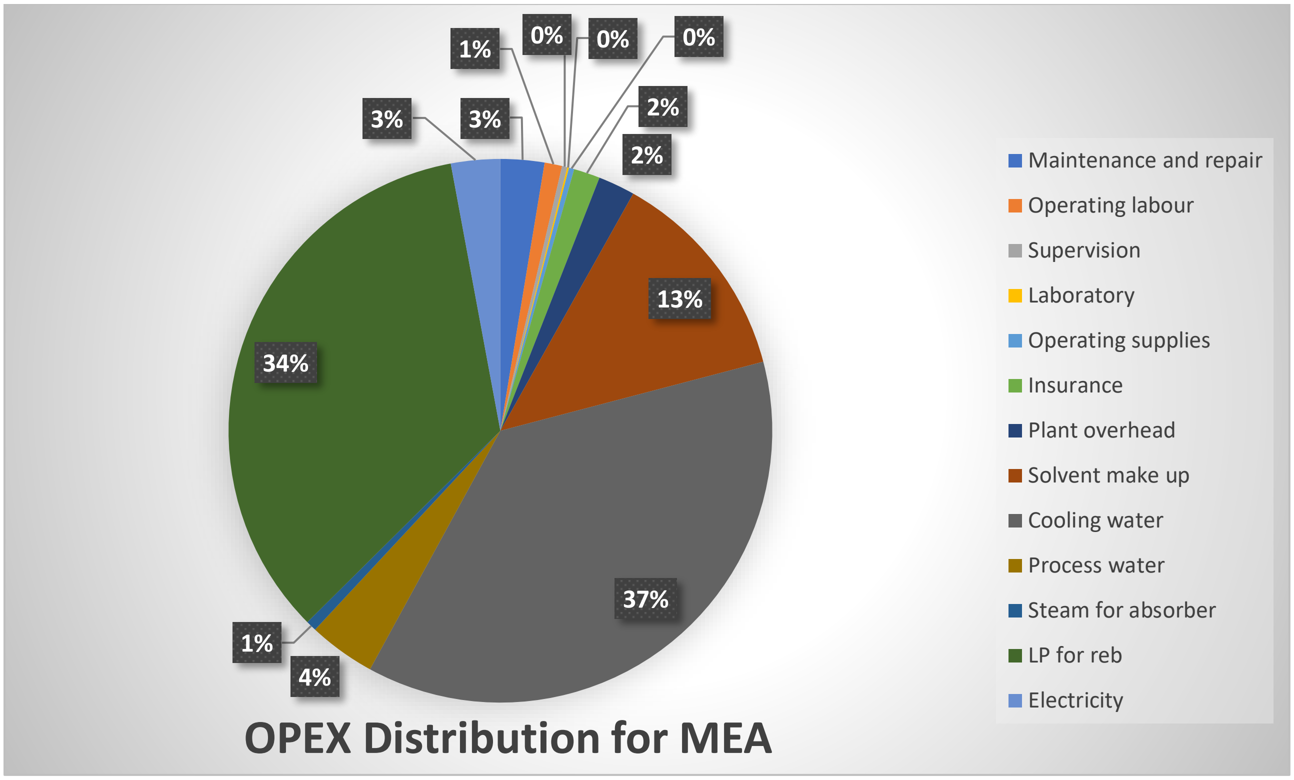

Figure 45: OPEX distribution for MEA at different minimum temperature differences

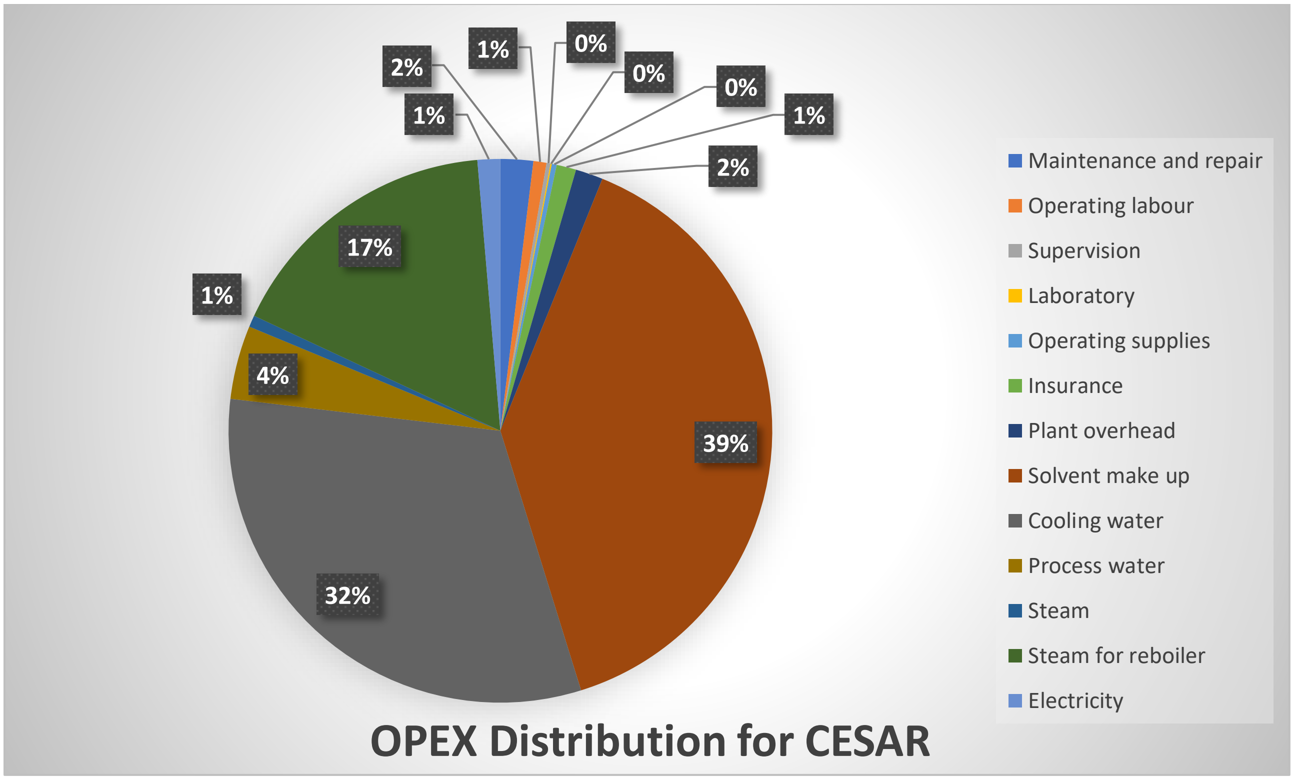

Figure 46: OPEX distribution for CESAR at different minimum temperature differences

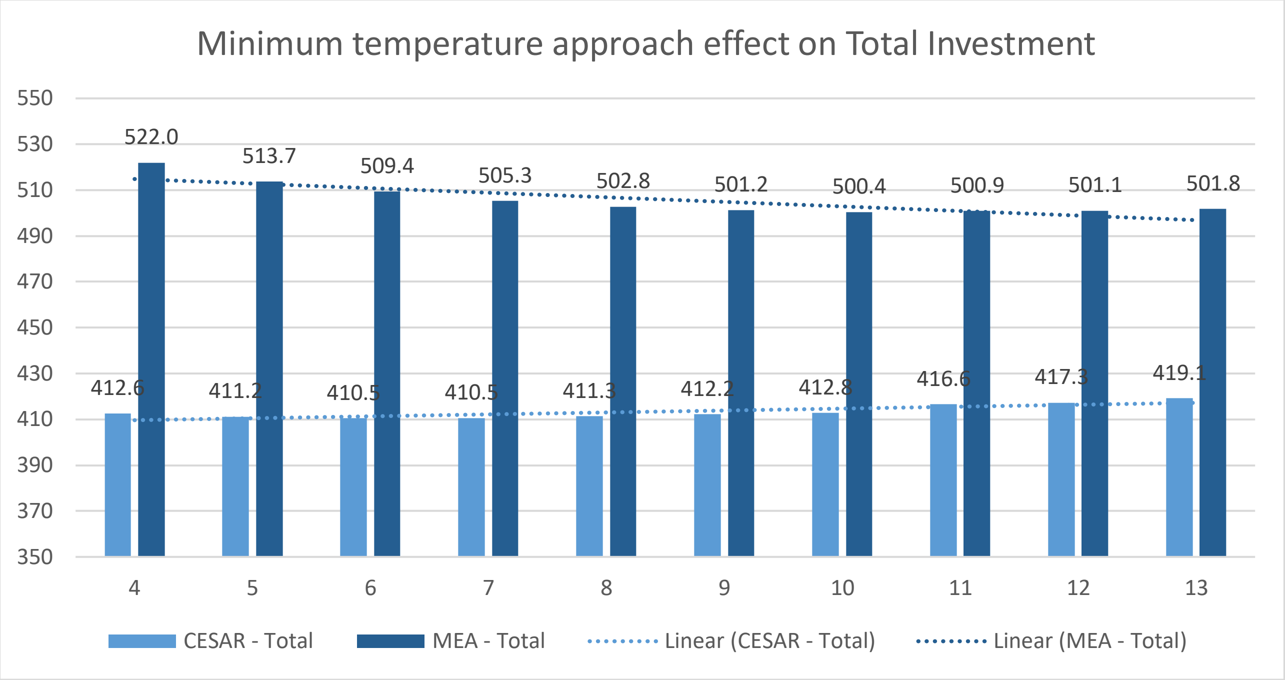

Figure 47: Effect of minimum temperature difference on total investment

10.3 Stripper pressure

The effect of stripper pressure was investigated from 1.3 bar to 2.2 bar. The smallest CAPEX of 255.7 million € is obtained at 1.9 bar for MEA, and 175.2 million € at 2.1 bar for CESAR. Although stripper pressure did not influence the CAPEX significantly, it was decided to make a comment about it as the CAPEX trends were not the same for MEA and CESAR. CAPEX trend for MEA showed decreasing trend in the first half of the sensitivity analysis, then it started showing increasing trend whereas CAPEX for CESAR showed decreasing trend through the analysis. Increasing stripper pressure decreases the SRD, therefore smaller reboiler will be needed. Due to this, smaller CAPEX might be expected. However, increasing stripper pressure will also result in different sizes of the pumps which also influences the CAPEX. The bigger the pressure difference the higher the pump size thus higher the CAPEX. Increase in the stripper pressure would also lead to a smaller stripper column, but the higher column thickness might be needed to withstand the increased stress in the column. Therefore, more detailed analysis is needed to investigate these different trends. S. Warudkar et al. [63] has studied the influence of stripper pressure on the process of PCC with amine solvent in the pressure range of 1.5-3.0 bar in ProMax. It was reported that bigger stripper columns are needed at lower pressures, which would increase CAPEX. Therefore, the CESAR-1 design looks more reasonable.

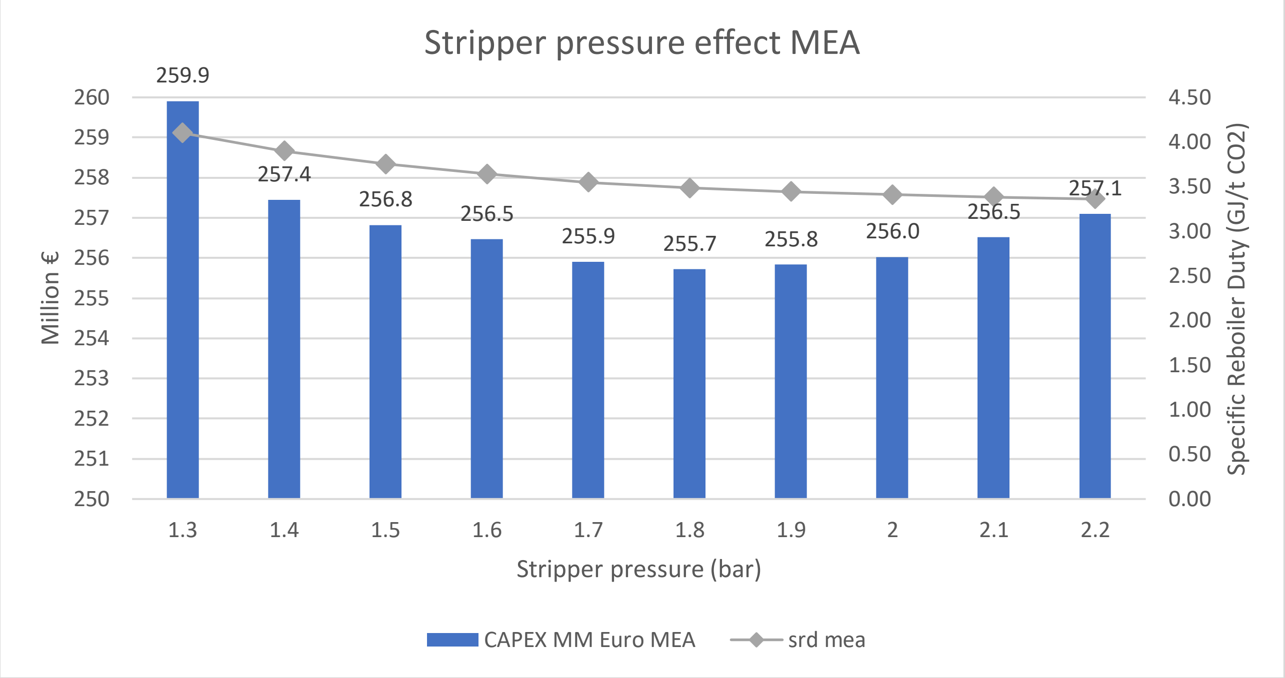

Figure 48: Effect of minimum temperature difference on CAPEX - MEA

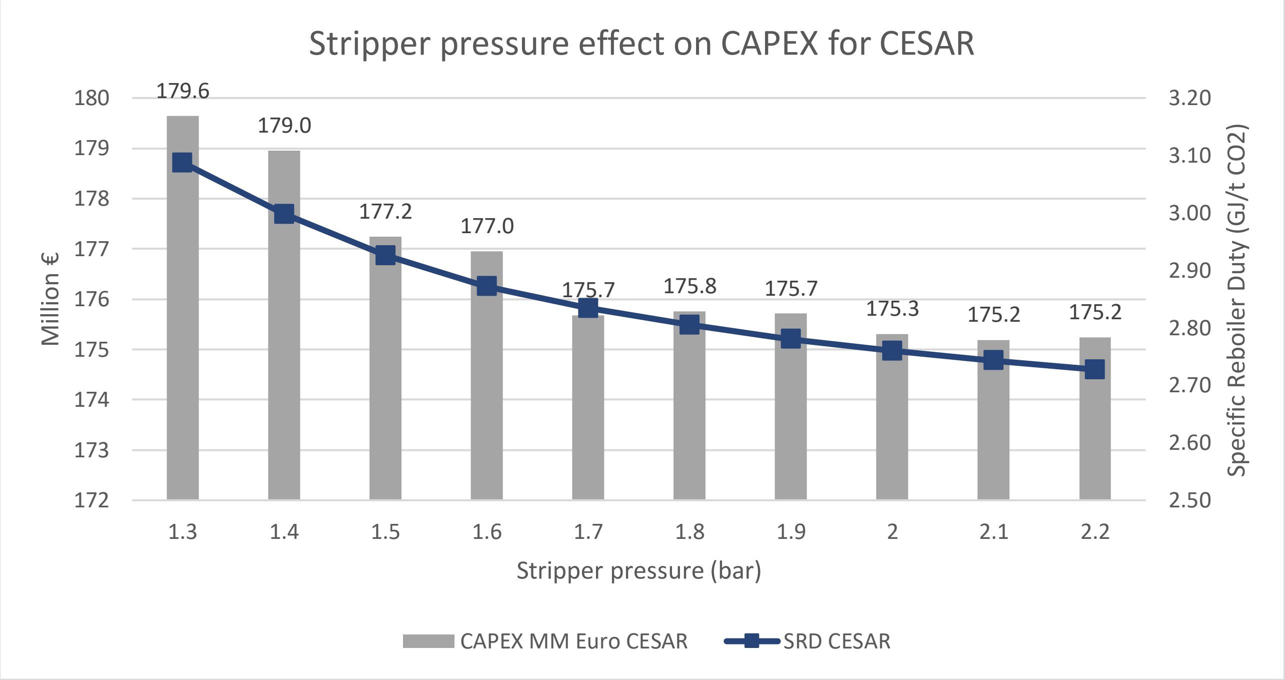

Figure 49:Effect of minimum temperature difference on CAPEX – CESAR

Figure 50 shows the effect of stripper pressure on OPEX. The trend is the same for both MEA and CESAR and the lowest OPEXs were obtained at 2.2 bar. Smaller SRD at higher pressures resulted in smaller OPEX. However, it should also be considered that the stripper pressure leads to temperature increase in the reboiler which may cause solvent degradation. Figure 51 and Figure 52 represent the distribution of OPEX which shows the same trend as in different L/G and minimum temperature approach. The biggest contributors are the cooling water, LP steam, and the solvent make-up.

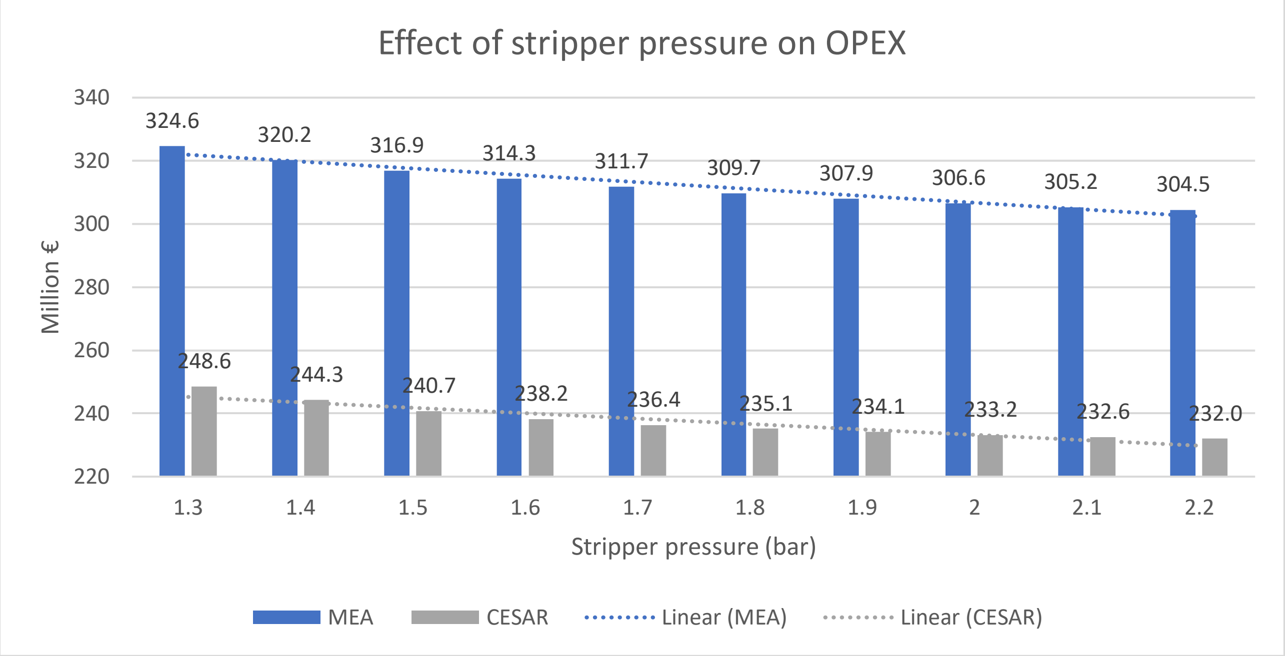

Figure 50: Effect of minimum temperature difference on OPEX

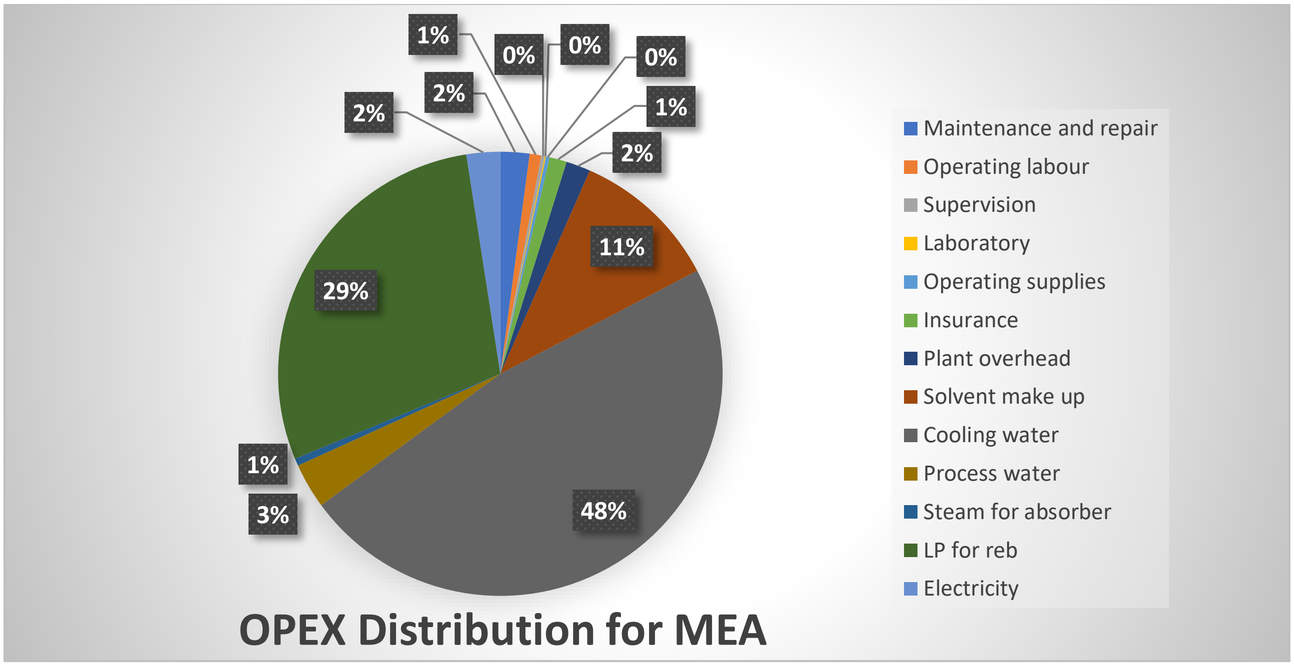

Figure 51:OPEX distribution for MEA at different stripper pressures

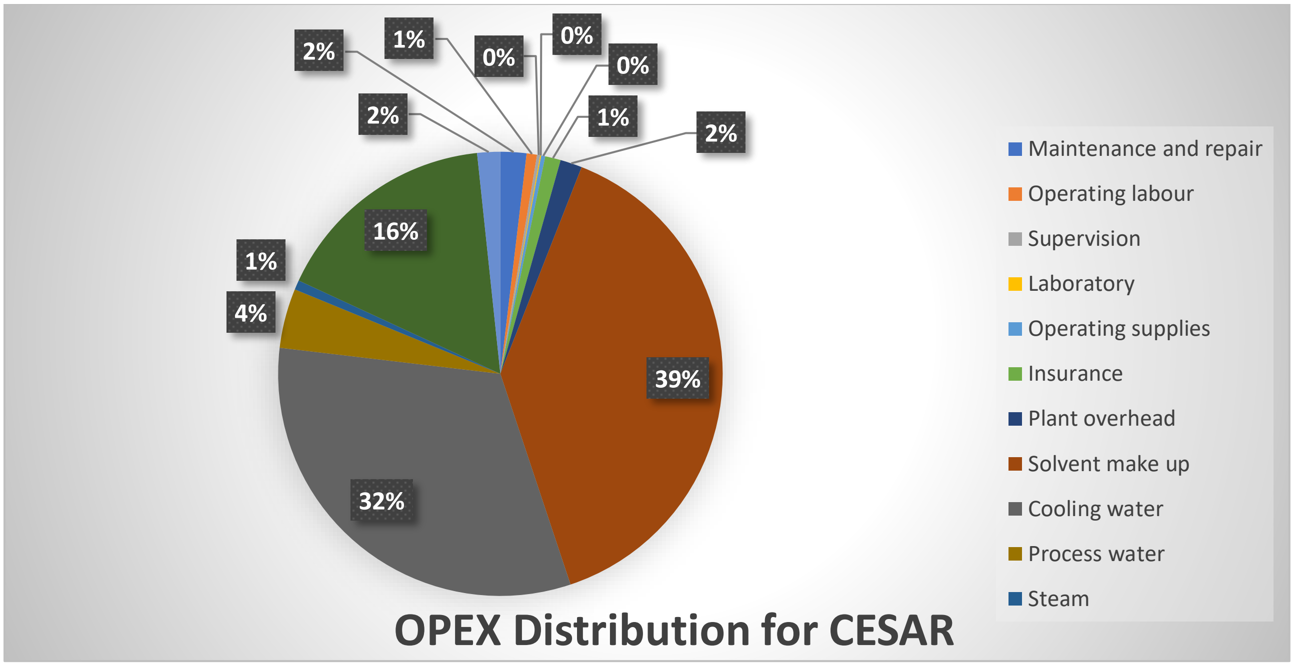

Figure 52: OPEX distribution for CESAR at different stripper pressures

The total investment shows the similar trend for both designs, but it decreases slightly more rapidly for MEA. More data points might be needed to find when we would observe the solvent degradation by increased reboiler temperature. However, with these data points, 2.2 bar pressure seem to be optimum for both designs.

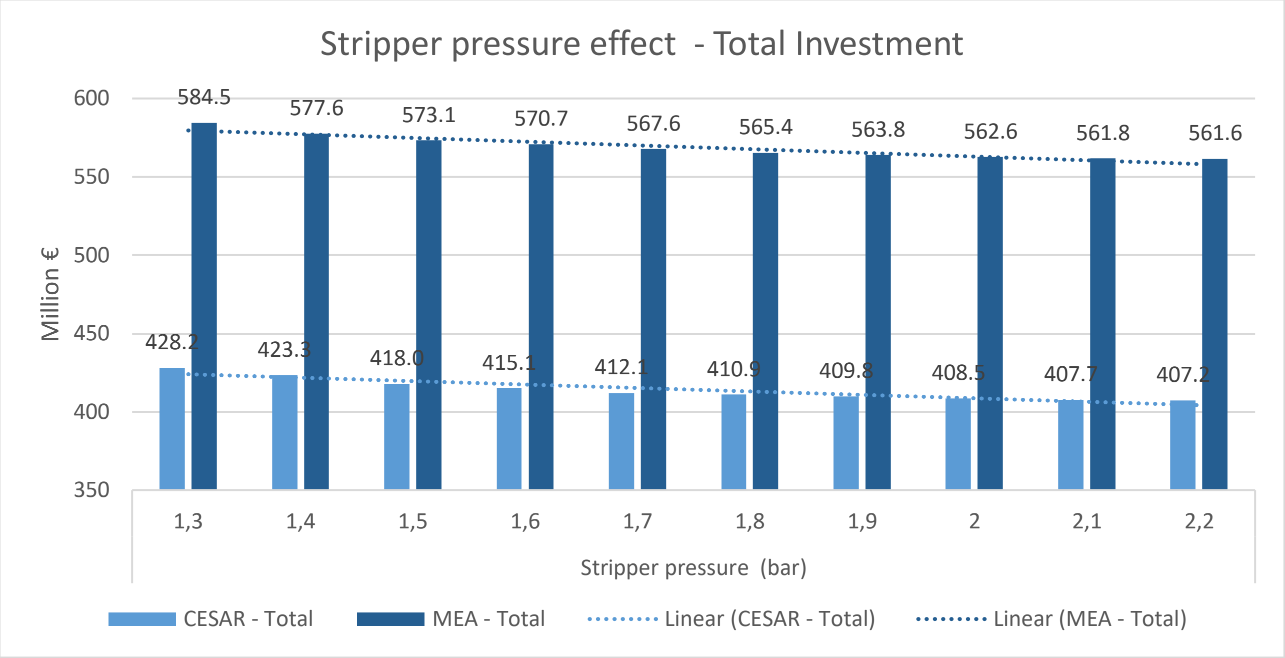

Figure 53: Effect of stripper pressure on total investment

10.4 Summary

The optimum L/G could be taken as 1.84 for CESAR-1 and 3.48 for MEA based on the costs. Optimum minimum temperature difference for both cases can be the lower end, $\Delta T_{min} = 4^{o}C$. Optimum stripper pressure is found as the higher end of the studied range, P=2.2 bar. The reference case [45] studied the PCC at $\Delta T_{min} = 5^{o}C$, and stripper pressure of 1.8 bar. The L/G ratio was not reported. With these values, the reported the CAPEX and OPEX of MEA is 172.98 M€ and 29.2 M€ and those of CESAR is 154.01 M€ and 35.05 M€. CAPEX value of CESAR is close to the reference value but the MEA is a lot higher. Different assumptions and methods in CAPEX estimation might be the reason of this difference. However, OPEX is extremely higher than the reference. As discussed, very high cooling water cost has a big contribution in the high OPEX. This could be overcome by locating the plant close to the water source and using the water from that source. However, then extra cost for desalination or water treatment plant will be added to the process economy. Alternatively, heat integration could be considered as absorption is exothermic, and desorption is endothermic process and extensive heat loss could be possible.

11 Conclusions

This project was a techno-economic evaluation of an absorption-based post combustion carbon capture. In this project, technical and economic performance of CESAR-1 solvent investigated and then benchmarked with most used solvent, MEA. The aim was to investigate at which conditions, CESAR-1 solvent is able to operate with lower reboiler duty and give low CAPEX and OPEX compared to MEA. First of all, pilot plant studies were performed to see if the design is suitable for big scale production. As a reference, Esbjerg Post-combustion Carbon Capture Pilot Plant was chosen, and conventional carbon capture and some process modifications were simulated. Based on the pilot plant results, it was concluded that the design reflects the reality well and it can be used for bigger scale studies. Real flue gas data from a big scale power plant was used while scaling up. To find the best operating conditions and to see the effect of different parameters on the design, sensitivity analyses were performed. It was found that L/G ratio of 3.75 gives to 3.5 GJ/t CO_2 SRD for MEA which was the best L/G in the sensitivity analysis. For CESAR-1, the optimum L/G is smaller around 2.0 corresponding to 2.8 GJ/t CO_2. Absorber feed temperature of 40°C was found to be the best condition for both designs giving 3.43 GJ/t CO_2 for MEA and 2.76 GJ/t CO_2 for CESAR. Minimum temperature difference of at $\Delta T_{min} = 4^oC$ gave the best results of SRD, 3.45 GJ/t CO_2 for MEA and 2.77 GJ/t CO_2 for CESAR. For the sensitivity analysis done by stripper pressure, 2.2 bar was found to be the best condition for both designs giving SRD of 3.43 GJ/t CO_2 with the MEA, and 2.73 GJ/t CO_2 with CESAR. The effect of stripper height was insignificant, the SRD lied around 3.40 GJ/t CO_2 for MEA, and around 2.80 GJ/t CO_2 for CESAR. The effect of absorber height was found to be more significant in the case of CESAR. For both designs, absorber height of 30 m showed the smallest SRD, 3.43 GJ/t CO_2 in MEA case and 2.72 GJ/t CO_2 in CESAR case. After sensitivity analysis, process economy was also investigated. CAPEX and OPEX was calculated for both designs. In every case, CAPEX and OPEX of CESAR were smaller than those of MEA. The most significant effect in the cost observed with varied L/G, and minimum temperature difference. For the rest of the parameters, cost lied around the same values with slight changes. For varied L/G ratios, the smallest cost was obtained at 1.84 for CESAR corresponding to 460 million €, and at 3.21 for MEA corresponding to 544 million €. $\Delta T_{min} = 13^o$ gave the smallest total cost of 419 million € for CESAR and 502 million € for MEA. However, the lowest CAPEX was obtained at $\Delta T_{min} = 4^o$. OPEX was very high in every case as the cooling requirement was very high. This result was off limit and unrealistic; however the reason is not known. Some solutions cold include heat integration and locating the plant to a near a water source so the water could be utilized from the source instead of purchasing. However, this would also bring additional water treatment cost.

To sum up, in every case SRD and CAPEX of CESAR was lower than MEA as expected. Thus, it can be used as a good alternative instead of state-of-art solvent, MEA. The optimum operating conditions should be further investigated, and profitability analysis should be made in the further work.

12 Bibliography

[1] "NASA Earth Observatory," NASA, 14 January 2022. [Online]. Available: https://earthobservatory.nasa.gov/images/149321/2021-continued-earths-warming-trend. [Accessed 18 May 2023].

[2] A. Olhoff, J. Christensen, W. F. Lamb, G. Grassi, :. T. Kuramochi, M. d. Elzen, T. Fransen, M. d. Elzen, J. Rogelj, J. Portugal-Pereira, N. Höhne, K. Levin, J. Roy, A. Mosnier and M. Springmann, "Emissions Gap Report 2022: The Closing Window," United Nations Environment Programme, 2022.

[3] "EPA United States Environmental Protection Agency," United States Environmental Protection Agency, [Online]. Available: https://www.epa.gov/ghgemissions/global-greenhouse-gas-emissions-data. [Accessed 18 May 2023].

[4] "C2ES Center for Climate and Energy Solutions," [Online]. Available: https://www.c2es.org/content/carbon-capture/. [Accessed 18 May 2023].

[5] E. Serin, "The London School of Economics and Political Science," Grantham Research Institute, 13 March 2023. [Online]. Available: https://www.lse.ac.uk/granthaminstitute/explainers/what-is-carbon-capture-and-storage-and-what-role-can-it-play-in-tackling-climate-change/. [Accessed 18 May 2023].

[6] D. M. Rabensteiner, "Evaluation of CO2 absorption solvents for post-combustion capture on the basis of pilot plant studies on hard coal-fired power plants," Graz University of Technology, Graz, 2016.

[7] Z. Chen, "A Review of Pre-combustion Carbon Capture Technology," in *Proceedings of the 2022 7th International Conference on Social Sciences and Economic Development (ICSSED 2022)*, Wuhan, 2022.

[8] J. Ciferno, J. Klara and J. Wimer, "CCS Economic Analyses: Outlook for Carbon Capture from Pulverized Coal and Integrated Gasification Combined Cycle Power Plants," Pittsburgh, 2007.

[9] N. S. M. Hatta, M. K. Aroua, F. Hussin and L. T. Gew, "A Systematic Review of Amino Acid-Based Adsorbents for CO2 Capture," *Energies,* vol. 15, no. 3753, 2022.

[10] M. K. GADOGBE, "COST-EFFECTIVENESS ANALYSIS (CEA) OF PROJECTED IMPACT OF CARBON CAPTURE AND STORAGE (CCS) TECHNOLOGIES IN ANTHROPOGENIC CLIMATE CHANGE MITIGATION," June 2014. [Online]. Available: https://www.researchgate.net/publication/312070045_COST-EFFECTIVENESS_ANALYSIS_CEA_OF_PROJECTED_IMPACT_OF_CARBON_CAPTURE_AND_STORAGE_CCS_TECHNOLOGIES_IN_ANTHROPOGENIC_CLIMATE_CHANGE_MITIGATION. [Accessed 31 May 2023].

[11] X. Wang and C. Song, "Carbon Capture From Flue Gas and the Atmosphere: A Perspective," *Frontiers Energy Research,* vol. 8, 2020.

[12] N. R. Sukor, A. H. Shamsuddin, T. M. I. Mahlia and M. F. M. Isa, "Techno-Economic Analysis of CO2 Capture Technologies in Offshore Natural Gas Field: Implications to Carbon Capture and Storage in Malaysia," *Processes,* vol. 8, no. 350, 2020.

[13] H. Hasse and H. P. Mangalapally, "Pilot Plant Experiments for Post Combustion Carbon Dioxide Capture by Reactive Absorption with Novel Solvents," *Energy Procedia,* vol. 4, pp. 1-8, 2011.

[14] A. S. Ahmed, M. R. Rahman and M. K. B. Bakri, "A Review Based on Low- and High-Stream Global Carbon Capture and Storage (CCS) Technology and Implementation Strategy," *Journal of Applied Science & Process Engineering,* vol. 8, no. 1, pp. 722-737, 2021.

[15] A. v. d. Haar, C. Trapp, K. Wellner, R. d. Kler and G. Schmitz, "Dynamics of Postcombustion CO2 Capture Plants: Modeling, Validation, and Case Study," *Industrial & Engineering Chemistry Research,* no. 56, pp. 1810-1822, 2017.

[16] S. S. Uhre, "The Effect of the Absorber Design and Operating Conditions on the MEA Emissions and Energy Consumption in an Absorption-Based Carbon Capture Plant," NTNU, 2021.

[17] J. N. Knudsen and J. N. J. Jimmy Andersen, "Results from test campaings at the 1 t/h CO2 PCC pilot plant in Esbjerg under the EU FP7 CESAR project," CESAR project EU, Esbjerg, 2011.

[18] W. Zhang, J. Chena, X. Luob and M. Wang, "Modelling and Process Analysis of Post-combustion Carbon Capture with a Novel Solvent of the blend of 2-amino-2-methyl-1-propanol (AMP) and Piperazine (PZ)," *International Journal of Greenhouse Gas Control,* vol. 63, pp. 37-46, 2017.

[19] D. Sachde and G. T. Rochelle, "Absorber Intercooling Configurations using Aqueous Piperazine for Capture from Sources with 4 to 27% CO2," *Energy Procedia,* no. 63, pp. 1637-1656, 2014.

[20] S. Reddya, J. R. Scherffius, J. Yonkoski, P. Radgen and H. Rode, "Initial Results from Fluor’s CO2 Capture Demonstration Plant Using Econamine FG PlusSM Technology at E.ON Kraftwerke’s Wilhelmshaven Power Plant," *Energy Procedia,* no. 37, pp. 6216-225, 2013.

[21] H.-T. Oh, Y. Ju, K. Chung and C.-H. Lee, "Techno-economic analysis of advanced stripper configurations for post-combustion CO2 capture amine processes," *Energy,* no. 206, 2020.

[22] B. Xue, Y. Yu, J. Chen, X. Luo and M. Wang, "A comparative study of MEA and DEA for post-combustion CO2 capture with different process configurations," *International Journal of Coal Science and Technology,* vol. 1, no. 4, pp. 15-24, 2017.

[23] J. Salazar, U. Diwekar, K. Joback, A. H. Berger and A. S. Bhown, "1.1 Solvents 1.1.1 State of art solvents 1.1.1.1 Thermal and oxidative degradation 1.1.1.2 Viscosity 1.1.2 Potential solvents," *Energy Procedia,* vol. 37, pp. 257-264, 2013.

[24] T. Yelland, "Carbon Clean," Carbon Clean, 17 August 2021. [Online]. Available: https://www.carbonclean.com/blog/solvent-based-carbon-capture. [Accessed 20 February 2023].

[25] M. T. Mota-Martinez, J. P. Hallett and N. M. Dowell, "Solvent selection and design for CO2 capture – how we might have been missing the point," *Sustainable Energy and Fuels*, no. 1, pp. 2078-2090, 2017.

[26] F. Meng, Y. Meng, T. Ju, S. Han, L. Lin and J. Jiang, "Research progress of aqueous amine solution for CO2 capture: A review," *Renewable and Sustainable energy Reviews*, no. 168, 2022.

[27] P. A. Smith and E. Block, "Encyclopedia Britannica," 6 February 2018. [Online]. Available: https://www.britannica.com/science/amine. [Accessed 20 February 2023].

[28] U. S. P. R. Arachchige, B. Singh, K. Prajapati and M. C. Melaaen, "Viscosities of Aqueous Solutions of Monoethanolamine (MEA), Diethanolamine (DEA) and N-Methyldiethanolamine (MDEA) at T = (90-150) °C," *ANNUAL TRANSACTIONS OF THE NORDIC RHEOLOGY SOCIETY*, vol. 22, pp. 185-190, 2014.

[29] "Merck," Merck KGaA, [Online]. Available: https://www.sigmaaldrich.com/DK/en/substance/piperazine8614110850. [Accessed 31 May 2023].

[30] "MERCK," Merck KGaA, [Online]. Available: https://www.merckmillipore.com/DK/en/product/2-Amino-2-methyl-1-propanol,MDA_CHEM-801465. [Accessed 31 May 2023].

[31] P.-C. Chen, J.-H. J. Hsun-Huang Cho and C.-H. Ku, "Selection of Mixed Amines in the CO2 Capture Process," *Journal of Carbon Research* , 2021.

[32] I. M. Bernhardsen and H. K. Knuutila, "A Review of potential amine solvents for CO2 absorption process: Absorption capacity, cyclic capacity and pKa," Trondheim, 2017.

[33] D. Tong, G. C. Maitlanda, M. J. Truslera and P. S. Fennell, "Solubility of carbon dioxide in aqueous blendsof 2-amino-2-methyl-1-propanol and piperazine," *Chemical Engineering Science,* no. 101, pp. 851-864, 2013.

[34] "DOW," [Online]. Available: https://www.dow.com/en-us/pdp.monoethanolamine-mea.87914z.html#tech-content. [Accessed 20 February 2023].

[35] C. Zhang, "Absorption principle and techno-economic analysis of CO2 absorption technologies: A review," in *IOP Conf. Series: Earth and Environmental Science*, China, 2021.

[36] M. v. d. Speka, R. Arendsen, A. Ramireza and A. Faaij, "Model development and process simulation of postcombustion carbon capture technology with aqueous AMP/PZ solvent," *International Journal of Greenhouse Gas Control,* no. 47, pp. 176-199, 2016.

[37] H. P. Mangalapally and H. Hasse, " Pilot Plant Experiments for Post Combustion Carbon Dioxide Capture by Reactive Absorption with Novel Solvents," *Energy Procedia,* no. 4, pp. 1-8, 2011.

[38] P. Tontiwachwuthikul, A. Meisen and C. Lim, "Oz ABSORPTION BY NaOH, MONOETHANOLAMINE AND 2-AMINO-2-METHYL-l-PROPANOL SOLUTIONS IN A PACKED COLUMN," *Chemical Engineering Science,* vol. 47, no. 2, pp. 381-390, 1992.

[39] W.-J. Choi, J.-B. Seo, S.-Y. Jang, J.-H. Jung and K.-J. Oh, "Removal characteristics of CO2 using aqueous MEA/AMP solutions in the absorption and regeneration process," *Journal of Environmental Sciences,* no. 29, pp. 907-913, 2009.

[40] T. Wang and Klaus-J.Jens, "Oxidative degradation of aqueous PZ solution and AMP/PZ blends for post-combustion carbondioxide capture," *International Journal of Greenhouse Gas Control,* no. 24, pp. 98-105, 2014.

[41] S. K. Dash, A. Samanta, A. N. Samanta and S. S. Bandyopadhyay, "Absorption of carbon dioxide in piperazine activated concentrated aqueous 2-amino-2-methyl-1-propanol solven," *Chemical Engineering Science,* vol. 66, pp. 3223-3233, 2011.

[42] S. A. Freeman, "Thermal Degradation and Oxidation of Aqueous Piperazine," Austin, 2011.

[43] S. Zhou, S. Wang and C. Chen, "Thermal Degradation of Monoethanolamine in CO2 Capture with," *Industrial & Engineering Chemistry Research,* no. 51, pp. 2539-2547, 2012.

[44] M. Campbell, S. Akhter, A. Knarvik, M. Zeeshan and A. Wakaa, "CESAR1 Solvent degradation and thermal reclaiming results from TCM testing," in *CESAR1 Solvent degradation and thermal reclaiming results from TCM testing*, Lyon, 2022.

[45] E. S. Fernandez, "NOVEL PROCESS DESIGNS TO IMPROVE THE EFFICIENCY OF POSTCOMBUSTION CARBON DIOXIDE CAPTURE," Delft University of Technology, Delft, 2013.

[46] G. S. Hwang and E. P. D. M. Haley M. Stowe, "Reaction mechanisms of aqueous monoethanolamine with carbon dioxide: a combined quantum chemical and molecular dynamics study," *Physical Chemistry Chemical Physics* , no. 17, pp. 831-839.

[47] B. Lv, B. Guo, Z. Zhou and G. Jing, "Mechanisms of CO2 Capture into Monoethanolamine Solution with Different CO2 loading during the Absorption/Aesorption Processes," *Environmental Science Technology,* no. 49, pp. 10728-10735, 2015.

[48] E. P. d. Silva and H. F. Svendsen, "Computational chemistry study of reactions, equilibrium and kinetics of chemical CO2 absorption," *International Journal of Greenhouse Gas Control,* vol. 1, no. 2, pp. 151-157, 2007.

[49] H. BOSCH, G. F. VERSTEEG and W. P. M. V. SWAAIJ, "KINETICS OF THE REACTION OF CO, WITH THE STERICALLY HINDERED AMINE 2-AMINO-2-METHYLPROPANOL at 298 K," *Chemical Engmeering Science,* vol. 45, pp. 1163-1173, 1990.

[50] C. Research, "AMP and MEA Carbamate Stability Comparison," CETRI, [Online]. Available: https://www.cetri.ca/amp-and-mea-carbamate-stability-comparison. [Accessed 15 May 2023].

[51] Y. Artantoa, J. Jansena, P. Pearsona, G. Puxty, A. Cottrell, E. Meulemana and P. Feron, "Pilot-scale evaluation of AMP/PZ to capture CO2 from flue gas of an Australian brown coal–fired power station," *International Journal of Greenhouse Gas Control,* no. 20, pp. 189-195, 2014.

[52] J. Ying, S. Raets and D. Eimera, "The Activator Mechanism of Piperazine in Aqueous Methyldiethanolamine Solutions," *Energy Procedia,* no. 114, pp. 2078-2087, 2017.

[53] L. E. Øi, "Comparison of Aspen HYSYS and Aspen Plus simulation of CO2 absorption into MEA from atmospheric gas," *Energy Procedia,* vol. 23, pp. 360-369, 2012.

[54] W. K. Lewis and W. G. Whitman, "Principles of Gas Absorption," *Industrial and Engineering Chemistry,* vol. 16, pp. 1215-1220, 1924.

[55] J. R. Welty, G. L. Rorrer and D. G. Foster, Fundamentals of Momentum, Heat, and Mass Transfer, New York: Wiley, 2014.

[56]

[57] I. Tönnies, H. P. Mangalapally and H. Hasse, "Pilot plant studies of new solvents for post combustion CO2 capture," Frankfurt, 2011.

[58] T. Singhal and S. D. Manjare, "Modelling Studies on Reactive Absorption of Carbon Dioxide in Monoethanolamine Solution from Flue Gas in Coal Based Thermal Power Plants," *Journal of Sustainable Development of Energy, Water and Environment Systems,* vol. 6, no. 3, pp. 481-493, 2018.

[59] K. Bochon and T. Chmielniak, "Energy and economic analysis of the carbon dioxide capture installation with the use of monoethanolamine and ammonia," *Archives of thermodynamics,* vol. 36, pp. 93-110, 2015.

[60] S. S. Uhre, "The Effect of the Absorber Design and Operating Conditions on the MEA Emissions and Energy Consumption in an Absorption-Based Carbon Capture Plant," Trondheim, 2021.

[61] A. Andreasen, *Oil & Gas Science and Technology,* vol. 76, no. 55, 2021.

[62] G. Léonard, "Optimal design of a CO2 absorption unit and assessment of solvent degradation," Liege, 2011.

[63] S. S. Warudkar, K. R. Cox, M. S. Wong and G. J. Hirasaki, "Influence of stripper operating parameters on the performance of amine absorption systems for post-combustion carbon capture: Part II. Vacuum strippers," *International Journal of Greenhouse Gas Control,* 2013.

[64] C. Nwaohaa, M. Beaulieu, P. Tontiwachwuthiku and M. D. Gibson, "Techno-economic analysis of CO2 capture from a 1.2 million MTPA cement plant using AMP-PZ-MEA blend," *International Journal of Greenhouse Gas Control,* no. 78, pp. 400-412, 2018.

[65] S. Shirdel, S. Valand, F. Fazli, B. Winther-Sørensen, S. A. Aromada, S. Karunarathne and L. E. Øi, "Sensitivity Analysis and Cost Estimation of a CO2 Capture Plant in Aspen HYSYS," *ChemEngineering,* vol. 6, no. 28, 2022.

[66] X. Luo and M. Wang, "Improving Prediction Accuracy of a Rate-Based Model of an MEA-Based Carbon Capture Process for Large-Scale Commercial Deployment," *Engineering,* vol. 3, no. 2, 2017.

[67] O. B. Kallevik, "Cost estimation of CO2 removal in HYSYS," Porsgrunn, 2010.

[68] U. S. P. R. Arachchig, M. Mohsin and M. C. Melaaen, "Optimized Carbon Dioxide Removal Model for Gas Fired Power Plant," *European Journal of Scientific Research,* vol. 86, no. 3, pp. 348-359, 2012.

[69] S. A. Aromada, N. H. Eldrup, F. Normann and L. E. Øi, "Simulation and Cost Optimization of different Heat Exchangers for CO2 Capture," in *Proceedings of SIMS*, 2020.

[70] A. VARANASI, "State of the Planet," Columbia CLimate School, Climate Earth and Society, 27 September 2019. [Online]. Available: https://news.climate.columbia.edu/2019/09/27/carbon-capture-technology/. [Accessed 18 May 2023].

[71] "European Comission CORDIS EU research results," 31 May 2011. [Online]. Available: https://cordis.europa.eu/project/id/213569. [Accessed 18 May 2023].

[72] J. N. Knudsen, J. Andersen, J. N. Jensen and O. Biede, " Evaluation of process upgrades and novel solvents for the post combustion CO2 capture process in pilot-scale," *Energy Procedia,* vol. 4, pp. 1558-1565, 2011.

[73] J. N. Knudsen, J. N. Jensen, P.-J. Vilhelmsen and O. Biede, "Experience with CO2 capture from coal flue gas in pilot-scale: Testing of different amine solvents," *Energy Procedia,* vol. 4, pp. 783-790, 2009.

[74] P. Brúder, A. Grimstvedt, T. Mejdell and H. F. Svendsen, "CO2 capture into aqueous solutions of piperazine activated 2-amino-2-methyl-1-propanol," *Chemical Engineering Science* , vol. 66, no. 3, pp. 6193-6198, 2011.

[75] H. Li, P. T. Frailie, G. T. Rochelle and J. Chen, "Thermodynamic modeling of piperazine/2-aminomethylpropanol/CO2/water," *Chemical Engineering Science,* vol. 117, no. 331-341, 2014.

[76] H. M. Kvamsdal, G. Haugen, H. F. Svendsen, A. Tobiesen, H. Mangalapally, A. Hartono and T. Mejdell, "Modelling and simulation of the Esbjerg pilot plant using the Cesar 1 solvent," *Energy Procedia,* no. 4, pp. 1644-1651, 2011.

[77] N. Sipöcz and F. A. Tobiesen, "Natural gas combined cycle power plants with CO2 capture – Opportunities to reduce cost.," *Int. J. Greenhouse Gas Control,* vol. 7, pp. 98-106, 2012.

[78] E. O. Agbonghae, K. J. Hughes, L. M. D. B. Ingham and M. Pourkashanian, The University of Sheffield , Sheffield, 2014.

[79] D. R. Woods, Rules of Thumb in Engineering Practice, John Wiley & Sons, 2007.

[80] A. Andreasen, Interviewee, *CAPEX tool by Rambøll which uses Woods and EDF method.* [Interview]. 2021 March 2023.

[81] S. A. Aromada, N. H. Eldrup and L. E. Øi, "Capital cost estimation of CO2 capture plant using Enhanced Detailed Factor (EDF) method: Installation factors and plant construction ccharacteristic factors," *International Journal of Greenhouse Gas Control,* vol. 110, no. 103394, 2021.

[82] C. Madeddu, M. Errico and R. Baratti, "Process analysis for the carbon dioxide chemical absorption–regeneration system," *Applied Energy,* no. 215, pp. 532-542, 2018.

[83] T. Nyssen, "Modelisation and optimisation of a CO2 capture process with a new benchmark solvent for the Sart-Tilman cogeneration plant," University of Liege , Liege, 2022.

[84] M. Biermann, F. Normann, F. Johnsson, R. Hoballah and K. Onarheim, "Capture of CO2 from Steam Reformer Flue Gases Using Monoethanolamine: Pilot Plant Validation and Process Design for partial capture," *Industrial Engineering & Chemistry Research,* no. 62, pp. 14305-14323, 2022.

[85] A. 1. Kohl and R. B. Nielsen, Gas Purification, Texas: Gulf Publishing Company, 1997.

[86] B. Xue, Y. Yu, J. Chen, X. Luo and M. Wang, "A comparative study of MEA and DEA for post-combustion CO2 capture with different process configurations," *International Journal of Coal Science and Technology,* vol. 4, no. 1, pp. 15-24, 2017.

[87] H.-B. Xie, Y. Zhou, Y. Zhang and J. K. Johnson, "Reaction Mechanism of Monoethanolamine with CO2 in Aqueous Solution from Molecular Modelling," *The Journal of Physical Chemistry A,* no. 114, pp. 11844-11852, 2010.

13 Appendix

This appendix includes the cost analysis of Absorber Feed Temperature, Stripper Height, and Absorber Height.

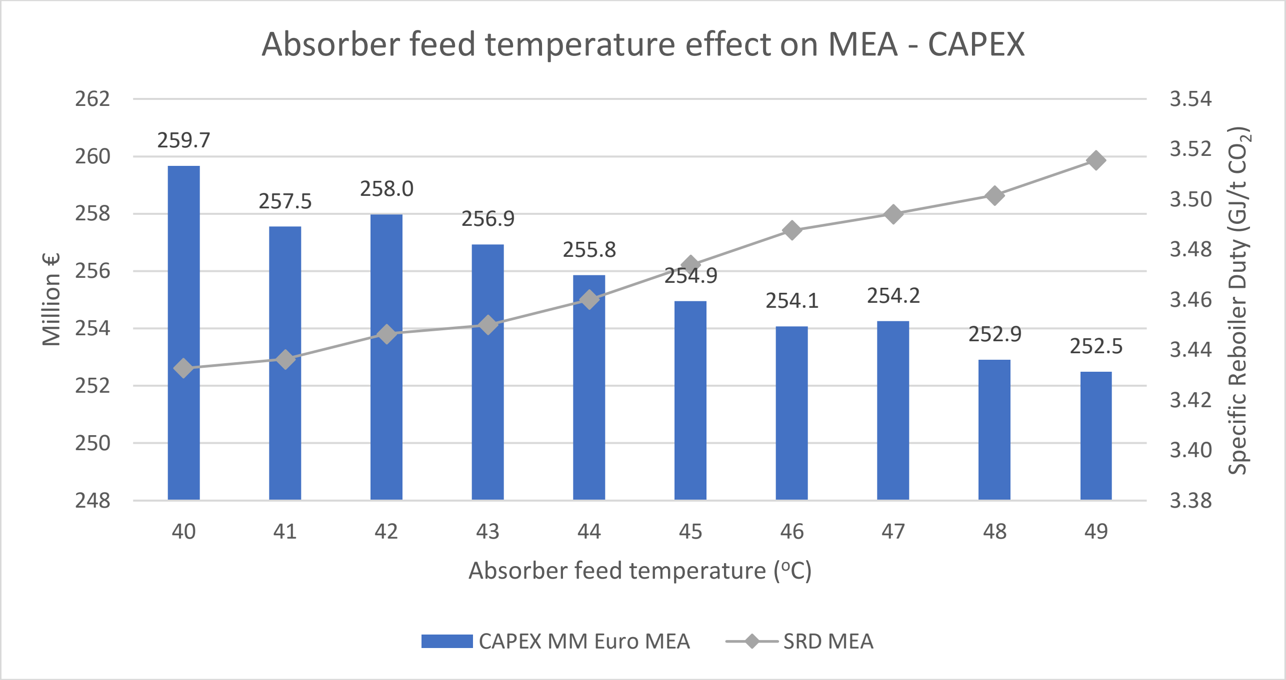

Figure 54: Effect of absorber feed temperature on CAPEX for MEA

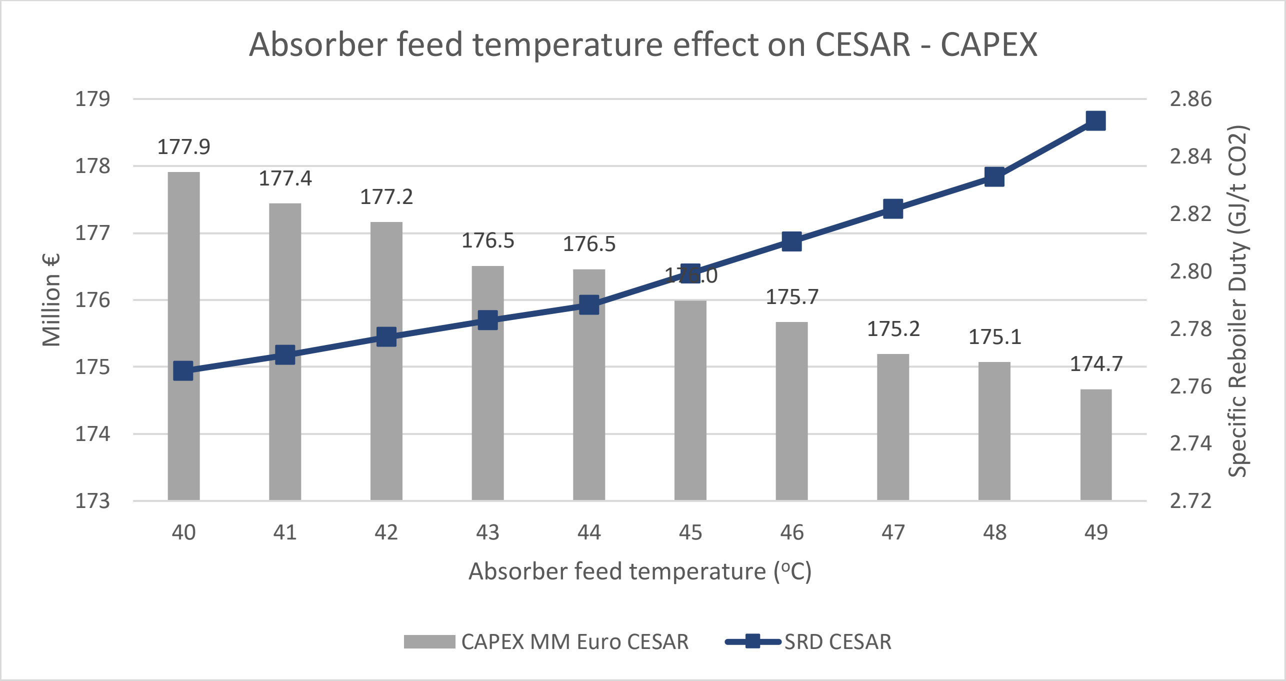

Figure 55:Effect of absorber feed temperature on CAPEX for CASER

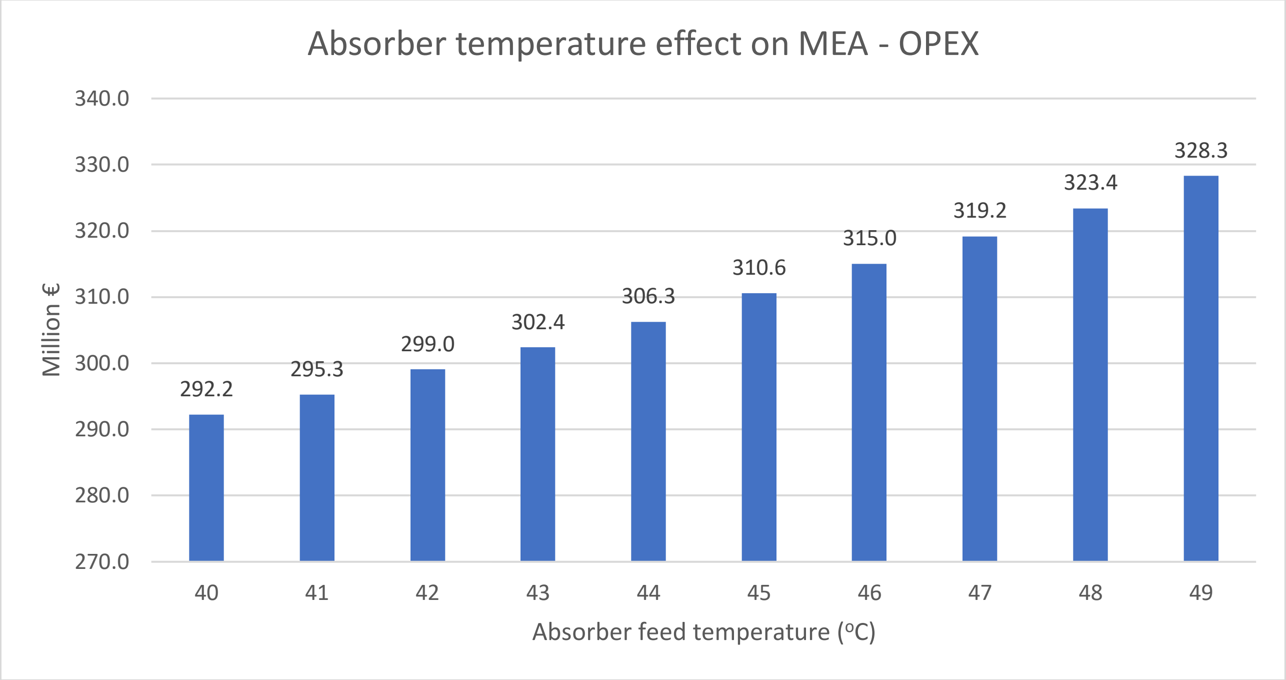

Figure 56: Effect of absorber feed temperature on OPEX for MEA

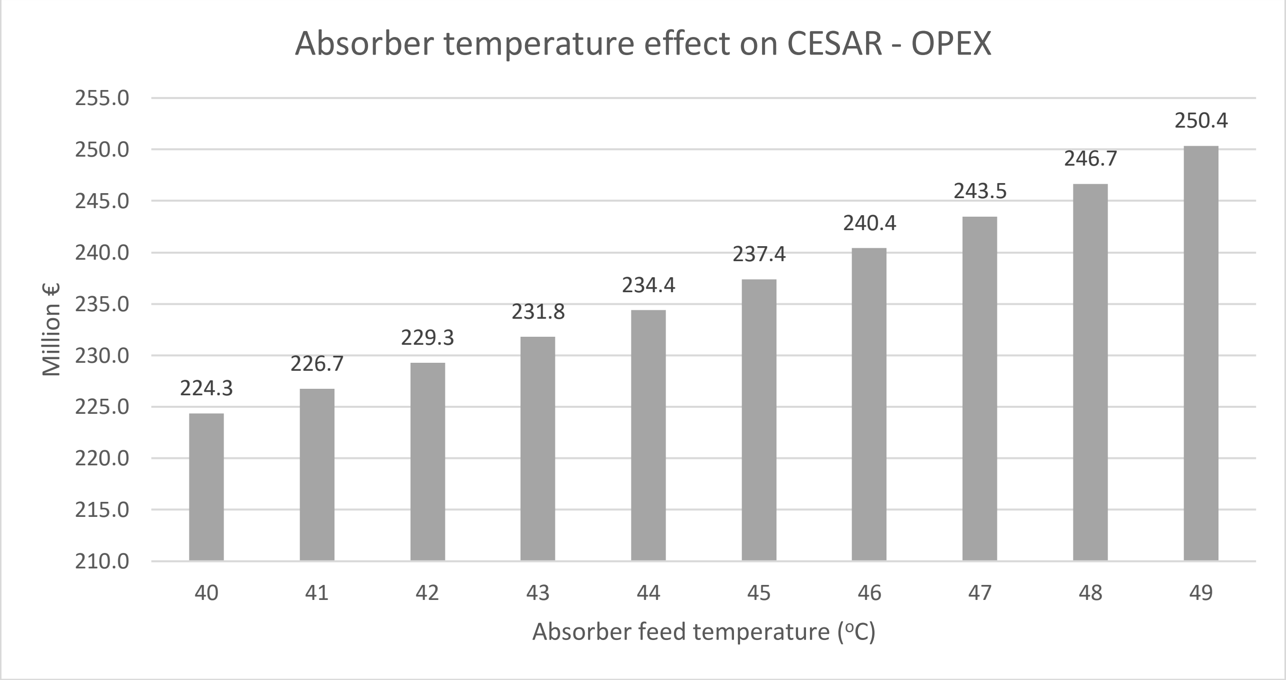

Figure 57:Effect of absorber feed temperature on OPEX for CESAR

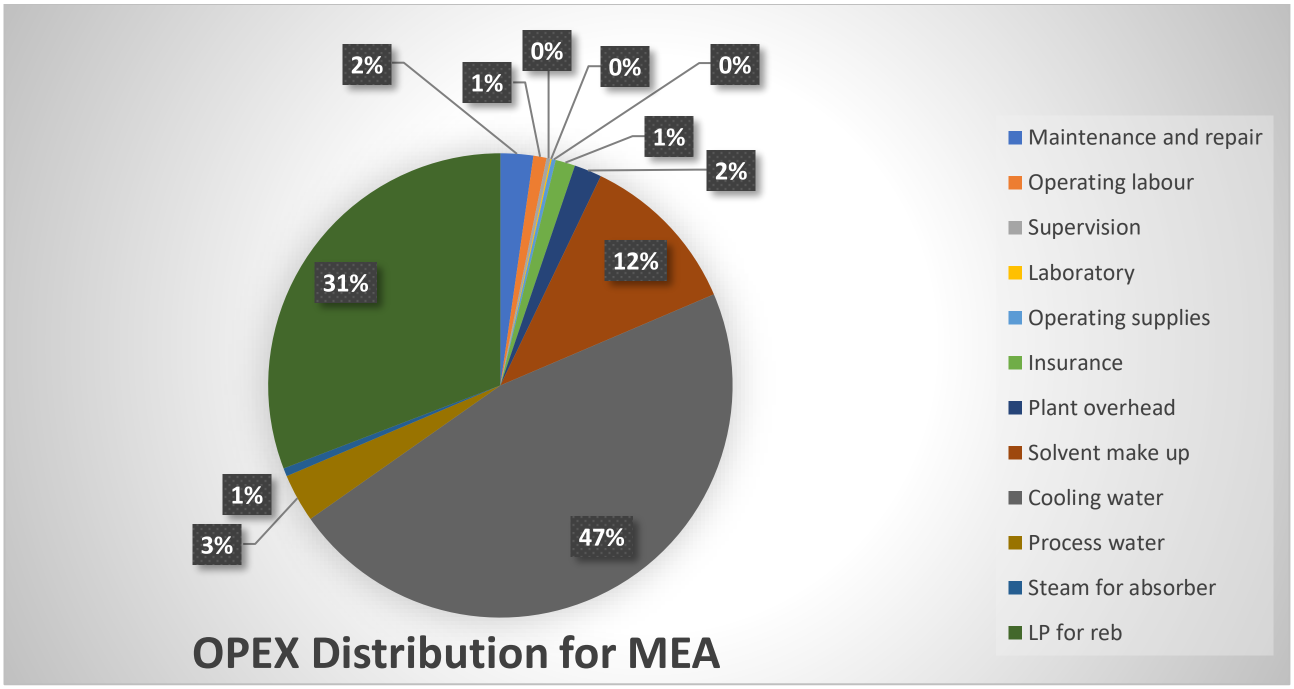

Figure 58: OPEX distribution for MEA for absorber feed temperature effect

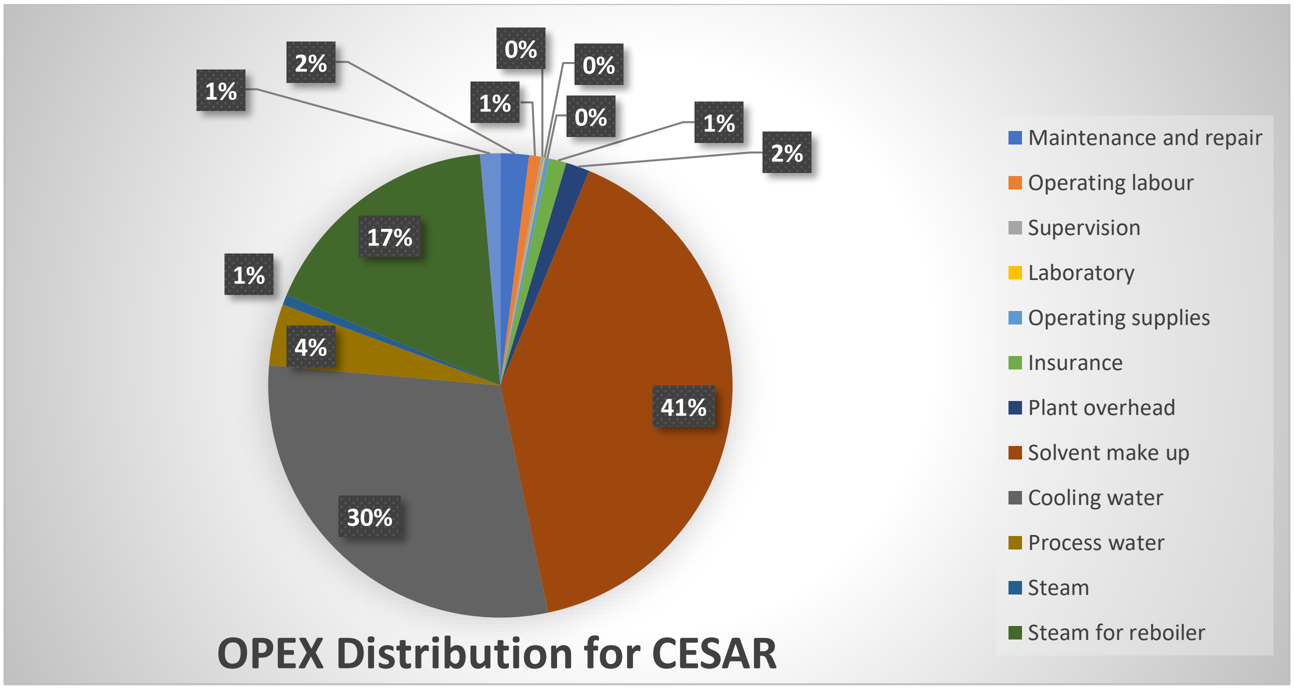

Figure 59: OPEX distribution for CESAR for absorber feed temperature effect

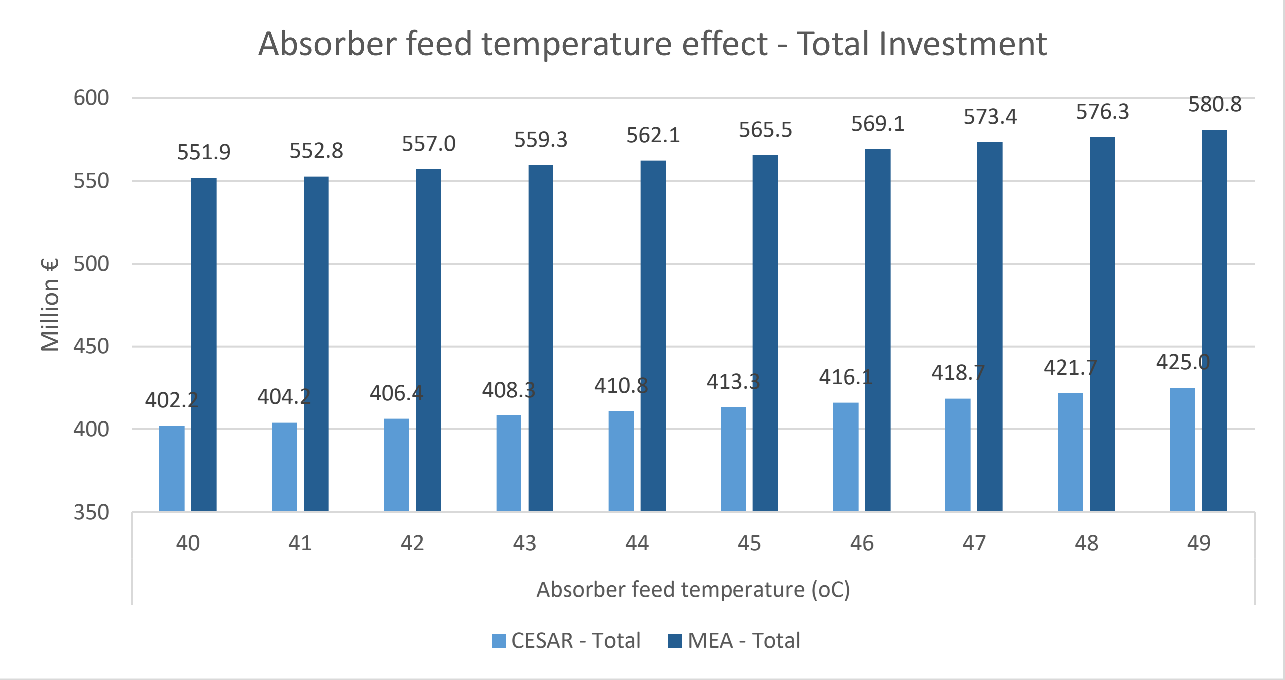

Figure 60: Absorber feed temperature effect on total investment

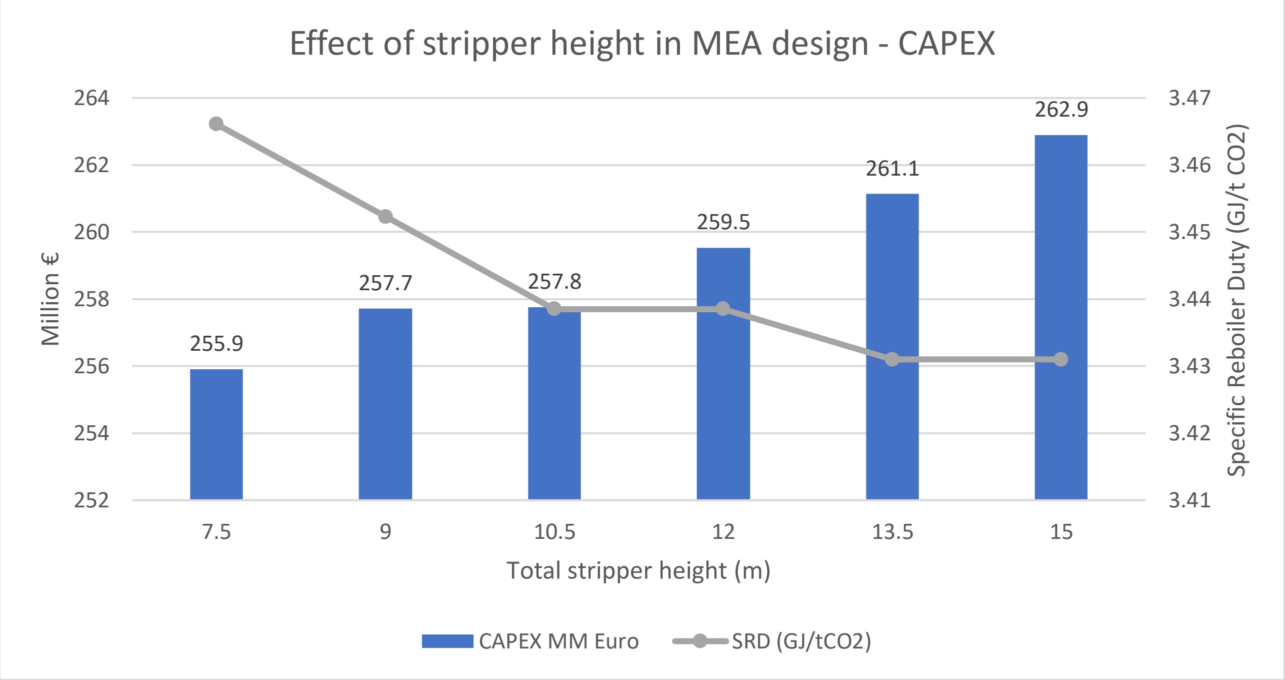

Figure 61: Effect of stripper height on CAPEX in MEA design

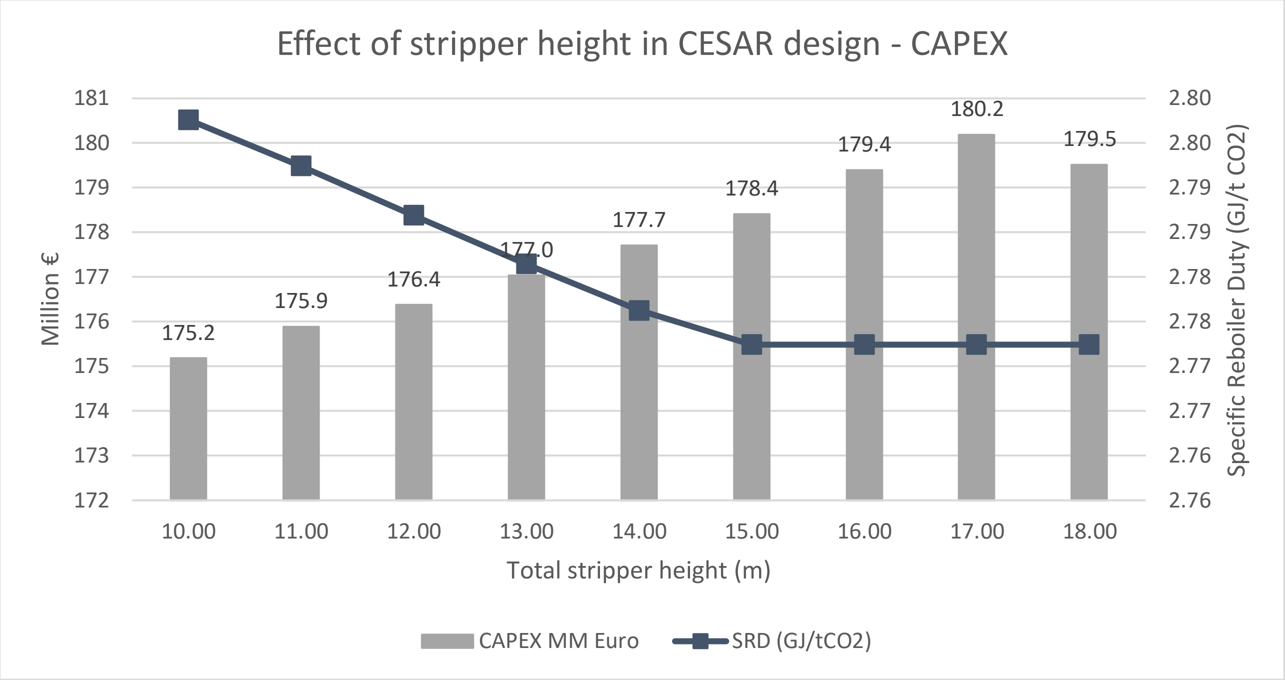

Figure 62: Effect of stripper height on CAPEX in CESAR design

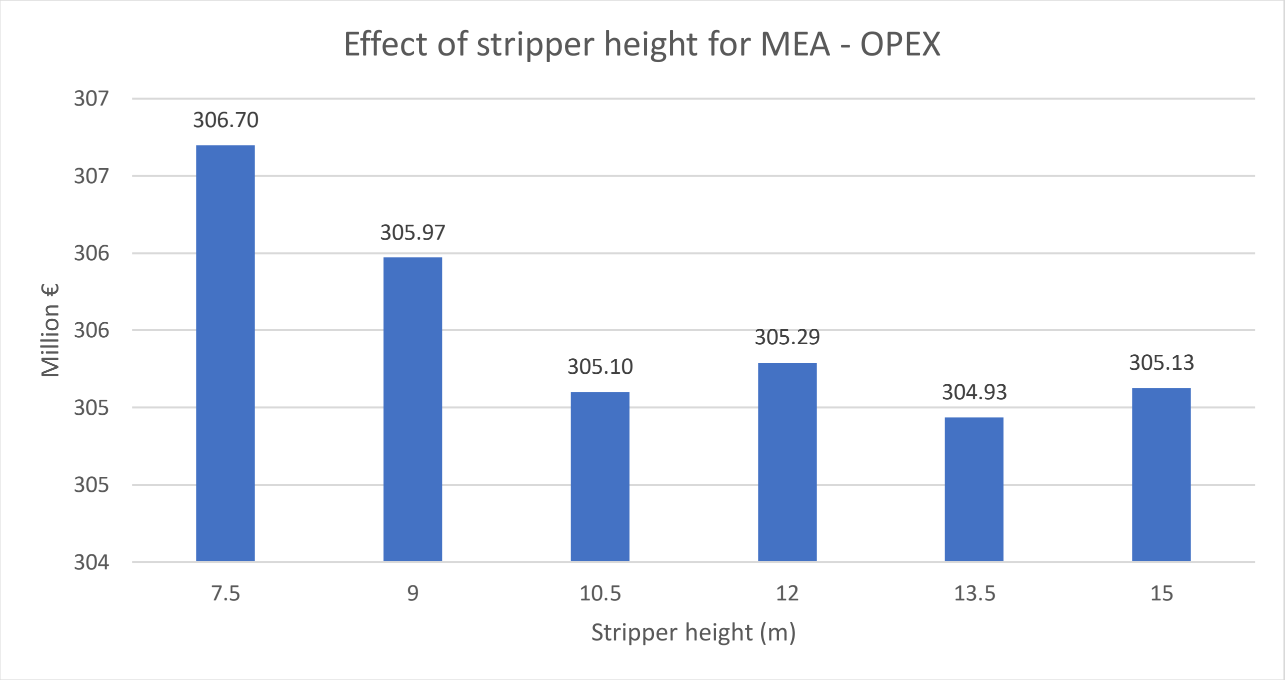

Figure 63: Effect of stripper height on OPEX in MEA design

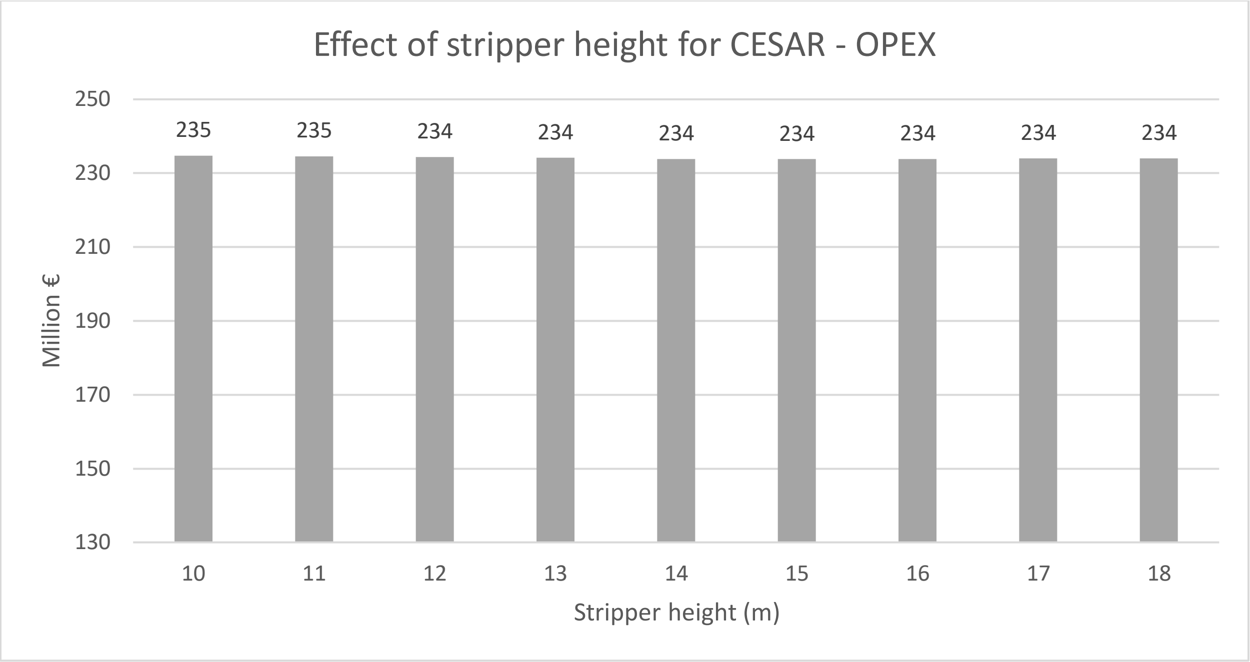

Figure 64: Effect of stripper height on OPEX in CESAR design

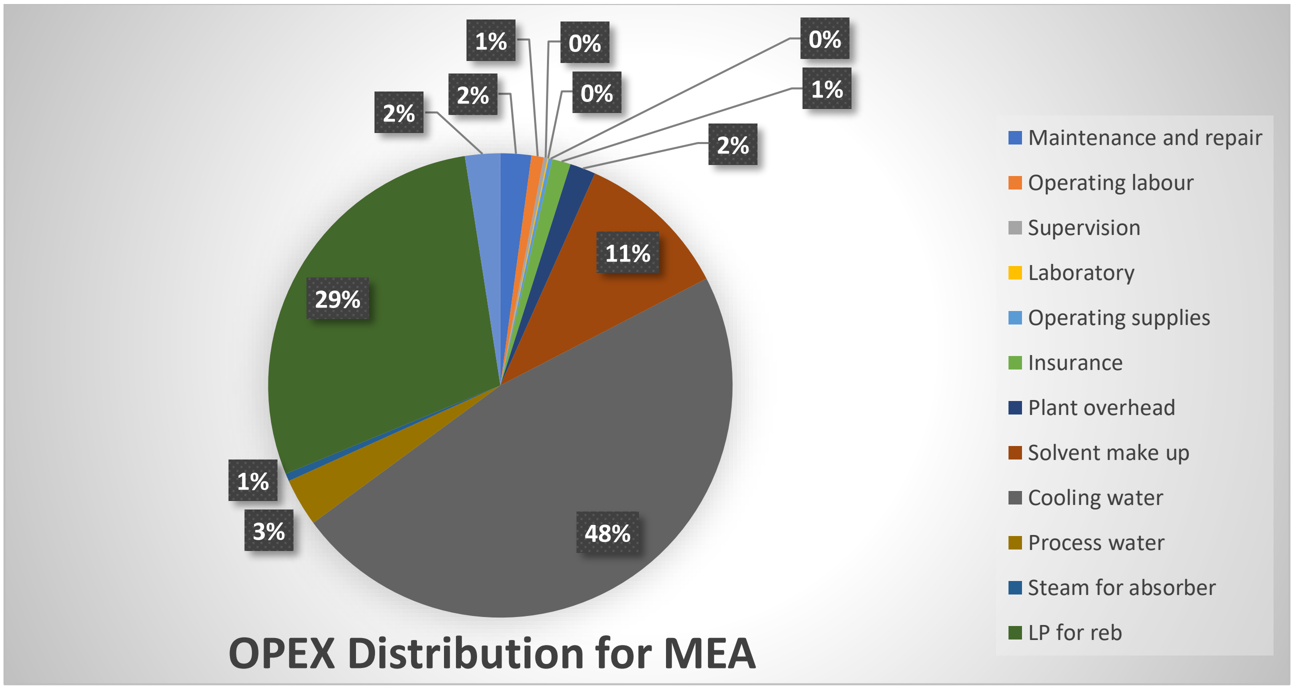

Figure 65: OPEX distribution for MEA for stripper height

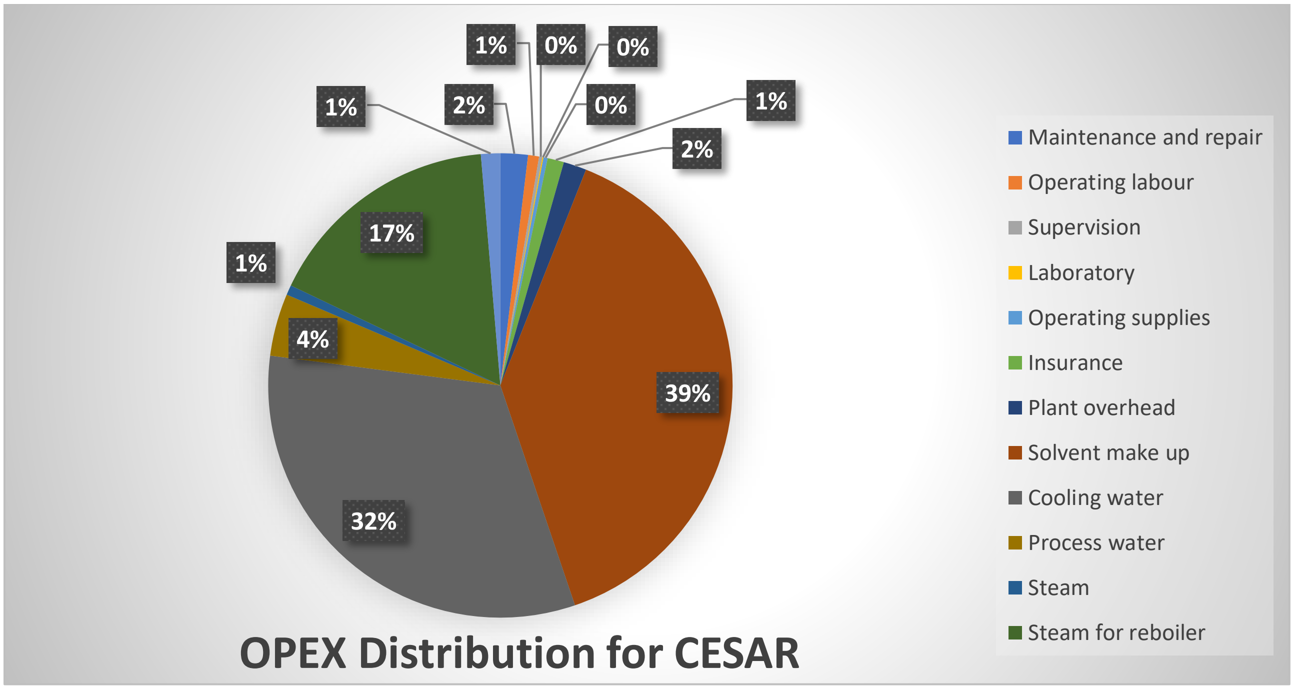

Figure 66:OPEX distribution for CESAR for stripper height

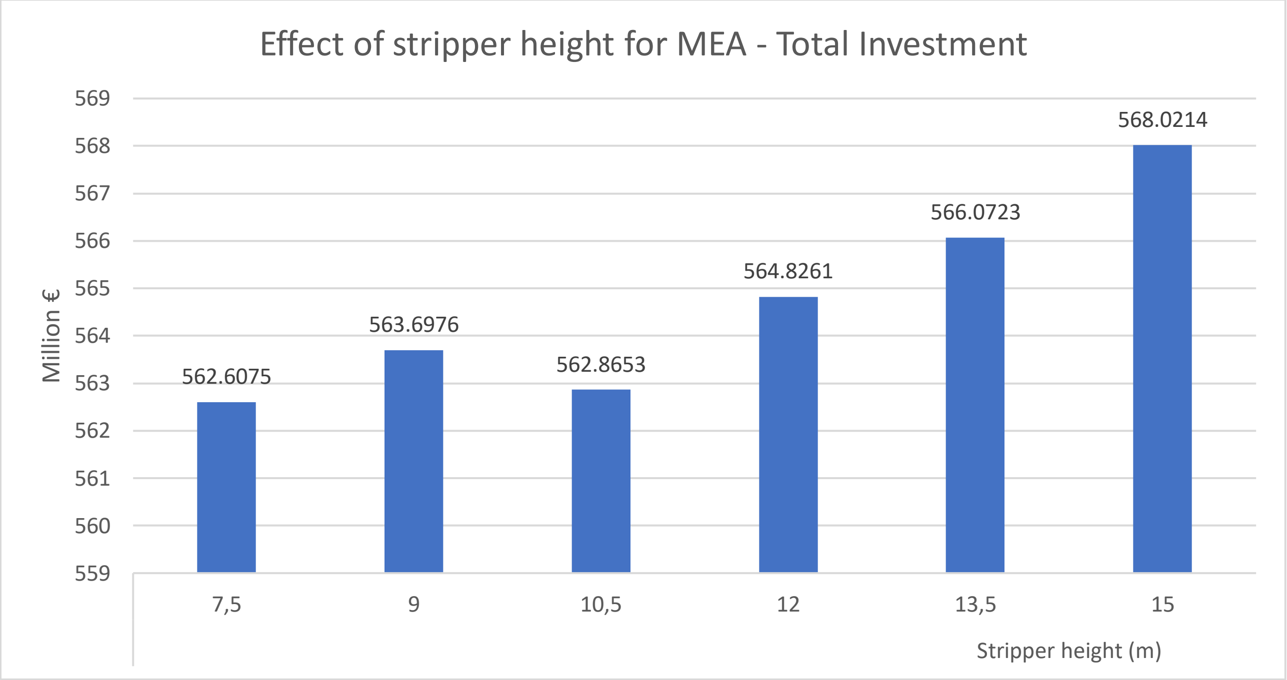

Figure 67: Effect of stripper height on total investment of MEA design

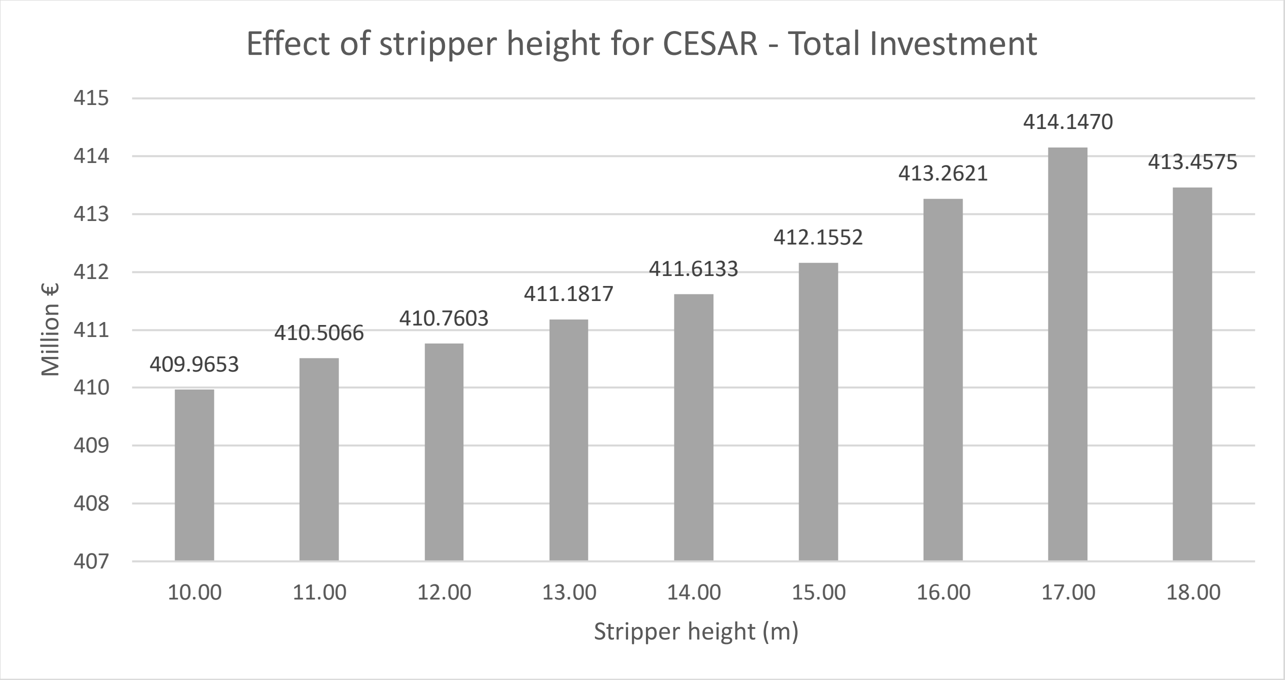

Figure 68:Effect of stripper height on total investment of CESAR design

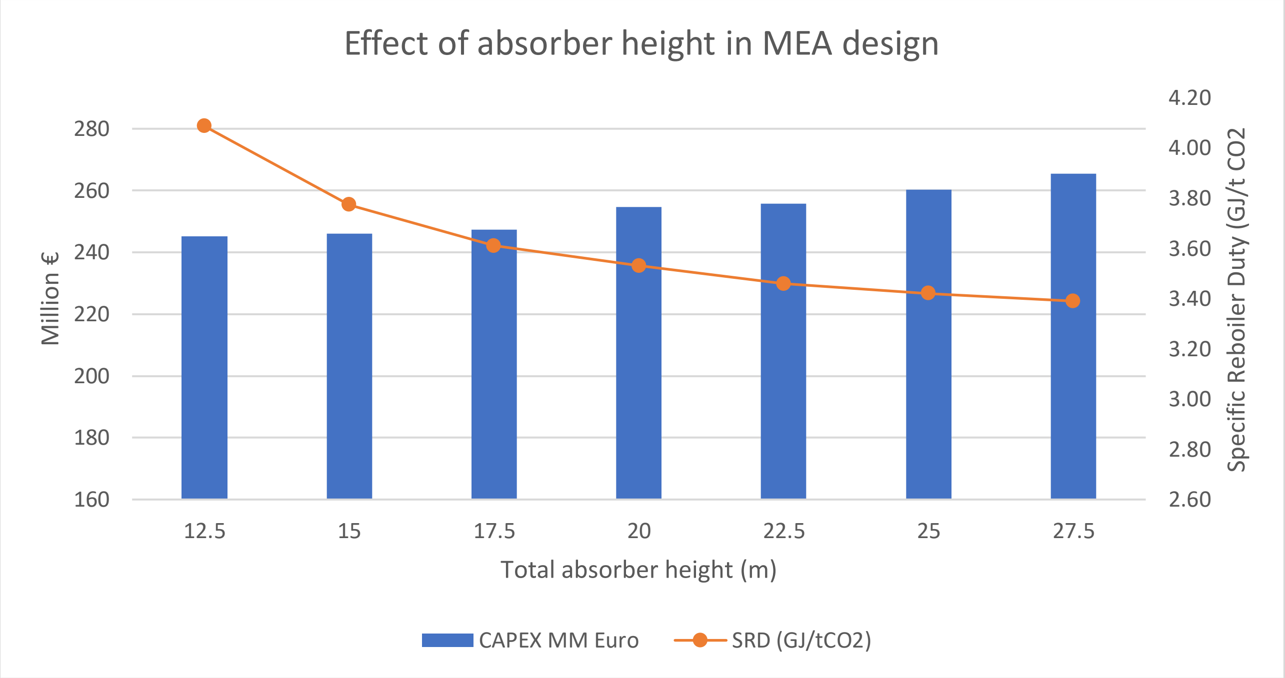

Figure 69:Effect of absorber height on CAPEX in MEA design

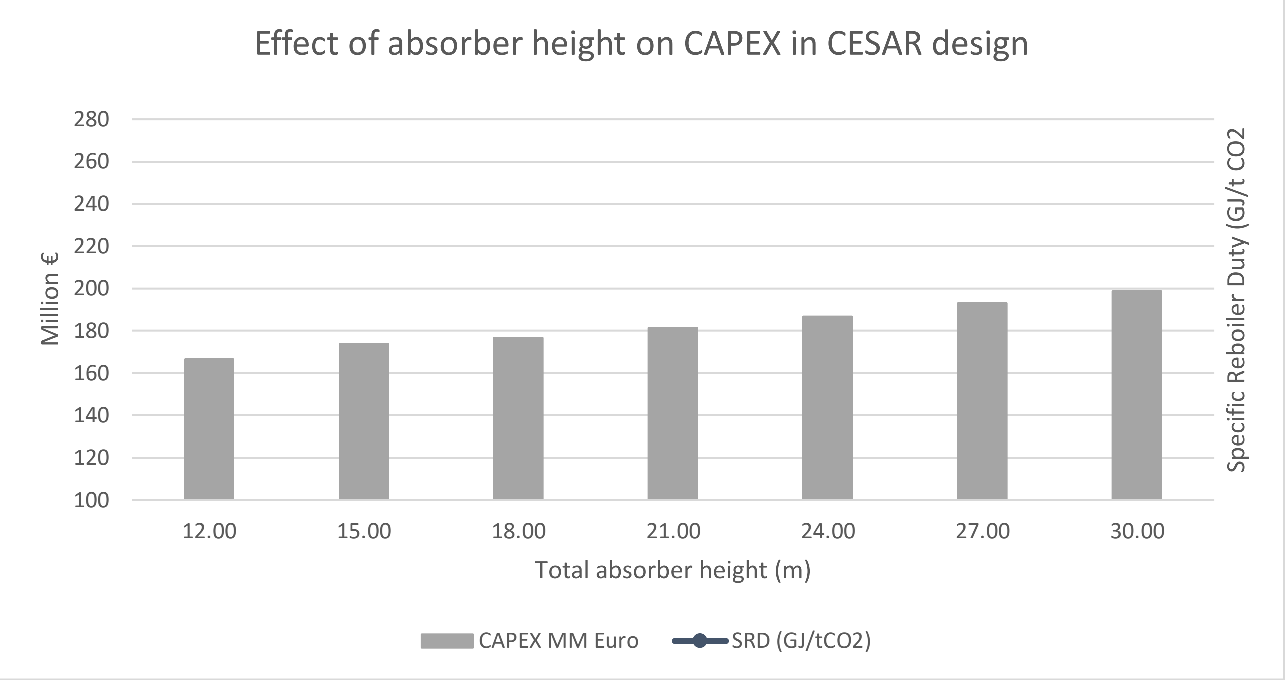

Figure 70:Effect of absorber height on CAPEX in CESAR design

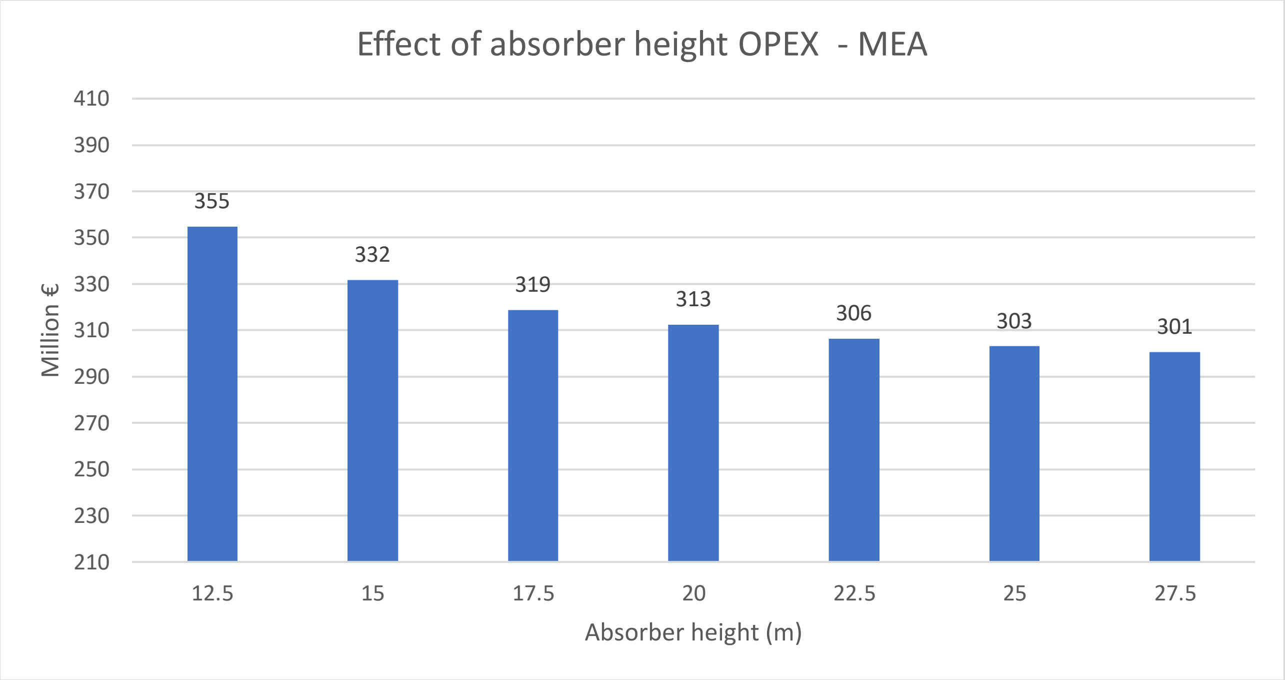

Figure 71:Effect of absorber height on OPEX for MEA

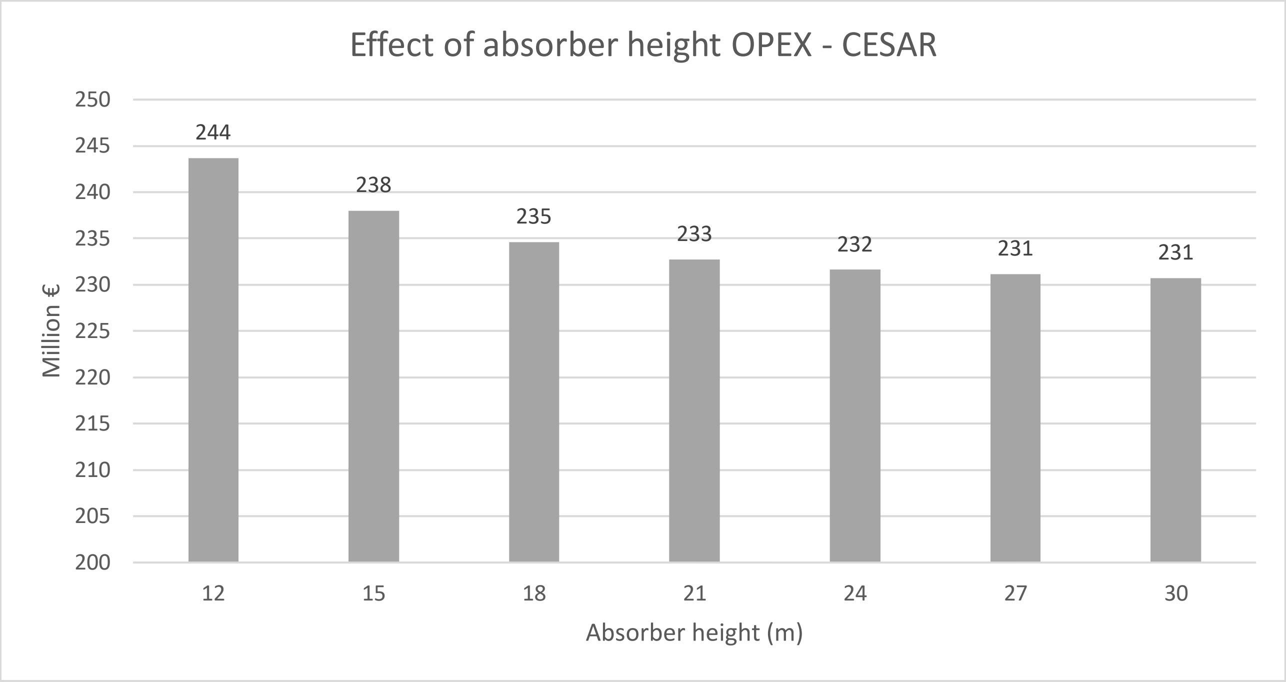

Figure 72: Effect of absorber height on OPEX for MEA

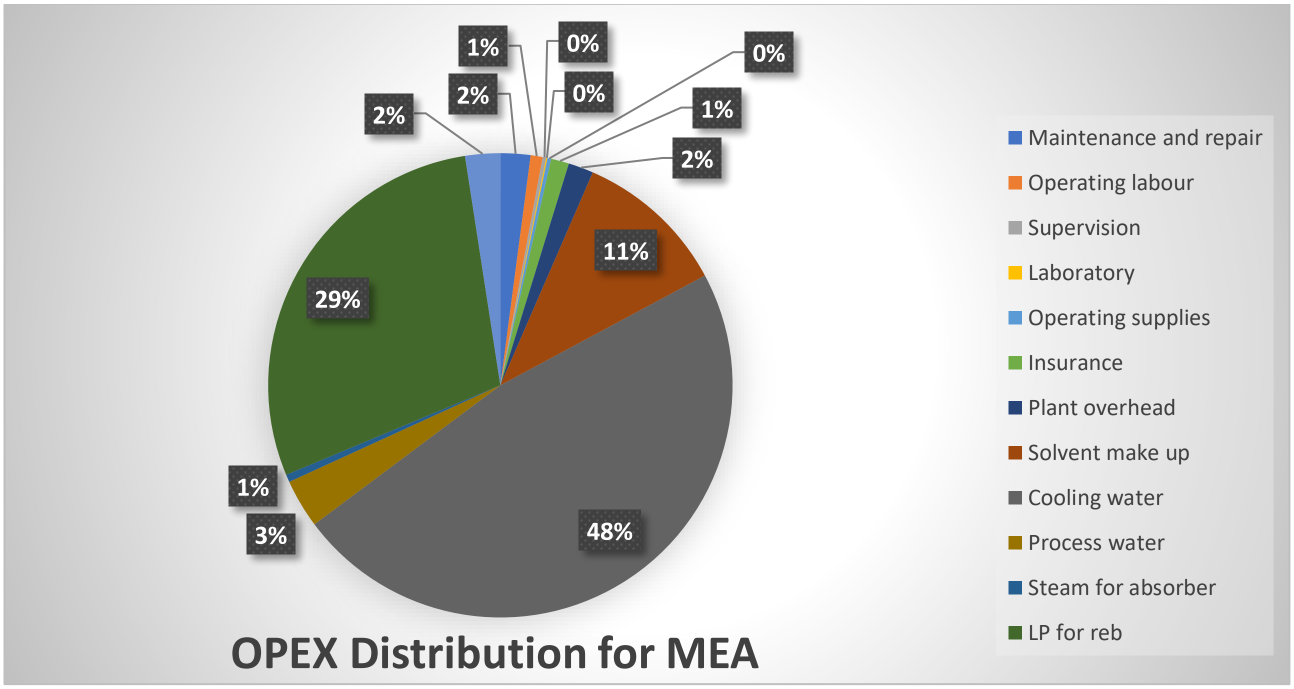

Figure 73:OPEX distribution for MEA for absorber height

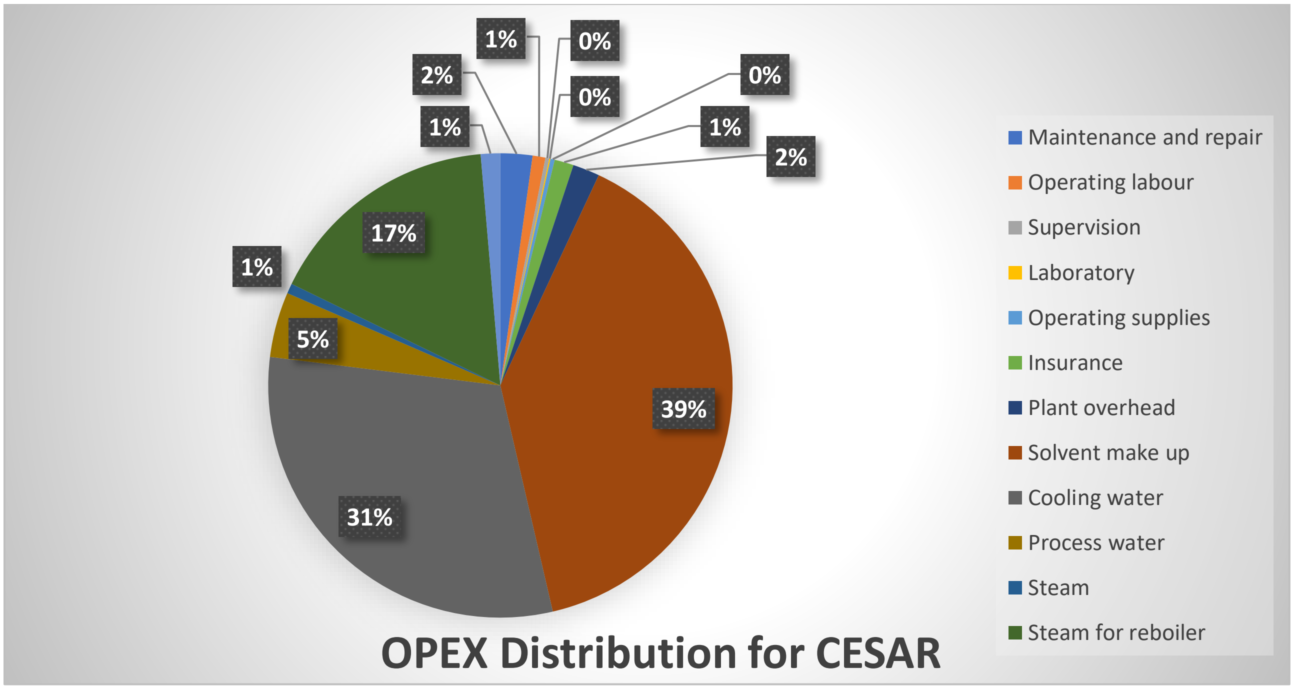

Figure 74: OPEX distribution for CESAR for absorber height

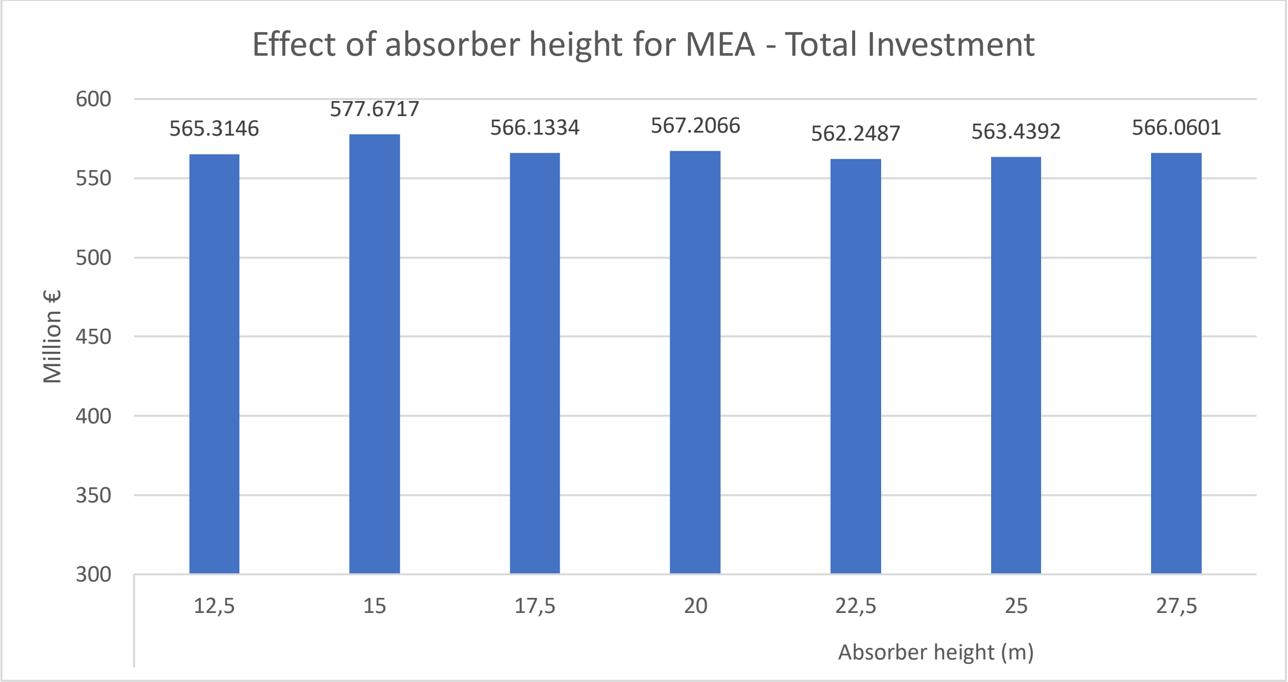

Figure 75: Effect of absorber height on total investment for MEA

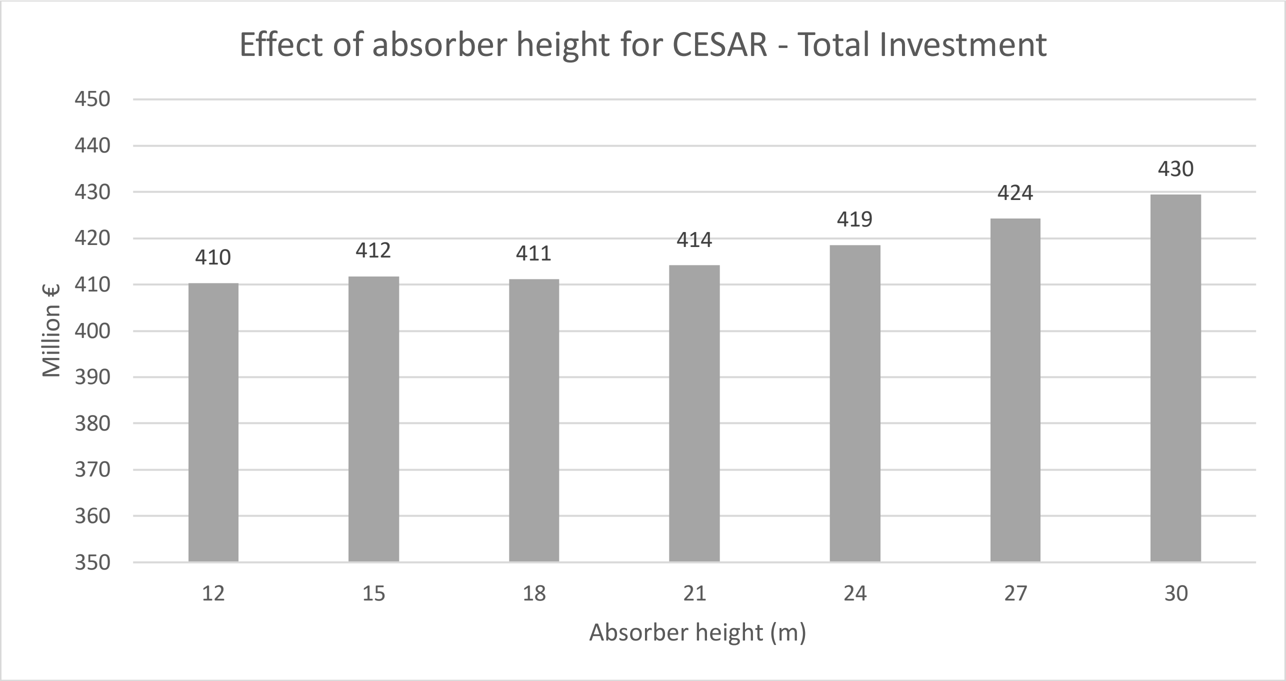

Figure 76: Effect of absorber height on total investment for MEA